

12-2015

# A plant-made cholera toxin B subunit enhances mucosal wound healing and protects against ulcerative colitis and colon cancer.

Keegan J Baldauf  
*University of Louisville*

Follow this and additional works at: <https://ir.library.louisville.edu/etd>

Part of the [Pharmacology Commons](#)

---

## Recommended Citation

Baldauf, Keegan J, "A plant-made cholera toxin B subunit enhances mucosal wound healing and protects against ulcerative colitis and colon cancer." (2015). *Electronic Theses and Dissertations*. Paper 2328.  
<https://doi.org/10.18297/etd/2328>

This Doctoral Dissertation is brought to you for free and open access by ThinkIR: The University of Louisville's Institutional Repository. It has been accepted for inclusion in Electronic Theses and Dissertations by an authorized administrator of ThinkIR: The University of Louisville's Institutional Repository. This title appears here courtesy of the author, who has retained all other copyrights. For more information, please contact [thinkir@louisville.edu](mailto:thinkir@louisville.edu).

A PLANT-MADE CHOLERA TOXIN B SUBUNIT ENHANCES MUCOSAL  
WOUND HEALING AND PROTECTS AGAINST ULCERATIVE COLITIS AND  
COLON CANCER

By

Keegan J. Baldauf  
B.S., Clarion University of Pennsylvania, 2005  
M.S., University of Louisville, 2012

A Dissertation  
Submitted to the Faculty of the  
School of Medicine of the University of Louisville  
in Partial Fulfillment of the Requirements  
for the Degree of

Doctor of Philosophy in Pharmacology and Toxicology

Department of Pharmacology and Toxicology  
University of Louisville  
Louisville, KY

December 2015



A PLANT-MADE CHOLERA TOXIN B SUBUNIT ENHANCES MUCOSAL  
WOUND HEALING AND PROTECTS AGAINST ULCERATIVE COLITIS AND  
COLON CANCER

By

Keegan J. Baldauf  
B.S., Clarion University of Pennsylvania, 2005  
M.S., University of Louisville, 2012

A Dissertation Approved on

October 26, 2015

by the following Dissertation Committee:

---

Nobuyuki Matoba, Ph.D.

---

Gavin E. Arteel, Ph.D.

---

Haribabu Bodduluri, Ph.D.

---

Susan Galandiuk, M.D.

---

Venkatakrishna Rao Jala, Ph.D.

---

Kenneth E. Palmer, Ph.D.

## DEDICATION

This dissertation is dedicated to my wife

Kristin M. Baldauf, Ph.D.,

And my Parents

Mr. Larry Baldauf and Mrs. Alice Baldauf,

who have supported me at home throughout this process

and

Nobuyuki Matoba, Ph.D.

who has given me the educational experience of a lifetime.

## ACKNOWLEDGEMENTS

I would like to thank my Mentor, Dr. Nobuyuki Matoba, for sharing his knowledge and always pushing me to achieve more. Also, I would like to thank my committee members, Dr. Gavin E. Arteel, Dr. Haribabu Bodduluri, Dr. Susan Galandiuk, Dr. Venkatakrishna Rao Jala, and Dr. Kenneth E. Palmer for stimulating conversations about my experiments throughout my time here. My wife, Kristin Baldauf, who from the beginning supported me and encouraged me throughout this process to press on when times were tough, deserves more thanks than I could possibly express here. Lastly, I want to thank my Parents and Kristin's family who were always available whenever we needed some help with our two sons, Carson and Caiden.

## ABSTRACT

### A PLANT-MADE CHOLERA TOXIN B SUBUNIT ENHANCES MUCOSAL WOUND HEALING AND PROTECTS AGAINST ULCERATIVE COLITIS AND COLON CANCER

Keegan J. Baldauf

October 26, 2015

This dissertation describes the previously unidentified effects of a plant-produced recombinant cholera toxin B subunit (CTBp) on the gastrointestinal (GI) tract and its ability to protect against inflammation in a mouse model of colonic injury and ulcerative colitis (UC). To comprehensively analyze CTBp's impacts on the GI tract, we employed global analysis methodologies based on multi-color flow cytometry to analyze immune cell populations in GI and systemic lymphatic compartments, gene expression microarray to decipher transcript-level changes in the colon and small intestine, and 16S rRNA sequencing to characterize fecal microbiota. Based on a drastic shift observed in the immune cell profile and gene expression pattern in the distal colon, we built a new working hypothesis that CTBp may enhance mucosal protection in the colon. To address this hypothesis, we used the Caco-2 human colonic cell line and the mouse dextran sulfate sodium (DSS) colitis model. After demonstrating the potential of CTBp as a mucosal healing and anti-colitic agent, the dissertation will be summarized and future directions discussed.

There are six chapters in this dissertation document. The first chapter covers the current knowledge base of CT and CTB. Additionally, the role of CTB in cholera vaccination and the protein's potential utility as a vaccine adjuvant and an anti-inflammatory agent are discussed. The second chapter focuses on the immunomodulatory effects of CTBp in the GI tract of mice upon oral administration. The third chapter discusses the mucosal protection potential of CTBp in Caco-2 cells and the acute DSS colitis model. The fourth chapter probes the long-term impacts of CTBp oral administration. In the fifth chapter, we explore the ability of CTBp to blunt chronic colitis in a mouse model. Lastly, the sixth chapter summarizes our findings in the present work and explores future directions for the CTBp research.



## TABLE OF CONTENTS

|   | PAGE |
|---|------|
| ABSTRACT .....  | v    |
| LIST OF TABLES .....  | x    |
| LIST OF FIGURES .....   | xi   |
| CHAPTER 1 CHOLERA TOXIN B: ONE SUBUNIT WITH MANY<br>PHARMACEUTICAL APPLICATIONS .....                                       | 1    |
| INTRODUCTION.....   | 2    |
| Cholera .....   | 2    |
| Cholera Toxin.....  | 3    |
| CTB AS A VACCINE ADJUVANT .....   | 10   |
| CTB IN INFLAMMATION .....   | 11   |
| CTB's Anti-Inflammatory Activity in Various Inflammatory Diseases.....  | 13   |
| Recombinant or Non-Recombinant CTB: Conflicting Results of CTB's<br>Anti-Inflammatory Activity in in Vitro Experiments..... | 18   |
| CONCLUSION .....  | 20   |
| CHAPTER 2: ORAL ADMINISTRATION OF CTB <sub>p</sub> SIGNIFICANTLY IMPACTS<br>THE GASTROINTESTINAL MUCOSA.....                | 22   |
| INTRODUCTION.....   | 23   |

|  | PAGE |
|--|------|
| METHODS .....  | 25   |
| RESULTS.....   | 32   |
| DISCUSSION.....  | 50   |
| CHAPTER 3: CTBp PROTECTS AGAINST DSS-INDUCED ACUTE COLITIS | 54   |
| INTRODUCTION.....  | 55   |
| METHODS .....  | 57   |
| RESULTS.....   | 62   |
| DISCUSSION.....  | 74   |
| CHAPTER 4: EFFECTS OF A LONG-TERM ORAL CTBp ADMINISTRATION | 77   |
| INTRODUCTION.....  | 78   |
| METHODS .....  | 80   |
| RESULTS.....   | 85   |
| DISCUSSION.....  | 94   |
| CHAPTER 5: CTBp MITIGATES CHRONIC COLITIS .....            | 97   |
| INTRODUCTION.....  | 98   |
| METHODS .....  | 101  |
| RESULTS.....   | 106  |
| DISCUSSION.....  | 111  |

|  | PAGE |
|--|------|
| CHAPTER 6: SUMMARY OF CTBp RESEARCH AND IMPLICATIONS FOR<br>FUTURE DIRECTIONS..... | 116  |
| SUMMARY OF THE PRESENT CTBp STUDIES .....  | 117  |
| PERSPECTIVES.....  | 123  |
| REFERENCES.....  | 131  |
| CURRICULUM VITAE.....  | 145  |

## LIST OF TABLES

| TABLE  | PAGE |
|--|------|
| Table 1.1 Gene Identity for qPCR analysis.....           | 30   |
| Table 2.1. Flow Cytometry Cell Type Marker Strategy..... | 33   |
| Table 3.1. Gene Identity for qPCR analysis.....          | 61   |

## LIST OF FIGURES

| FIGURE   | PAGE |
|--|------|
| Figure 1.1. CT crystal structure. ....   | 5    |
| Figure 1.2. CT, not rCTB, inhibits the release of TNF- $\alpha$ by Raw 264.7 cells stimulated with LPS. ....                                   | 19   |
| Figure 2.1. T cell populations in different lymphoid tissues one week after the second CTBp or PBS oral administration. ....                   | 35   |
| Figure 2.2. CD45+ immune cell populations in different lymphoid tissues one week after the second CTBp or PBS oral administration. ....        | 36   |
| Figure 2.3. T cell populations in different lymphoid tissues two weeks after the second CTBp or PBS oral administration. ....                  | 37   |
| Figure 2.4. CD45+ gated Immune cell populations in different lymphoid tissues two weeks after the second CTBp or PBS oral administration. .... | 38   |
| Figure 2.5. CTBp significantly alters the Immune Cell profile in the colon. ....   | 39   |
| Figure 2.6. Principal coordinate analysis revealed separation of GI tract gene expression profiles of mice vaccinated with PBS and CTBp. ....  | 41   |
| Figure 2.7. TGF $\beta$ -dependent pathways are significantly altered by CTBp in the colon. ....   | 42   |
| Figure 2.8. TGF $\beta$ associated gene expression pathways in the colon induced by CTBp oral administration. ....                             | 44   |

| FIGURE   | PAGE |
|--|------|
| Figure 2.9. qPCR analysis of representative genes to verify the microarray analysis. ....  | 45   |
| Figure 2.10. Wound healing pathway-focused qPCR analysis of colon gene expression. ....  | 46   |
| Figure 2.11. No significant change in overall microbiome was observed two weeks following CTBp vaccination. ....   | 47   |
| Figure 2.12. CTBp does not significantly alter the microbiome at the Phylum level but several species were significantly altered in the Firmicutes Phylum. . . | 49   |
| Figure 3.1. CTBp enhanced wound healing in Caco2 cells. ....   | 63   |
| Figure 3.2. Study design for recovery acute colitis experiment.....  | 64   |
| Figure 3.3. CTBp blunts body weight loss from DSS exposure. ....   | 65   |
| Figure 3.4. Histopathological analysis of colon 1 week after DSS exposure. ....  | 66   |
| Figure 3.5. Masson’s trichrome stain of distal colon cross sections. ....  | 67   |
| Figure 3.6. Study design for recovery acute colitis experiment.....  | 67   |
| Figure 3.7. CTBp blunts inflammation immediately after DSS exposure. ....  | 68   |
| Figure 3.8. CTBp blunts pro-inflammatory genes in DSS colitis after a 1 week recovery.....   | 69   |
| Figure 3.9. Pro-fibrotic cytokine gene expression significantly elevated 1 week after DSS exposure with PBS but not CTBp.....                                  | 70   |
| Figure 3.10. 30 µg CTBp blunts inflammatory gene expression and protein levels immediately after DSS exposure. ....  | 71   |

| FIGURE  | PAGE |
|---|------|
| Figure 3.11. Immunohistochemistry analysis of macrophages in distal colon sections. ....  | 73   |
| Figure 4.1. Chronic administration of CTBp significantly alters T cell populations. ....  | 86   |
| Figure 4.2. Chronic administration of CTBp significantly alters CD45+ cell populations. ....  | 87   |
| Figure 4.3. CTBp increased immune cell populations proportionally to the total population, as well as the total white blood cell population. .... | 89   |
| Figure 4.4. No changes in serum chemistry were noted following CTBp administration. ....  | 90   |
| Figure 4.5. Serum IFN $\gamma$ was significantly decreased by the long-term CTBp administration. ....   | 91   |
| Figure 4.6. Treatment with CTBp and cage did not significantly alter the overall microbiome. ....   | 92   |
| Figure 4.7. OTU's significantly decreased by CTBp oral administration. ....   | 93   |
| Figure 5.1. Study design for chronic colitis and colon cancer model. ....   | 106  |
| Figure 5.2. CTBp protects against colitis associated colon cancer. ....   | 107  |
| Figure 5.3. CTBp significantly enhances genes related to suppression of tumor development. ....   | 109  |
| Figure 5.4. CTBp treatment blunted tissue inflammatory cytokine protein levels. ....  | 110  |

FIGURE

PAGE

Figure 6.1. CTBp significantly enhances wound healing compared to native CTB.

..... 126



CHAPTER 1 CHOLERA TOXIN B: ONE SUBUNIT WITH MANY  
PHARMACEUTICAL APPLICATIONS<sup>1</sup>

---

<sup>1</sup> Toxins. 2015 Mar;7:974-96.

## INTRODUCTION

### Cholera

Cholera is a highly contagious acute dehydrating diarrheal disease caused by *Vibrio cholerae*. There are over 200 serogroups of *V. cholerae* known to date; however, only 2 (O1 and 139 serotypes) are responsible for the vast majority of outbreaks (1, 2). The pathology of cholera results from *V. cholerae* colonization in the small intestine and subsequent production of the cholera toxin (CT). *V. cholerae* are found in coastal waters and deltas due to their preference for salinity in water; however under proper conditions (warm and sufficient nutrients), *V. cholerae* can grow in low salinity environments (3). Natural disasters (e.g., floods, monsoons, and earthquakes) and poor sanitation are major players in the spread of cholera epidemics. Symptomatic individuals can shed the organism from 2 days to 2 weeks after infection and recently shed organisms (5–24 h after shedding) have hyperinfectivity; in this state the infectious dose is 10 to 100 times lower than non-shed organisms ( $\sim 10^6$  bacteria) (4, 5). This can lead to the rapid spread of cholera in densely populated areas without proper management of patients and their waste.

The most common symptom of cholera is a life-threatening amount of watery diarrhea, causing an extreme loss of water, up to 1 L per hour, which can lead to death within hours of the first onset of symptoms if left untreated (3). The diarrhea is usually painless and not accompanied by the urge to evacuate the bowels. Early in the illness, vomiting can be a common symptom as well.

Cholera is considered endemic in over 50 countries, but it can manifest as an epidemic, as has recently been the case in Haiti (2010–present), a country previously not exposed to cholera (6-8). Reported world incidences of cholera increased from 2007 until a peak of approximately 600,000 cases in 2011 (9). In 2012, the number of reported cases decreased to approximately 245,000 with 49% of the cases resulting from the ongoing outbreak in Haiti and the Dominican Republic. However, the World Health Organization (WHO) estimates the actual global burden of the disease to be between 3 and 5 million cases per year and 100,000 to 130,000 deaths per year (10). Additionally, a more virulent strain of *V. cholerae* O1 is making inroads in Africa and Asia (11). The WHO suggests there should also be concern for the spread of antibiotic-resistant strains of *V. cholerae*. This has already been shown with *V. cholerae* O139 and some isolates from *V. cholerae* O1 El Tor, which have acquired resistance traits for cotrimoxazole and streptomycin (3). It is clear that cholera, despite its long history, is still an emerging disease that is necessary to combat.

### **Cholera Toxin**

CT produced by *V. cholerae*, is the main virulence factor in the development of cholera. The molecular characteristics of CT and its toxic effects in humans have been well characterized (12-14). CT is an 84 kD protein made up of 2 major subunits, CTA and CTB (15, 16) (Fig. 1.1). The CTA subunit is responsible for the disease phenotype while CTB provides a vehicle to deliver CTA to target cells. CTA is a 28 kD subunit consisting of 2 primary domains, CTA1 and CTA2, with the toxin activity residing in the former and the latter acting as an anchor into

the CTB subunit (17). The CTB subunit consists of a homopentameric structure that is approximately 55 kD (11.6 kD monomers) and binds to the GM1-ganglioside; found in lipid rafts, on the surface of intestinal epithelial cells (13). The exact mechanism of delivering CTA1 into the intracellular space is still not fully resolved; however, the current understanding is that CT is endocytosed and travels through a retrograde transport pathway from the Golgi apparatus to the endoplasmic reticulum (ER) (12-14, 17, 18). Recently, it has been shown that CT can also move from the apical to basolateral surface of epithelial cells via transcytosis, enabling transport of whole CT through the intestinal barrier (19). CTA is dissociated from CTB after the toxin reaches the ER and translocated to the cytosol via the ER-associated degradation pathway (15). Intoxication occurs when CTA1 enters the cell cytosol and catalyzes the ADP ribosylation of adenylate cyclase, which leads to increased intracellular cAMP. The increase in intracellular cAMP results in impaired sodium uptake and increased chloride outflow, causing water secretion and diarrhea (12, 17).

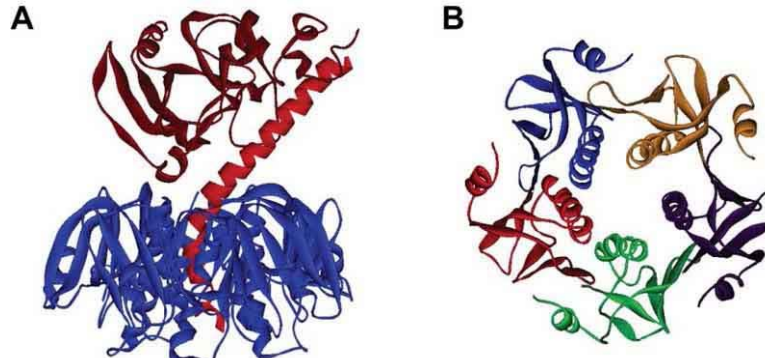


**Figure 1.1. CT crystal structure.**

**A.)** CT (side view; PBD ID: 1XTC). The CTA subunit is shown in red (CTA1 in dark red and CTA2 in light red) and the CTB subunit is shown in blue. **B)** CTB (top view; PBD ID: 1XTC with CTA subunit removed). Each monomer of the B subunit is shown in a different color. Images were created in Accelrys Discovery Studio Visualizer 2.5.

The emergence of a more virulent strain of *V. cholerae*, coupled with the increasing number of endemic and newly exposed countries suggests a growing need for a consistent vaccination strategy. Currently, there are 2 WHO pre-qualified vaccines for cholera: Dukoral<sup>®</sup> (SBL Vaccin AB, Stockholm, Sweden) and Shanchol<sup>®</sup> (Shantha Biotechnics Limited, Basheerbagh, India). Dukoral<sup>®</sup> contains killed *V. cholerae* (Inaba and Ogawa serotypes of *V. cholerae* O1) and recombinant (r) CTB, while Shanchol<sup>®</sup> contains the killed *V. cholerae* (serogroups O1 and O139) (20).

Due to the cross-reactivity of anti-CTB antibodies to heat labile enterotoxin (LTB), Dukoral<sup>®</sup> is also effective against enterotoxigenic *Escherichia coli* (ETEC), an advantage not offered by Shanchol<sup>®</sup>. On the other hand, Shanchol<sup>®</sup> is a less expensive cholera vaccine than Dukoral<sup>®</sup> because the latter includes costs related to rCTB, *i.e.*, recombinant production, a buffer to neutralize stomach acid to prevent rCTB degradation and additional storage space and logistics. In a vaccination cost analysis study performed in 2012, it was found to cost approximately US\$10 to purchase 2 doses of Dukoral<sup>®</sup> and approximately US\$3

to deliver those doses (21). However, these costs could be reduced by developing cost-effective rCTB production methods (see below) and formulating the vaccine in a solid oral dosage form able to pass through the stomach and dissolve in the small intestine (22).

Interestingly, a field trial performed in 1985 suggests that a whole cell-killed vaccine with CTB (WCB) may be more efficacious than a whole cell-killed vaccine without CTB (WC) (23). Children 2 to 10 years old were almost completely and significantly protected (92%) from cholera after 3 vaccinations with WCB compared to a non-significant 53% protection for WC for the first 6 months after vaccination. Hence, children were far better protected with the CTB-containing vaccine. In older populations (>10 years old) both vaccines showed similar protective efficacy over 6 months; the WCB vaccine protected 77% of the adults compared to 62% with the WC vaccine. Additionally, perhaps most importantly, the WCB vaccine significantly protected against severe cholera episodes (89% protective) *versus* no significant protection by the WC vaccine (44% protective). Lastly, within approximately the first 6 months following vaccination, the WCB vaccine significantly protected the recipients while WC vaccine recipients lost protective efficacy approximately 3 months after vaccination. This short-term enhanced protection could provide a significant implication for a reactive vaccination strategy to contain outbreaks. The same population was also tracked for 3 years following vaccination and differences between WCB and WC vaccination were further elucidated (24). Again, it was found that 2–5 year old children, who received all 3 vaccine doses, were

significantly protected when receiving the WCB vaccine for up to 2 years following vaccination when compared to the placebo group. At no point was WC vaccine significantly protective of the 2–5 year old cohort in this study. For up to 3 years following vaccination both WCB and WC protected study participants over the age of 5.

Additionally, the number of doses needed to see strong protection against cholera was another point of differentiation. WCB vaccination required 2 doses to provide significant protection while the same level of protection was not achieved with the WC vaccine until a third dose was administered. It should be noted that WCB contains non-recombinant CTB (purified from CT) and thus should not be confused with the currently available Dukoral<sup>®</sup>, which contains rCTB.

In this regard, a more recent work has been performed to evaluate the protective efficacy of Dukoral<sup>®</sup> in adults and children (25). The study by Alam *et al.*, divided children into 2 groups: young (median age 5) and older (median age 10) and had an adult group with a median age of 32. Significant antibody responses in all groups were seen 3 days following the first dose in all study groups and continued to day 42 in all groups. However at day 90, the next time point in the study, both groups of children lost the antibody response while the adult antibody response persisted until at least 270 days following the second vaccination. Additionally, a 2005 study in Mozambique showed that an rCTB whole cell-killed vaccine was able to protect at similar levels of the WCB vaccine used in Bangladesh (26). The results from this study also confirmed that the

vaccine containing rCTB may have improved protection in severe cases of cholera. Confounding these results, a field trial performed in Peru in 1994 is often reported as having negative results (increased cholera infection) in rCTB vaccine recipients (27). However, the study did report positive protection after a booster third dose was given just prior to the start of the next cholera outbreak season in Peru. Additionally, this study evaluated only 2 time points, 1 year and 2 year protection, which could have overlooked the early protection (<6 months after vaccination) observed previously with WCB (28). Lastly, the fact that a single booster provided protection during the second year of the study suggests that an rCTB containing vaccine does in fact protect against cholera outbreaks.

Shanchol<sup>®</sup> has been studied in both Bangladesh and Haiti; participants in both studies showed strong immune responses to the 2 dose vaccine regimen (20, 29). In 2012, Shanchol<sup>®</sup> was used in an outbreak in Guinea and found to be effective in protecting adults from cholera infection (30). These findings were thought to be in line with results seen with Dukoral<sup>®</sup>, but there was no rCTB vaccine group in this study to compare to. An advantage to Shanchol<sup>®</sup> is that it has been tested in children as young as 1 year old and protection has been noted in this young population (29). The lack of a large scale study comparing Shanchol<sup>®</sup> and Dukoral<sup>®</sup> makes any comparison difficult.

A recent paper may help elucidate the potential benefit of including rCTB in any cholera vaccine. Although mice do not develop cholera, a model of pulmonary *V. cholerae* infection has recently been established (31). In this model, severe pneumonia was induced in mice and was found to be fatal within



several days of inoculation with *V. cholerae*. Interestingly, mice vaccinated intranasally, twice with Dukoral<sup>®</sup> prior to *V.cholerae* challenge, were significantly protected compared to controls. Unvaccinated animals died within 24 h of the challenge while none of the mice vaccinated died for up to 7 days following challenge. Notably, Dukoral<sup>®</sup> without rCTB showed no protection in this model, while protection was restored upon inclusion of rCTB. These results provide unequivocal evidence that rCTB is essential in protecting mice from the lethal pneumonia induced by *V. cholerae* infection. Coupled with the earlier findings with WCB vaccines in the field trial, it is suggested that, in the case of cholera outbreaks, vaccines containing rCTB may provide immediate benefit to vaccine recipients that would not be seen in rCTB-free vaccines.

## **CTB AS A VACCINE ADJUVANT**

In addition to its toxic properties, CT is also known to have strong mucosal immunogenic properties that have been investigated for beneficial use as well as inducing an allergic response in animal models (32-37). CT has also been shown previously to have adjuvant potential when incorporated into mucosal vaccines (38-40). However, the toxicity of CT made its use in humans undesirable and work now focuses on removing the toxicity from the molecule while maintaining the adjuvant effect. The CTB subunit was previously shown to induce an immune response without the toxicity associated with the CTA subunit (41). CTB has proven to be a strong adjuvant to uncoupled antigens when administered via the nasal route but less so when administered orally (15, 42, 43). However, the nasal route of administration is not preferred due to the potential risk for developing Bell's palsy, which was found to be the case for *E. coli* enterotoxin B subunit (44-46). Fortunately, it was found that by coupling the antigen to CTB, a much stronger response is achieved via the oral administration route (47). We should also point out that the adjuvant potential of CTB has also been shown in large animal models, indicating that the adjuvant potential is scalable to higher species (48-50).

The utility of CTB becomes apparent when looking at the various disease states in which it has been used as an adjuvant: bacterial and viral infections, allergy, and diabetes have been targeted (51-53). Also, an interesting approach to resolving cocaine addiction has been attempted by binding rCTB to succinylnorcocaine, which has been tested in a Phase IIb randomized double-blind placebo-controlled trial (54, 55). The hypothesis behind the vaccine was that the

anti-cocaine antibodies may block the uptake of cocaine in the brain from the blood. While the results were inconclusive, with only ~40% of participants achieving inhibitory antibody concentrations in the blood, this study shows potential utility of CTB-based vaccines in addiction therapy. While antigen-CTB coupling has been most commonly achieved by chemical crosslinking to specific functional groups of amino acid residues or genetic fusion to the *N*- or *C*-terminus of CTB, an alternative approach has been seen in the literature that uses the CTA2 domain to link antigens to CTB (52, 56, 57). For example, this approach was used for a vaccine against West Nile virus, in which the domain III (DIII) region of the virus was used as the antigen genetically fused to the CTA2 domain (see Figure 1). The DIII-CTA2 protein was co-expressed with rCTB to form a chimeric CT-like molecule, DIII-CTA2/B (52). Intranasal delivery of DIII-CTA2/B in mice produced DIII-specific antibodies that could trigger complement-mediated killing. Although not as heavily studied as conventional CTB *C/N*-terminal fusion methods, the CTA2/B strategy may provide a useful means to develop a vaccine comprising a relatively large antigen.

For a general overview of the work on CTB as a vaccine adjuvant, readers are referred to thorough reviews published previously (41, 58, 59).

## **CTB IN INFLAMMATION**

Besides the mucosal vaccine adjuvant activity summarized above, recent studies have revealed that CTB can also induce anti-inflammatory and regulatory T cell responses. Indeed, the protein was shown to suppress immunopathological reactions in allergy and autoimmune diseases (reviewed in: (59)). In a mouse model, the airway administration of CTB ameliorated experimental asthma (60).

Furthermore, the anti-inflammatory and immunoregulatory effects of CTB are effectively conferred on bystander protein antigens that are chemically or genetically linked to CTB; oral administration of rCTB chemically cross-linked to a peptide from the human 60 kD heat shock protein was shown to mitigate uveitis of Behcet's disease in a Phase I/II clinical trial (61). Meanwhile, rCTB was also shown to mitigate the intestinal inflammation of Crohn's disease in mice and humans (59). Below, we will highlight some of these and a few other recent findings regarding CTB as an anti-inflammatory agent.

## **CTB's Anti-Inflammatory Activity in Various Inflammatory Diseases**

Type 1 Diabetes Mellitus induces cellular oxidative stress which leads to chronic inflammation and secondary effects such as: atherosclerosis, blindness, and stroke (62). CTB has been used to target multiple anti-inflammatory agents that alone were either short lived or could not effectively induce an immune response. An example of this comes from Odumosu *et al.*, who fused glutamic acid decarboxylase (GAD) to rCTB (GAD-rCTB) and showed suppression of dendritic cell activation in human umbilical cord blood isolated dendritic cells (63). Dendritic cells are often implicated in islet  $\beta$ -cell loss in Type 1 Diabetes so this presents an attractive therapeutic option. Additionally, the group showed that pro-inflammatory cytokines, IL-12 and IL-6, were down-regulated while IL-10 was significantly increased *in vitro* using dendritic cells. Another study was performed incorporating GAD with rCTB and a recombinant vaccinia virus (rVV) by Denes *et al.*, which co-administered the rVV-rCTB-GAD generated in their lab with Complete Freund's adjuvant (CFA) to see if multiple adjuvants could further enhance the immune response to the vaccine (64). Vaccination with both rVV-rCTB-GAD alone and CFA alone showed some measureable protection in the NOD mouse model of diabetes compared to control animals given PBS at approximately 39 weeks of age. However, when rVV-rCTB-GAD and CFA were combined, hyperglycemia was delayed further to 43 weeks of age. Overall, the study showed by combining the vaccines, NOD mice could be protected from hyperglycemia and pancreatic islet inflammation better than either vaccine alone.

CTB had previously been shown to protect against uveitis resulting from Behcet's disease in a clinical trial performed in 2004 (61). This work linked a T cell proliferative peptide (p336–351) to rCTB, which conferred protection on 5 of 8 patients following withdrawal of all immunosuppressive drugs. Other CTB conjugates have also been evaluated in a mouse model of uveitis and shown promise more recently (65). Shil and colleagues delivered two components of the Renin-angiotensin system (RAS) to the retina, ACE2 and Ang-(1–7) by fusing them to rCTB and administering them orally to mice. Protection was noted by decreased inflammatory cytokines (e.g., IL-6, IL-1 $\beta$ , and TNF- $\alpha$ ) and inflammation scoring. Additionally, these components were significantly elevated in the retina of the mice. This study showed that CTB can also be used as a delivery system to inflamed tissue and not just to enhance an immune response.

Atherosclerosis, an inflammatory condition, has recently become a target for rCTB fusion proteins (66-68). In 2010, a mouse model of atherosclerosis showed protection by nasal administration of an rCTB fusion protein (p210-CTB) (67). The p210 portion is derived from the apolipoprotein B-100 (ApoB100) peptide sequence as an alternative to a low density lipoprotein. Indeed this vaccination strategy reduced atherosclerotic lesion formation and provided some clues to mechanism. IL-10 was significantly upregulated by p210-CTB, while transforming growth factor- $\beta$  (TGF- $\beta$ ) was not, which led the authors to hypothesize that T regulatory 1 (T<sub>R</sub>1) cells may be responsible for the protection. However, FoxP3 was upregulated thus the authors could not rule out some level of protection from the FoxP3<sup>+</sup> T regulatory cell

population as well. Interestingly, T<sub>R</sub>1 cells are believed to play a more important role when immunity is conferred through nasal administration (69).

A second rCTB-linked protein targeting both ApoB100 and cholesteryl ester transfer protein (implicated in atherosclerosis pathogenesis) was explored more recently, in a proof of concept study, in which antibodies were detected in mouse serum to the target proteins (68). In this study, the route of administration was by foot pad injection, so it will be interesting to see if altering the route of administration will have impacts on the efficacy and/or mechanism of protection from atherosclerosis. Liver inflammation and fibrosis were also significantly blunted by an intranasal administration of a rCTB-Sm-p40 egg antigen immunodominant peptide fusion in mice following infection with *Schistosoma mansoni*, which results in schistosomiasis (70). This protection was associated with a significant increase in TGF- $\beta$  in the mesenteric lymph node (MLN) CD4 T cells and granuloma cells. The studies on atherosclerosis and this study suggest that CTB may have a compartmentalized effect on TGF- $\beta$  production in tissues, since both conjugates were administered intranasally, yet only the MLN CD4 T cells and liver granuloma cells showed elevated TGF- $\beta$ .

Organ transplantation can lead to rejection through inflammation. In a rat model of kidney transplantation, an anti-inflammatory D-amino acid decapeptide, RDP58, chemically conjugated to CTB was shown to enhance the survival time compared to the therapeutic compound alone (71). Allergic inflammation in mouse airways has also been shown to be reduced by CTB administration, not only in a

preventative sense but also in mice that have already been sensitized to airway inflammation (60).

Lastly, CTB has shown in animal models as well as clinical trials to be effective in decreasing inflammation in Inflammatory Bowel Disease (IBD). IBD is subcategorized into Crohn's disease and ulcerative colitis. In 2001, Boirivant *et al.* showed that oral administration of rCTB protected against Trinitrobenzene Sulfonic Acid (TNBS) induced intestinal inflammation, which is a mouse model resembling Crohn's disease (72). This finding was further explored to reveal that IL-12 and IFN- $\gamma$  were significantly downregulated by rCTB administration in TNBS induced colitis (73). In addition, rCTB inhibited both STAT-4 and STAT-1 activation and downregulated T-bet expression. These results showed a possible mechanism for protecting against inflammation by inhibiting Th1 cell signaling. The protection seen in the TNBS colitis model was confirmed in a human clinical trial, in which rCTB significantly decreased inflammation in mild to moderately active Crohn's disease (74). However, IFN- $\gamma$  did not correlate with the reductions in Crohn's disease activity index in the patients.

This might suggest that CTB reduced inflammation in humans through more than inhibition of Th1 cell signaling. On the other hand CTB's effect in ulcerative colitis, which is another form of IBD involving inflammatory signaling and pathogenesis that is different from that of Crohn's disease, is currently not known. As noted earlier in the atherosclerosis and liver fibrosis studies, CTB's anti-inflammatory potential seems to be mediated by different pathways despite having the same route of administration. In this regard, it is of particular interest to



investigate whether oral administration of CTB may have therapeutic potential in both Crohn's disease and ulcerative colitis.

## **Recombinant or Non-Recombinant CTB: Conflicting Results of CTB's Anti-Inflammatory Activity in *In Vitro* Experiments**

While a number of studies have reported the anti-inflammatory activity of CTB *in vitro* and *in vivo*, the quality of the CTB used in those studies has not been consistent, which may have had a significant impact on the results of some of those studies. Hence, before concluding this section, we would like to point out the potential influence that the quality of the CTB may have on the outcome of anti-inflammatory studies, particularly those using cell culture experiments. Many of the early studies have used non-recombinant CTB obtained from a commercial source, which is prepared from the CT holotoxin by chemical dissociation of CTA and CTB subunits. As a result, there is a trace amount of CT and CTA subunit remaining in the CTB product (75). In a conventional *in vitro* assay using the murine macrophage cell line RAW264.7, we found that a commercial CTB product (Sigma-Aldrich, St. Louis, MI, USA; C9903), which contains  $\leq 0.5\%$  of CT according to the datasheet provided, significantly inhibited the production of TNF $\alpha$  induced by lipopolysaccharides (LPS), while rCTB produced in *E. coli* (purified to  $>95\%$  homogeneous pentamer, with  $<0.003$  endotoxin unit/ $\mu\text{g}$ ) failed to show such an effect (Fig. 1.1A) (76). Notably, in this assay picomolar concentrations ( $<10$  ng/mL) of CT exerted strong anti-inflammatory activity (Fig. 1.2B). These results indicate that the trace amount of CT contamination in non-recombinant CTB products could have a major impact on results generated in similar assay systems. Hence, care should be taken when choosing the source of CTB for anti-inflammatory studies. It should be noted that some of the

groundbreaking studies showing CTB's anti-inflammatory activity outlined above, including human clinical studies, have used rCTB. Consequently, there is compelling evidence for the immunotherapeutic potential of rCTB in various inflammatory disorders.

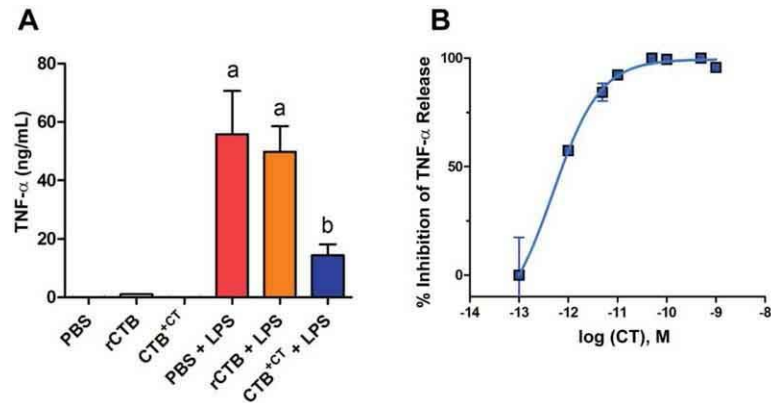


**Figure 1.2. CT, not rCTB, inhibits the release of TNF- $\alpha$  by Raw 264.7 cells stimulated with LPS.**

**A)** Commercial non-recombinant CTB containing a trace amount of CT (CTB+CT) significantly reduces the production of TNF- $\alpha$  due to LPS stimulation. Raw 264.7 cells were pretreated with 10  $\mu$ g/ml rCTB (produced in *E. coli* (76)), CTB+CT (Sigma-Aldrich, catalog no. C9903), or PBS, and a final concentration of 1  $\mu$ g/ml LPS was added and incubated for 24 hours. TNF- $\alpha$  levels in cell supernatants were determined using a commercial ELISA kit (eBioscience). Data represent the mean  $\pm$  SEM (n=4). a: P < 0.001, compared to PBS; b: P < 0.05, compared to PBS+LPS and rCTB+LPS (one-way ANOVA with Bonferroni multiple comparison tests). **B)** Picomolar levels of CT inhibit the production of TNF- $\alpha$ . Raw 264.7 cells were pretreated for 2 h with varying concentration of CT, and a final concentration of 0.1  $\mu$ g/ml LPS was added and incubated for 6 h. The 50% inhibitory concentration (IC<sub>50</sub>) of CT was determined by non-linear regression analysis (GraphPad Prism 5.0) to be 0.49 pM. Data represent the mean  $\pm$  SEM (n=2). The TNF- $\alpha$  level of PBS + LPS was 4516.8  $\pm$  791.1 pg/ml (mean  $\pm$  SEM; n=2).

## CONCLUSION

While first being recognized for its role in the delivery of the virulence factor of *V. cholerae*, the works highlighted here show CTB's broad utility as a cholera vaccine immunogen, vaccine adjuvant (through co-administration or conjugation), immune modulator and/or anti-inflammatory agent. This has led to the development of various rCTB expression systems in an effort to make the protein more efficient and widely available. Given that CTB appears to provide additional efficacy to killed bacteria-based cholera vaccines, development of alternative rCTB production and delivery methods may significantly contribute to cholera prevention and control. We have therefore developed a novel CTB variant that can be rapidly mass produced in *Nicotiana benthamiana* plants (CTBp) to aid in reactive vaccination in response to outbreaks (76). Also, because of the capacity to induce potent mucosal humoral immune responses, antigen-CTB fusion provides a promising strategy for vaccines against enteric pathogens and mucosally transmitted diseases.

On the other hand, the immunotherapeutic potential of CTB in inflammatory diseases warrants further investigations; despite a number of studies demonstrating CTB's anti-inflammatory effects, the underlying mechanism remains to be fully disclosed. This could be partly due to the inconsistent quality of CTB used in those studies and also attributed to different pathways altered by CTB, depending on the route/mode of administration and inflammatory conditions. Since many inflammatory diseases involve chronic and recurring inflammation, long-term immunological and toxicological impacts of repeated CTB administration need to be

investigated. In this regard, the impacts of orally administered CTB on the GI tract are poorly understood despite its use in an internationally licensed oral cholera vaccine. Our investigation in the following chapters will therefore focus on unveiling the global changes and elucidating their mechanisms following oral administration of CTB. The results help fill the above-mentioned gaps in our knowledge about CTB, which in turn may help to pinpoint further use cases for a protein that has shown potential utility in many disease states.

CHAPTER 2: ORAL ADMINISTRATION OF CTB<sub>p</sub> SIGNIFICANTLY  
IMPACTS THE GASTROINTESTINAL MUCOSA

## INTRODUCTION

As discussed in Chapter 1, CTB is a non-toxic, GM1-ganglioside-binding subunit of CT, the main virulence factor of *Vibrio cholerae*. CTB consists of a pentameric structure of approximately 55 kDa and is currently used in the World Health Organization (WHO)-prequalified oral cholera vaccine Dukoral®, due to its capacity to induce CT-neutralizing antibodies (77-79). Oral administration of CTB has also been shown to produce a strong antibody response in the gut and systemic compartments (76, 80). A number of studies have highlighted CTB's strong immunogenicity in other mucosal surfaces. For instance, vaginal administration of CTB revealed that two doses of CTB significantly induced specific IgA and IgG in cervical secretions and serum (81). In the lungs, CTB was able to prevent allergic inflammation by induction of IgA specific to ovalbumin (60). Thus, the induction of the antibody response at mucosal surfaces has been well studied. However, there is little information regarding the global impacts of CTB on targeted mucosa, including the GI tract upon oral administration.

Previously, our lab has attempted to produce recombinant CTB in plants (*Nicotiana benthamiana*) using a plant virus vector overexpression system, with the aim of economically manufacturing the protein at a large scale to facilitate global cholera vaccination (76). When the original CTB was expressed in *N. benthamiana*, the protein was found to be *N*-glycosylated due to the presence of eukaryote-common *N*-glycosylation signal at the near N-terminus of CTB, leading to some concern of an allergenic response associated with plant-specific

glycoforms (82). Therefore, we replaced the responsible asparagine residue with a serine to eliminate the glycosylation. An additional modification to the protein was the addition of a hexapeptide SEKDEL sequence to the C-terminus for endoplasmic reticulum (ER) retention via the KDEL receptor, which was critical for high-level accumulation in *N.benthamiana* leaf tissue. Despite these modifications, the plant-made aglycosylated CTB variant (CTBp) maintained GM-1-ganglioside binding affinity and oral immunogenicity for the induction of anti-cholera holotoxin neutralized antibodies, which were similar to those of original CTB. These results demonstrate that CTBp is a viable alternative to *E. coli*-produced recombinant CTB that is currently used in Dukoral® Vaccine. The efficient plant-based production of CTBp facilitates the extensive investigation of immunomodulatory mechanisms previously undescribed for CTB and exploration of its potential pharmaceutical uses besides cholera vaccination. Hence, we used CTBp in all the work described in this dissertation.

In this chapter, we characterize the global impact of oral CTBp administration on the GI tract by employing flow cytometry to elucidate changes in lymphocyte populations in several immune compartments in mice. In addition, microarray analysis was performed on RNA samples from the small intestine and colon to determine if CTBp altered gene expression along the GI tract.



## **METHODS**

### *Animals*

8 week old C57BL/6J female mice were obtained from Jackson Laboratories (Bar Harbor, Maine) and allowed to acclimate for one week. Animals were housed according to the University of Louisville's Institutional Animal Care and Use Committee standards.

### *Study Design and Dosing Regimen*

For the characterization of the global impacts of CTBp oral administration, animals were orally administered with PBS or 30  $\mu$ g CTBp twice at a 2-week interval after neutralization of stomach acids with a sodium bicarbonate solution, as described previously (76). CTBp was produced in *N. benthamiana* and purified to >95% homogeneity as a pentamer molecule with an endotoxin level of <1 endotoxin units (EU)/mg, as described previously (76). One or two weeks after the second dose, mice were sacrificed using carbon dioxide inhalation followed by a thoracotomy. Fecal, colon, small intestine, spleen, mesenteric lymph nodes and Peyer's patches were collected. These specimens were used for flow cytometry and gene expression analyses described below.

### *Lymphocyte Isolation*

Mesenteric lymph nodes, spleens, colon, and small intestine were removed from the animals at sacrifice. Peyer's patches were isolated from the small intestines prior to isolation of lymphocytes from the small intestine. Lamina propria lymphocytes (LPLs) were isolated from the colons and small intestines by using a series of washing and collagenase steps. Epithelial cells, mucus and fat tissue were removed by incubating with EDTA at 37°C. The colon and small intestine were cut into small pieces and incubated with collagenase at 37°C Cell suspensions. Mesenteric lymph node immune cells were isolated by mincing the tissue and using a syringe plunger to release the cells into suspension. The cell suspensions were filtered, sequentially, through 100 and 40 µm cell strainers. Cells were counted in a hemocytometer. Splenocytes were isolated by crushing the spleens on metal mesh and separating the supernatant. ACK buffer was used to lyse red blood cells and following several washes the cells were filtered through a 70 µm cell strainer. Peyer's patch lymphocytes were isolated by chopping up the Peyer's patches with fine surgical scissors and incubating the pieces in collagenase at 37°C. After allowing the suspension to settle, the supernatant was removed and saved for lymphocyte isolation. The collagenase step was repeated and the second suspension was isolated. The suspensions were centrifuged and supernatants were discarded. After a second wash the cells were combined and filtered through a 70 µm cell strainer.

### *Flow Cytometry*

Cells were stained using antibodies and a Cell staining kit (Catalog no. 00-5523-00) from eBiosciences, Inc. (San Diego, CA). Briefly, tubes containing  $1 \times 10^6$  cells were washed with flow cytometry staining buffer 2 times. Fc Block was added to each tube in flow cytometry staining buffer (supplied in kit) for 10 minutes.

For adaptive immune cell populations, surface staining antibodies were then added to each tube (anti-CD3-FITC, anti-CD4-APC-Cy7, anti-CD25-PerCP) and allowed to incubate at  $4^\circ\text{C}$  for 30 minutes. After removing excess antibodies, fixation/permeabilization buffer (supplied in kit) was added to the tubes and incubated overnight. The following morning the tubes were washed with permeabilization buffer 2 times and again incubated for 10 minutes with Fc block. Internal cell antibodies (Gata3-PE, T-Bet-PE-Cy7, FoxP3-APC, IL-17-eFlour450) were added to each tube and incubated for 30 minutes at  $4^\circ\text{C}$ . The tubes were washed 2 times with permeabilization buffer (supplied in kit) and finally cells were suspended in flow cytometry staining buffer.

For innate immune cell populations, surface staining antibodies were added to each tube (CD19-APC, CD3-FITC, CD49b-PE, F4/80-PeCy7, CD11c-PerCP-Cy5.5, CD8-APC-eFluor 780, and CD45-eFlour450) and incubated at  $4^\circ\text{C}$  for 30 minutes. After removing excess antibodies, fixation buffer was added to the tubes and incubated overnight. The cells were washed 2 times with flow cytometry staining buffer and resuspended in flow cytometry staining buffer. Events ( $1 \times 10^5$ ) were counted on a BD FACSCanto™ II and analyzed with the BD FACSDiva Software v6.1.3.

### *F4/80+ immunohistochemistry*

Colons were removed and washed with PBS. A portion of the distal colon was fixed with paraformaldehyde overnight and stored in 70% Ethanol until paraffin embedding and sectioning. Sections were deparaffinized with Citrisolv and rehydrated through several ethanol washing steps ending with incubation in distilled water. Antigen retrieval was performed overnight with a 2100 Retriever (Electron Microscopy Sciences) using Buffer B designed specifically for the Retriever. Tissue sections were blocked for endogenous peroxidase, avidin, biotin, and serum from the animal in which the secondary antibody was raised. Primary antibody (F4/80; ab111101) was incubated with the tissue sections for 2 hours at room temperature. The Vectastain Elite ABC kit (rabbit anti-goat; Vector Labs) was used to label the primary antibody. F4/80+ cells were visualized with the ImmPACT DAB Substrate Kit (Vector Labs) and then dehydrated through an ethanol gradient and finally incubated with Citrisolv. Sections were scanned using a Aperio ScanScope CS (Leica Biosystems) and positive cells were counted in 10 representative sections (40x magnification) from each colon. The 10 sections were averaged and that was the score for each animal.

### *RNA Isolation*

Sections from the small intestine and distal colon were stored in *RNAlater*<sup>™</sup> (Qiagen, Valencia, CA) at -20°C until RNA was isolated. Colon tissue (approximately 14 mg) was placed in QIAzol lysis reagent in a 2.0 mL conical bottom centrifuge tube with Zirconia/Silica beads. A Bead Bug<sup>™</sup> (Catalog no.

S8452-SK, Denville Scientific Inc., MA) was used to homogenize the tissue. An RNeasy<sup>®</sup> Microarray Tissue Kit from Qiagen (Catalog no. 73304) was used to purify the RNA from the tissue homogenate. RNA was stored at -80°C until use.

#### *Microarray gene expression analysis*

Total RNA was amplified and labeled following the Affymetrix (Santa Clara, CA) standard protocol for whole transcript expression analysis, followed by hybridization to Affymetrix Mouse Gene 2.0 ST<sup>®</sup> arrays. The arrays were processed following the manufacturer recommended wash and stain protocol on an Affymetrix FS-450 fluidics station and scanned on an Affymetrix GeneChip<sup>®</sup> 7G scanner using Command Console 3.3. The resulting .cel files were imported into Partek Genomics Suite 6.6 and transcripts were normalized at the gene level using RMA as normalization and background correction method (83). Contrasts in a 1-way ANOVA were set up to compare the treatments of interest.

#### *Quantitative RT-PCR gene expression analysis*

Gene expression was carried out by qPCR using quality verified by Nanodrop 1000 (Thermo Scientific) RNA samples. First strand cDNA was obtained from reverse transcription of 150 ng RNA using a SUPERSCRIPT VILO cDNA synthesis kit (Life Technologies) according to the manufacturer's instructions. Template cDNA were added to a reaction mixture containing 10 µl of 2×TaqMan<sup>®</sup> Fast Advanced Master Mix (Life Technologies) and endonuclease free water to 20 µl and loaded in TaqMan<sup>®</sup> Array Standard 96 well Plates (Applied Biosystems). These plates contain pre-spotted individual TaqMan<sup>®</sup>

Gene Expression probes for the detection of genes of interest as well as the house keeping genes *18S*,  $\beta$ -*actin* (ACTB), and *GAPDH* (Table 2.1). PCR amplification was carried out on a 7900HT Fast Real-Time PCR System (Applied Biosystems) with the following conditions: 95°C, 20 min; 40 cycles (95°C, 1 min); 20 min at 60°C. The 7500 Software v2.0.6 (Applied Biosystems) was used to determine the cycle threshold (Ct) for each reaction and derive the expression ratios relative to control. Wound healing pathway analysis was performed with a RT2 Profiler PCR Mouse Wound Healing Array (Cat. No. PAMM-121Z) (Qiagen) under the same conditions described above.

**Table 1.1 Gene Identity for qPCR analysis**

| Gene Name   | Gene ID | Entrez Gene ID |
|---|---------|----------------|
| Angiogenin, ribonuclease A family, member 4             | Ang4    | 219033         |
| Angiopoietin 1  | Angpt1  | 11600          |
| ATP-binding cassette, sub-family A (ABC1), member 1     | Abca1   | 11303          |
| Cathepsin K   | Ctsk    | 13038          |
| Collagen, type 1, alpha 1                               | Col1a1  | 12842          |
| Collagen, type 1, alpha 2                               | Col1a2  | 12843          |
| Collagen, type 3, alpha 1                               | Col3a1  | 12825          |
| Collagen, type XIV, alpha 1                             | Col14a1 | 12818          |
| Decorin   | Dcn     | 13179          |
| Malate dehydrogenase 1, NAD                             | Mdh1    | 17449          |
| Matrix Metalloproteinase 2                              | Mmp2    | 17390          |
| Mitogen-activated protein kinase kinase kinase kinase 4 | Map4k4  | 26921          |
| SMAD family member 6                                    | Smad6   | 17130          |
| Tissue inhibitor of metalloproteinase 4                 | Timp4   | 110595         |
| Transgelin  | Tagln   | 21345          |

### *Microbiome analysis*

Fecal samples were collected at the end of the acclimation period and at the time of study termination. Bacterial DNA was isolated using the PowerFecal® DNA Isolation Kit (Mo Bio Laboratories, Inc.). Briefly, fecal samples were added to a bead tube with solution and lysed with a bead beater. Through a series of centrifugation and elution steps Fecal DNA was isolated. DNA concentration was

determined using the Quant-iT dsDNA Broad-Range Kit (Life Technologies). Samples were then sent to Second Genome, Inc. for analysis. Upon arrival, samples were enriched for bacterial 16S V4 rDNA region by utilizing fusion primers designed against conserved regions and tailed with sequences to incorporate Illumina flow cell adapters and indexing barcodes. Amplified products were concentrated using a solid-phase reversible immobilization method and quantified by electrophoresis using an Agilent 2100 Bioanalyzer®. Samples were loaded into a MiSeq® reagent cartridge and then loaded into the instrument. Amplicons were sequenced for 250 cycles with the MiSeq instrument. Second Genome's PhyCA-Stats™ analysis software package was used to analyze the results.

### *Statistics*

Graphs were prepared and analyzed using Graphpad Prism version 5.0 (Graphpad Software). To compare two data sets, we conducted an unpaired, two-tailed Student's *t* test. To compare three or more data sets, we conducted a one-way ANOVA with a Bonferroni post-test.

## RESULTS

### *Colon lamina propria leukocyte profile was significantly altered by CTBp*

CTB is a strong mucosal immunogen and induces a robust mucosal antibody response upon oral administration (47, 84); therefore, we characterized the immune cell populations in various immune compartments in CTBp-vaccinated mice. We evaluated both innate and adaptive immune cell populations in the small intestine lamina propria and colon lamina propria, mesenteric lymph node, Peyer's patches and spleen using flow cytometry. For this analysis, mice were given PBS or 30 µg CTBp, orally, twice separated by a two week interval, the standard regimen used for oral cholera vaccination (76), and sacrificed one or two weeks after the second dose. We designed two panels of markers, based on the literature, in order to evaluate innate and adaptive immune cell populations (Table 3.1) (85, 86).



**Table 2.1. Flow Cytometry Cell Type Marker Strategy.**

| Cell Type             | Cell Subtype         | Surface Markers used | Internal Markers Used |
|-----------------------|----------------------|----------------------|-----------------------|
| Adaptive Immune Cells |                      |                      |                       |
|                       | T Helper 1           | CD3+CD4+             | Tbet+                 |
|                       | T Helper 2           | CD3+CD4+             | Gata3+                |
|                       | T Regulatory         | CD3+CD4+CD25+        | FoxP3+                |
|                       | T Helper 17          | CD3+CD4+             | ROR $\gamma$ T+       |
|                       | CD8+ T Cells         | CD45+CD3+CD8+        |                       |
|                       | B Cells              | CD45+CD19+           |                       |
| Innate Immune Cells   |                      |                      |                       |
|                       | Natural Killer Cells | CD45+CD49b+          |                       |
|                       | Dendritic Cells      | CD45+CD11c+          |                       |
|                       | Macrophages          | CD45+F4/80+          |                       |

Overall, the immune profiles were not significantly affected in mesenteric lymph nodes or spleen at either time point (Fig. 2.1 through 2.4). One week after CTBp administration, a significant increase of the B cell population (CD45<sup>+</sup>CD19<sup>+</sup>) was observed in Peyer's patches, whereas T-regulatory (FoxP3<sup>+</sup>CD25<sup>+</sup>) and T<sub>H</sub>1 (TBet<sup>+</sup>) cells were significantly increased in lamina propria of colon and small intestines, respectively, compared to the PBS group (Fig. 2.1 and 2.2). In addition, there was a trend of increase in CD8<sup>+</sup> T cells ( $P = 0.0667$ ; Fig. 2.1) in the small intestine. However, these changes did not persist through the following week (Fig. 2.3, 2.4).

Meanwhile, subsets of innate immune cell populations in the lamina propria of colon, but not of small intestine, significantly increased two weeks post

CTBp oral administration (Fig. 2.5B); macrophages (F4/80<sup>+</sup>), dendritic cells (CD11c<sup>+</sup>) and natural killer cells (CD49b<sup>+</sup>) were significantly increased when compared to the control PBS group. The increase of these cell types was associated with a relative decrease in B cells within CD45<sup>+</sup> cell population (Fig. 2.5A, B). The increase in macrophages in colon lamina propria was confirmed by immunohistochemistry analysis in CTBp treated mice compared to the PBS-fed control mice despite the lack of abnormality or inflammation in the mucosa (Fig. 2.5C).

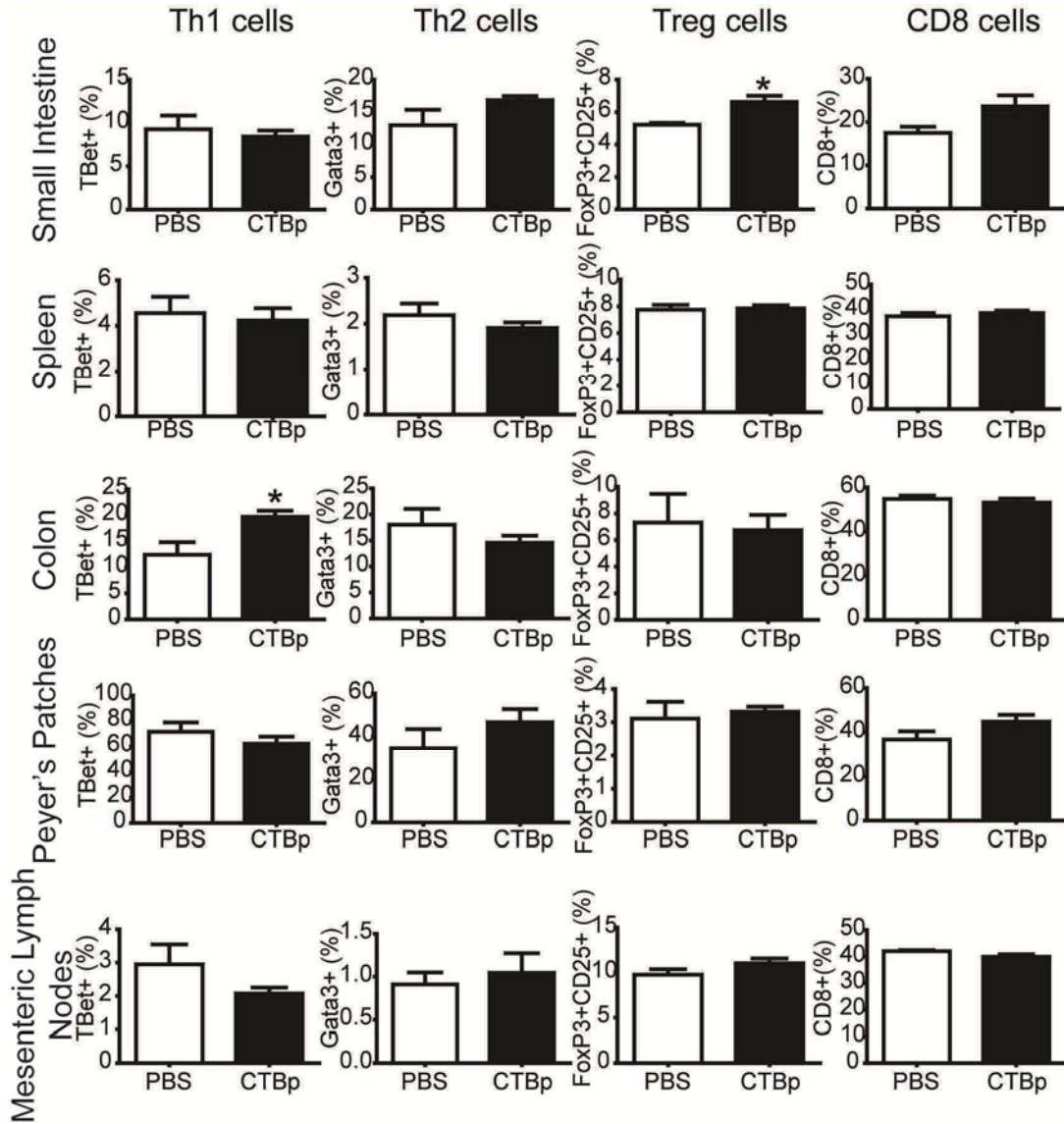


**Figure 2.1. T cell populations in different lymphoid tissues one week after the second CTBp or PBS oral administration.**

Animals were orally administered twice at a two-week interval with PBS or 30  $\mu$ g CTBp and one week later the mice were sacrificed. Small intestine and colon lamina propria, Peyer's patches, mesenteric lymph nodes, and spleen lymphocytes were isolated after several wash steps and collagenase incubation steps as necessary. CD4<sup>+</sup> and CD8<sup>+</sup> cells gated on T lymphocyte subpopulation (CD45<sup>+</sup>CD3<sup>+</sup>). Data are presented as mean  $\pm$  standard error of the mean (SEM) of at least four biological replicates comprised of two pooled mice each. Unpaired t test was performed with \* P < 0.05 compared to PBS group.

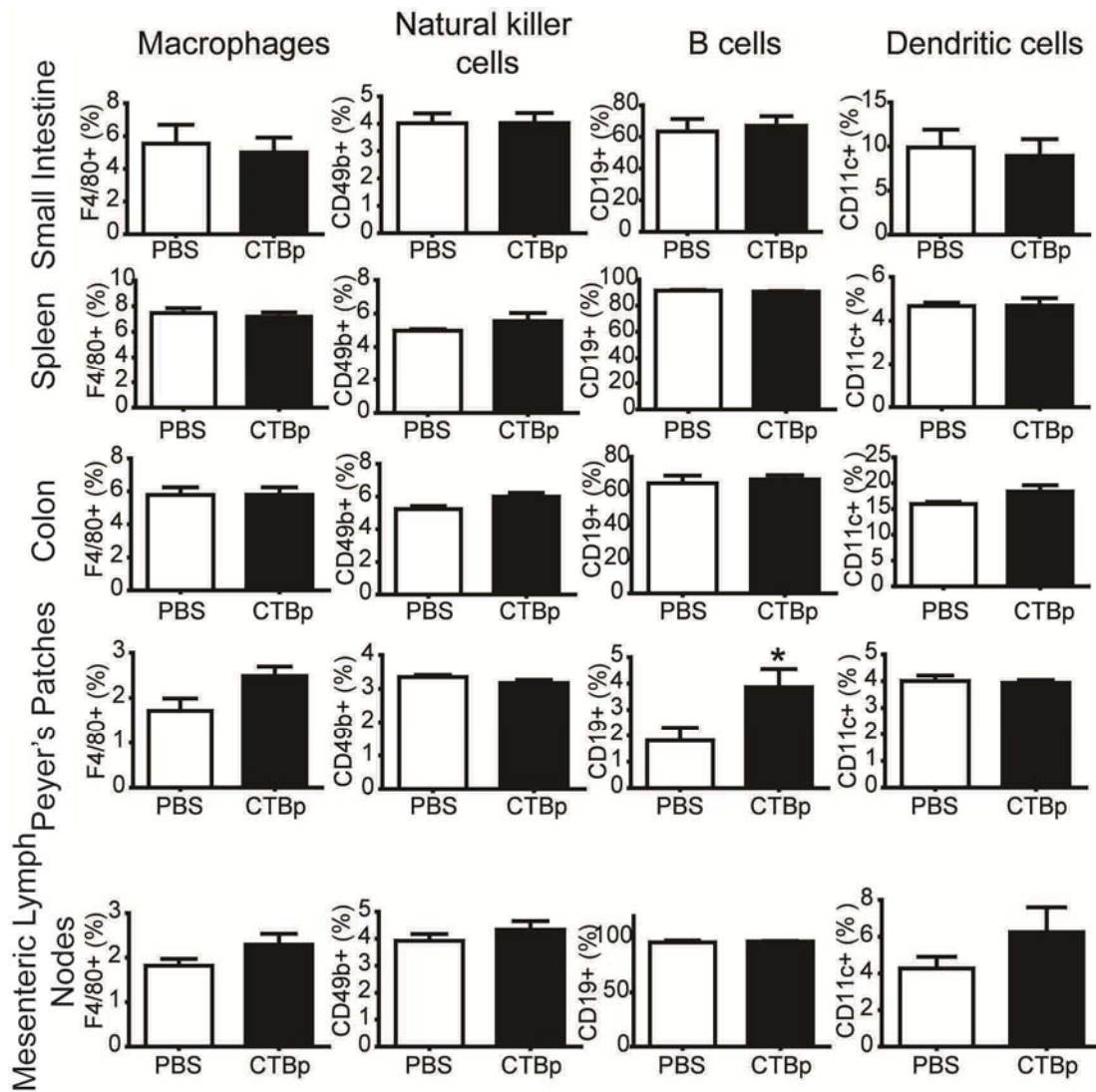


**Figure 2.2. CD45<sup>+</sup> immune cell populations in different lymphoid tissues one week after the second CTBp or PBS oral administration.**

Animals were orally administered twice at a two-week interval with PBS or 30  $\mu$ g CTBp and one week later the mice were sacrificed. Small intestine and colon lamina propria, Peyer's patches, mesenteric lymph nodes, and spleen lymphocytes were isolated after several wash steps and collagenase incubation steps as necessary. CD45<sup>+</sup> cells were further divided into B (CD19<sup>+</sup>), macrophage (F4/80<sup>+</sup>), dendritic (CD11c<sup>+</sup>) and natural killer (CD49b<sup>+</sup>) subpopulations. Data are presented as mean  $\pm$  standard error of the mean (SEM) of at least four biological replicates comprised of two pooled mice each. Unpaired t test was performed with \*  $P < 0.05$  compared to PBS group.

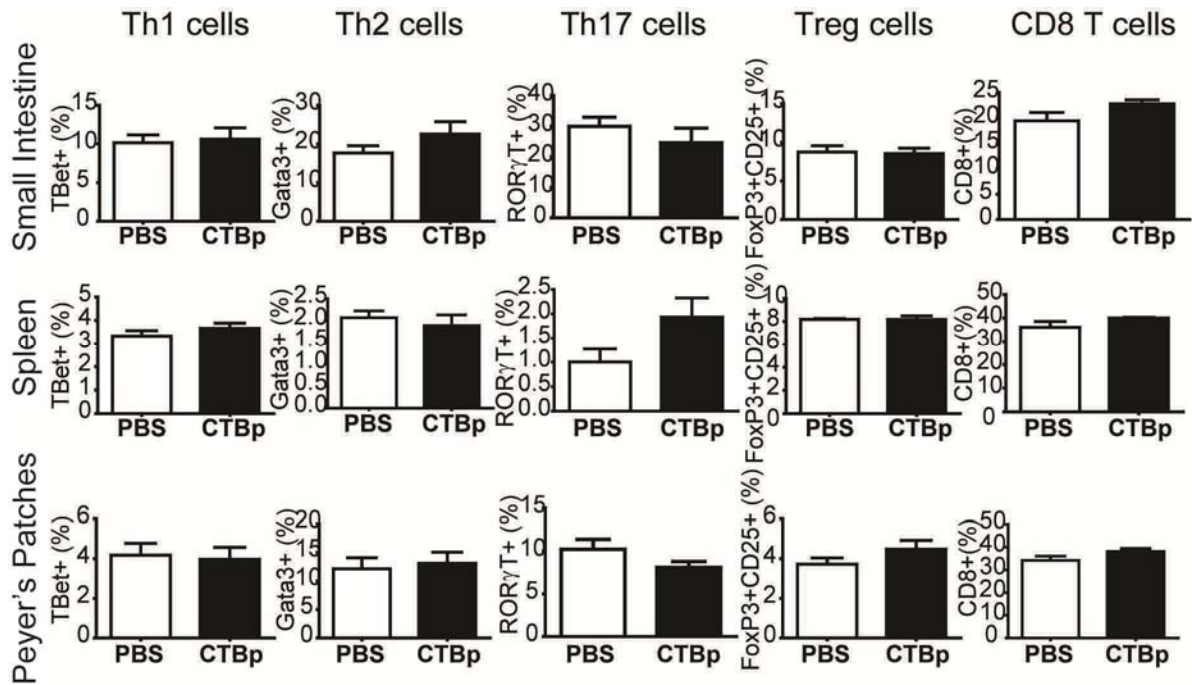


**Figure 2.3. T cell populations in different lymphoid tissues two weeks after the second CTBp or PBS oral administration.**

Animals were orally administered twice a two-week interval with PBS or CTBp and two weeks later the mice were sacrificed. Small intestine lamina propria, Peyer's patches, and spleen lymphocytes were isolated after several wash steps and collagenase incubation steps as necessary. CD4<sup>+</sup> and CD8<sup>+</sup> cells gated on gated on T lymphocyte subpopulation (CD45<sup>+</sup>CD3<sup>+</sup>). Data are presented as mean  $\pm$  standard error of the mean (SEM) of at least four biological replicates comprised of two pooled mice each. Unpaired t test was performed with \*P < 0.05 compared to PBS group.

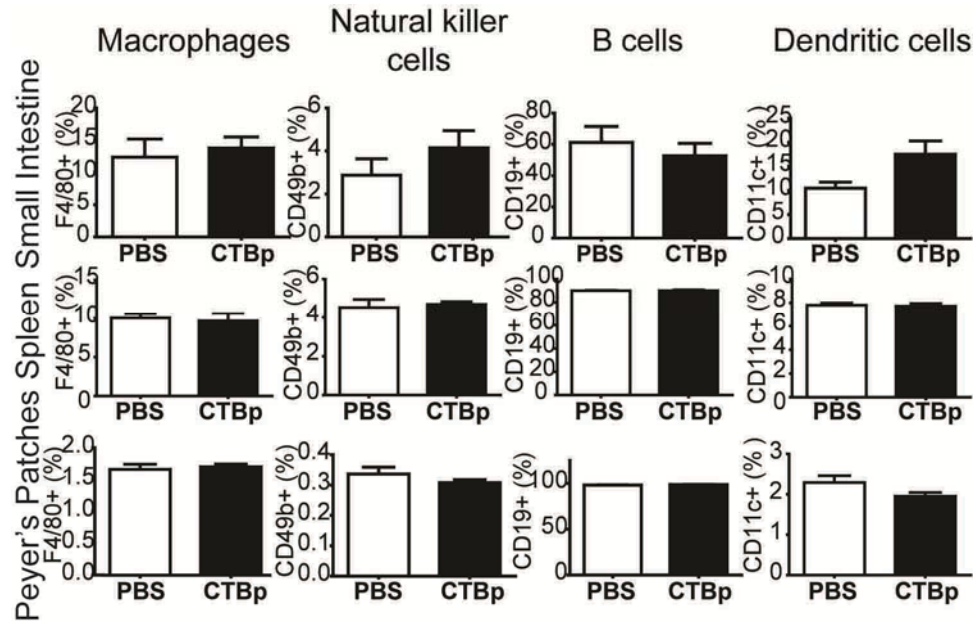


**Figure 2.4. CD45+ gated Immune cell populations in different lymphoid tissues two weeks after the second CTBp or PBS oral administration.**

Animals were orally administered twice a two-week interval with PBS or CTBp and two weeks later the mice were sacrificed. Small intestine lamina propria, Peyer's patches, and spleen lymphocytes were isolated after several wash steps and collagenase incubation steps as necessary. CD45+ cells were further divided into B (CD19+), macrophage (F4/80+), dendritic (CD11c+) and natural killer (CD49b+) subpopulations. Data are presented as mean  $\pm$  standard error of the mean (SEM) of at least four biological replicates comprised of two pooled mice each. Unpaired t test was performed with \*P < 0.05 compared to PBS group.

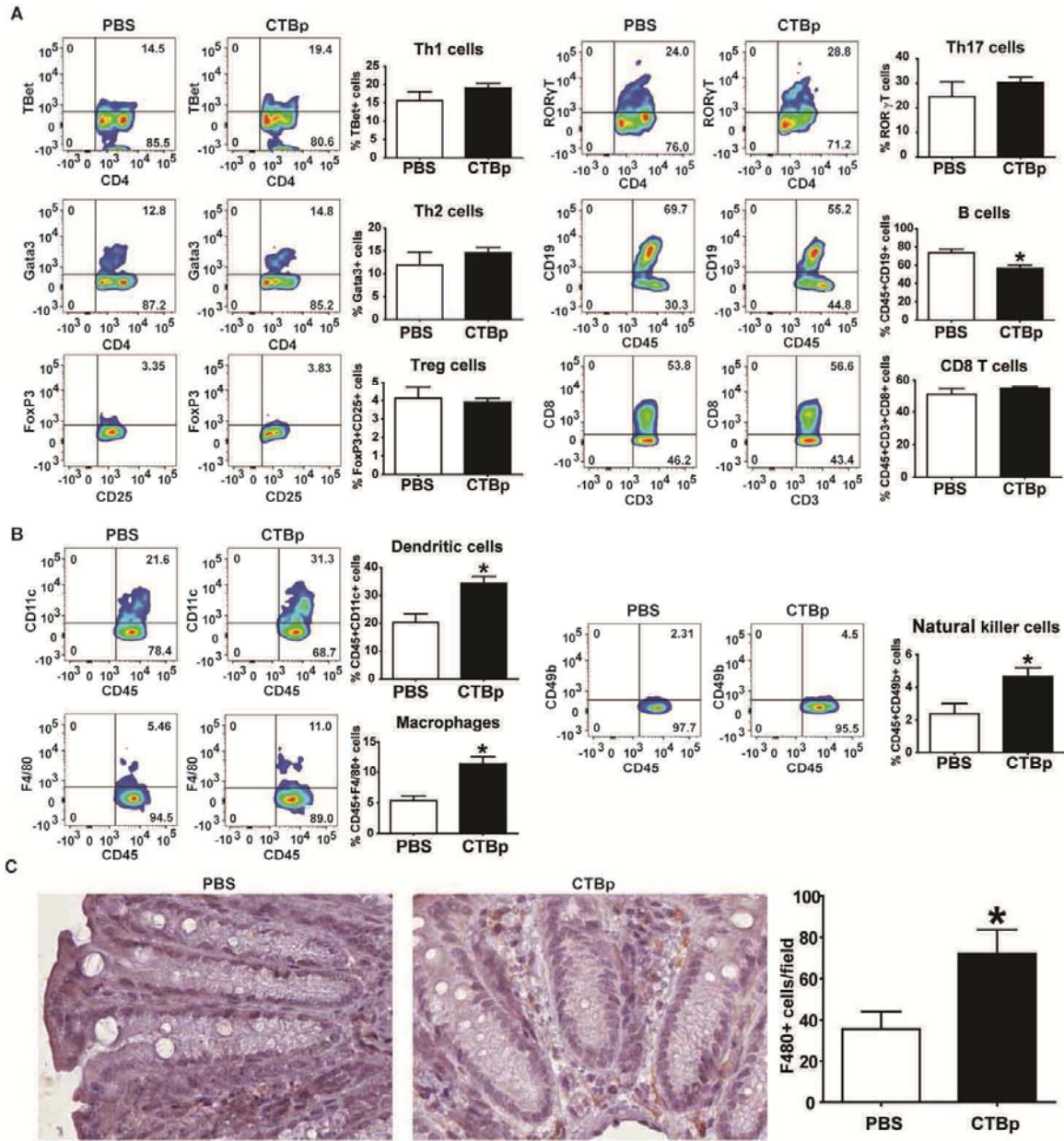


**Figure 2.5. CTBp significantly alters the Immune Cell profile in the colon.**

Animals were vaccinated twice at a two-week interval with PBS or CTBp and two weeks later the mice were sacrificed. Colon lamina propria leukocytes were isolated and stained for surface and internal markers specific for immune cell subtypes. CD4+ and CD8+ cells gated on T lymphocyte subpopulation (CD45+CD3+). Additionally, CD45+ cells were further divided into B (CD19+), macrophage (F4/80+), dendritic (CD11c+) and natural killer (CD49b+) subpopulations. Dot plots are representative samples taken from each group. Data are presented as mean  $\pm$  standard error of the mean (SEM) of at least four biological replicates comprised of two pooled mice each. Unpaired t test was performed with \*  $P < 0.05$  compared to PBS group. **A**) Adaptive immune cell populations in the colon lamina propria. **B**) Innate immune cell populations in the colon lamina propria. **C**) Immunohistochemistry analysis of macrophage (F4/80+) cells in the distal colon lamina propria isolated from mice 2 weeks post the second CTBp oral administration. Paraffin embedded colon cross sections were incubated with F4/80 primary antibody (1:100 dilution) and a biotinylated secondary antibody. After addition of a Horseradish peroxidase (HRP) and 3,3'-diaminobenzidine tetrahydrochloride solution (DAB), positive cells were counted in 10 high power fields per section and averaged for each colon. Mean  $\pm$  SEM is shown. Unpaired t test was performed with \*  $P < 0.05$  compared to PBS group. Animals per group: PBS (n = 6) and 30  $\mu$ g CTBp (n = 7)

*CTBp has a more pronounced effect on colon gene expression than small intestine*

Next, we performed microarray analysis of transcripts isolated from the small intestine and colon to determine if CTBp affected gene expression in the GI tract. A heat map was generated to compare the gene expression profiles in colon and small intestine specimens. We followed the same dosing regimen used to profile the immune cell populations and sacrificed the animals two weeks after the second dose; to further evaluate the time point of greatest change in immune cell populations shown above.

Orally administered CTBp had profound impacts on the gene expression profile of the entire intestinal tract (Fig. 2.6, Fig. 2.7). However, while gene expression profiles in the small intestine samples clustered relatively tightly, colons from CTBp-treated mice showed a completely separated pattern compared with the other samples (Fig. 2.7A). At a global level, 871 genes were significantly altered in the colon between CTBp and PBS groups ( $P < 0.01$ ; one-way ANOVA), while ~5 fold less (184) genes were significantly altered in the small intestine (Fig. 2.7B). Of these significant genes, 539 were induced and 332 were suppressed in the colon. By comparison, the small intestine was fairly evenly split between induced and suppressed genes, with 97 and 87 altered genes, respectively, and there was no overlap with genes affected in the colon.



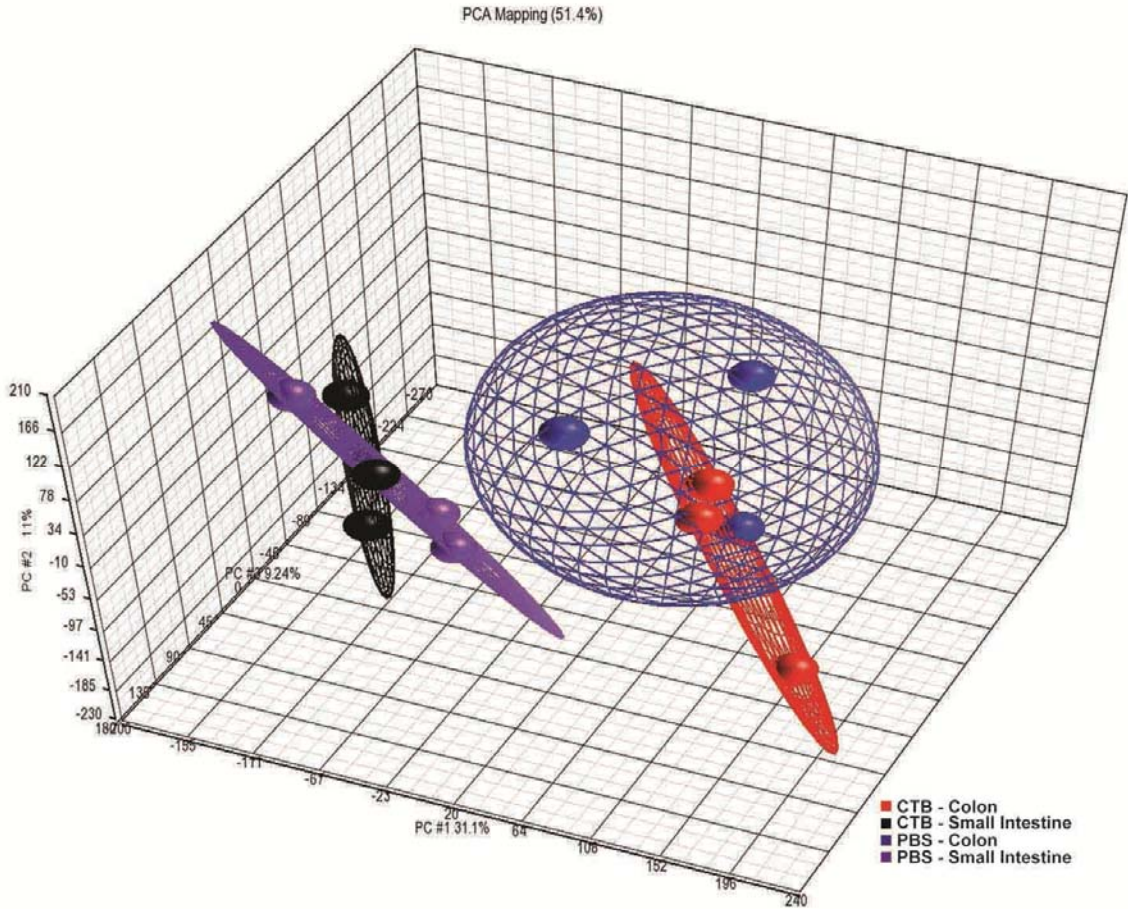


**Figure 2.6. Principal coordinate analysis revealed separation of GI tract gene expression profiles of mice vaccinated with PBS and CTBp.**

PBS or CTBp were administered twice to mice at a two-week interval. Two weeks after the final dose, animals were sacrificed and the small intestine and colon was removed. RNA was purified from small intestine and colon tissue sections. Total RNA was amplified and labeled then whole transcript expression analysis was performed as described in Materials and Methods. Principal coordinate analysis was performed using Partek Genomics Suite 6.6 (St. Louis, MO). N = 3 for all groups.

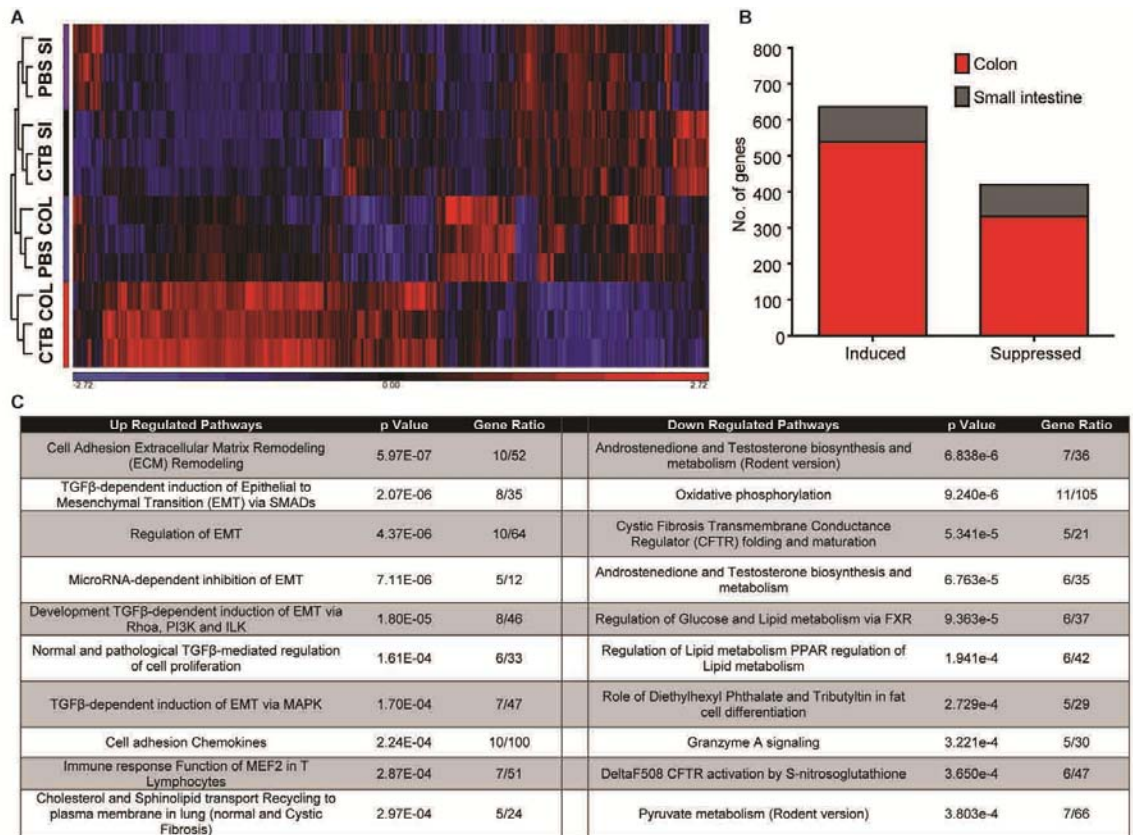


**Figure 2.7. TGFβ-dependent pathways are significantly altered by CTBp in the colon**

PBS or CTBp were administered twice to mice at a 2 week interval. Two weeks after the final dose animals were sacrificed and the small intestine and colon were removed for RNA purification. Total RNA was amplified and labeled then whole transcript expression analysis was performed. **A**) Heat map showing differentially expressed genes in the small intestine and colon following PBS or CTBp administration. **B**) Significantly altered genes in the colon and small intestine following PBS or CTBp administration. Significance was determined as p value of < 0.01. **C**) Ten most significantly affected pathways by CTBp administration in the colon as determined by MetaCore™ ontologies enrichment analysis using a P < 0.01 and fold change of < -1.2 or > 1.2.

### *CTBp enhances TGFβ-associated gene expression pathways in the colon*

We used the pathway analysis software in MetaCore™ (version 6.22 build 67265) to dissect gene expression alterations in the colon after CTBp administration. Extracellular matrix (ECM) remodeling and epithelial to mesenchymal transition (EMT) pathways were among the most significantly induced pathways by CTBp oral administration. In particular, TGFβ-dependent pathways heavily populated the most significantly induced (Fig. 2.7C). Indeed, when evaluating individual gene expression from the microarray analysis *Tgfβ1*,

*Tgfβ11* receptor, and *Smad4* are significantly induced by CTBp oral administration (Fig. 2.8). These results suggest that CTBp may facilitate epithelial wound healing (87, 88). By contrast, such strong induction of TGFβ-related pathways was not observed in the small intestine. Suppressed pathways in the colon epithelium included several metabolic pathways, cystic fibrosis transmembrane conductance regulator (CFTR) pathways, and an apoptosis associated pathway. Genes associated with lipid, bile acid, pyruvate, and androstenedione and testosterone metabolic pathways were significantly blunted by CTBp. *Hspa5*, *Hspa8*, *Hsp90aa1*, and *Stip1*, which are implicated in the progression of colon cancer, were significantly suppressed in several pathways (89-94). To confirm microarray data, quantitative real-time-PCR (qPCR) was performed on selected induced (i.e., collagen, decorin, mitogen-activated protein KKKK 4, and tissue inhibitor of metalloproteinase 4), suppressed (malate dehydrogenase 1 and angiogenin), or unaltered genes (ATP binding cassette and SMAD family member 6) and a high agreement between microarray and qPCR results was obtained (Fig. 2.9). Notably, a wound healing pathway-focused qPCR analysis revealed that many key genes, including: *Col1a1*, *Col1a2*, *Col3a1*, *Col14a*, *Mmp2*, *Ctsk*, *Tagln*, and *Angpt1* were significantly upregulated by CTBp oral administration (Fig. 2.10).

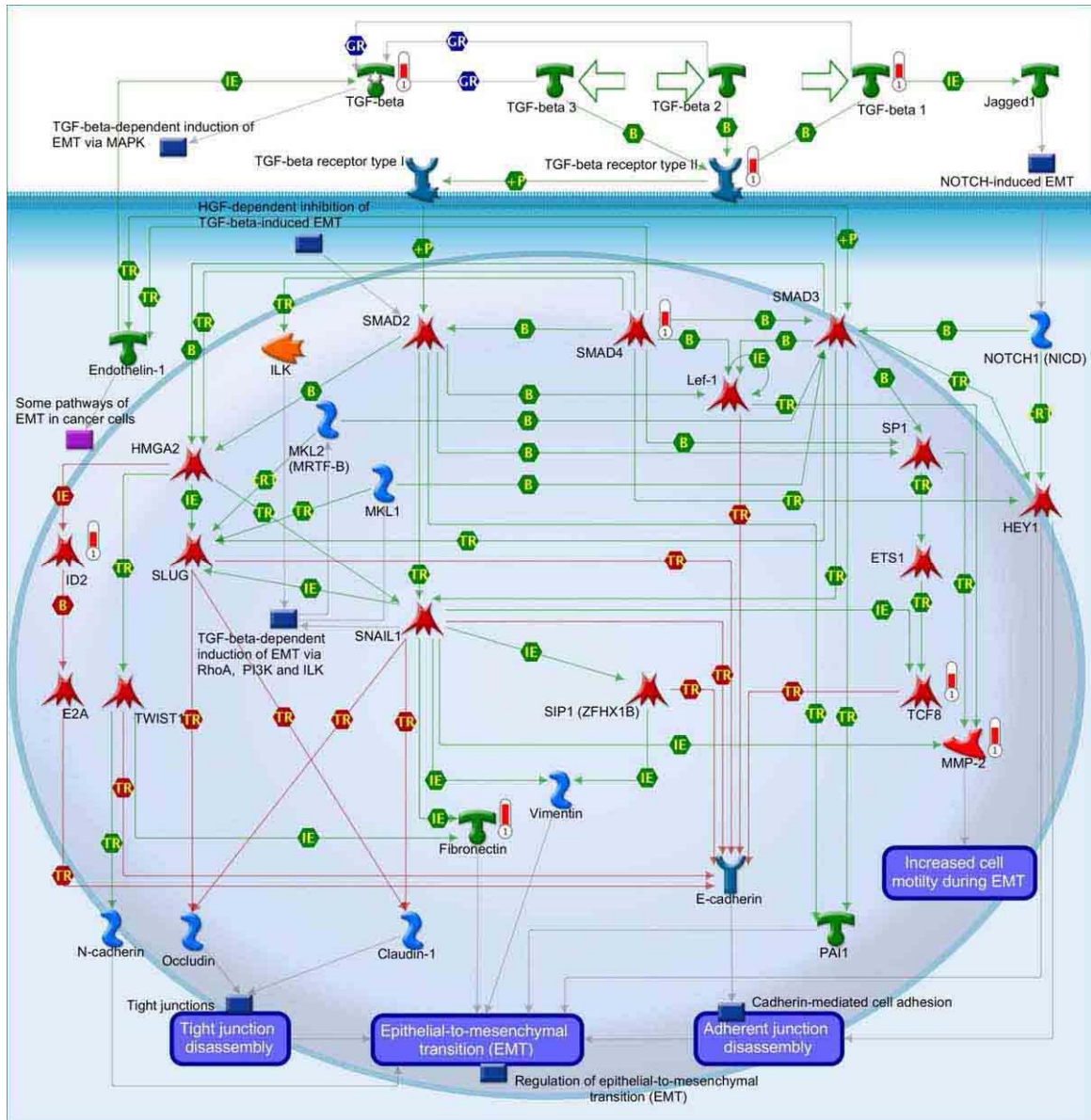


**Figure 2.8. TGFβ associated gene expression pathways in the colon induced by CTBp oral administration.**

Pathway analysis of colon gene expression from microarray analysis is shown. Red bars are indicative of significant induction of the gene. Pathway analysis was performed by MetaCore™ ontologies enrichment analysis using  $P < 0.01$  and a fold change of  $< -1.2$  or  $> 1.2$ . Definitions: EMT = Epithelial to Mesenchymal Transition, MAPK = Mitogen-activated protein kinase, HGF = Hepatocyte Growth Factor.

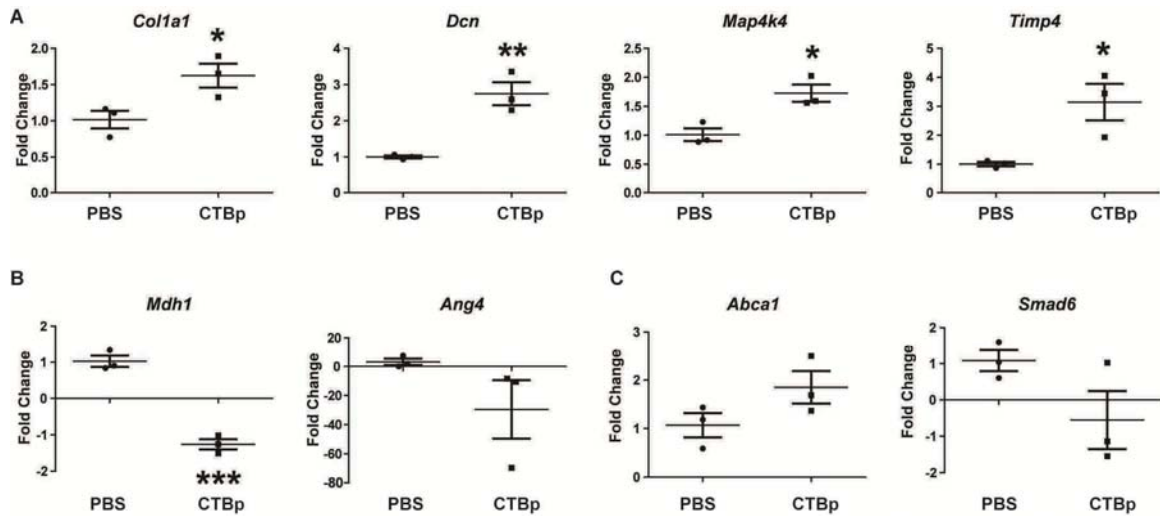


**Figure 2.9. qPCR analysis of representative genes to verify the microarray analysis.**

RNA samples from the distal colon tissue were isolated using the Qiagen RNeasy Microarray Tissue Mini Kit and analyzed by Applied Biosystems TaqMan Array 96- Well FAST plate in an Applied Biosystems 7500 Fast Real-Time PCR System. N = 3 per group. \*P < 0.05, \*\*P < 0.01 and \*\*\*P < 0.001; unpaired *t* test. **A)** Microarray-identified significantly induced genes including: *Col1a1*, *Dcn*, *Map4k4* and *Timp4*. **B)** Microarray identified suppressed genes including: *Mdh1* and *Ang4*. **C)** Unchanged genes in microarray analysis including: *Abca1* and *Smad6*.

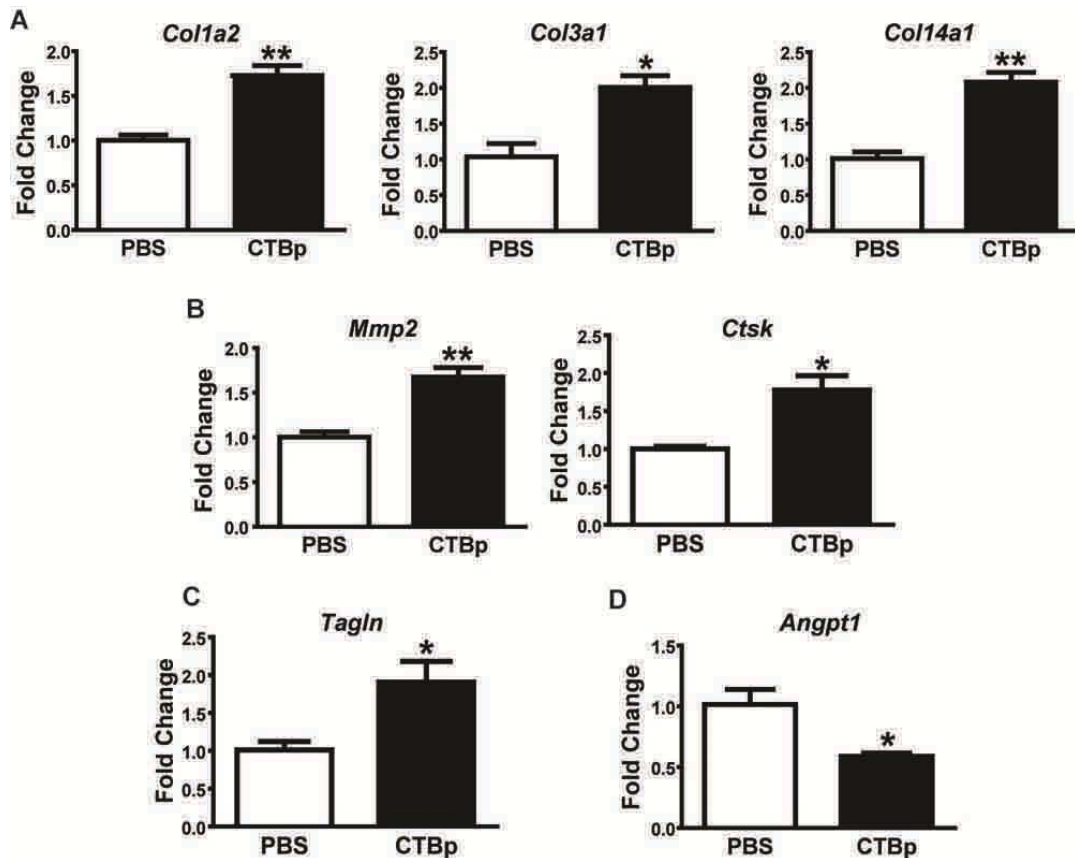


**Figure 2.10. Wound healing pathway-focused qPCR analysis of colon gene expression.**

Two weeks post vaccination, RNA samples were isolated using the Qiagen RNeasy Microarray Tissue Mini Kit and analyzed by RT2 Profiler PCR Mouse Wound Healing Array (Qiagen, Cat. No. PAMM-121Z) in an Applied Biosystems 7500 Fast Real-Time PCR System. N = 3 per group. A 1.5 fold change from PBS cutoff was used to filter data prior to testing for significance. Seven significantly changed genes in: **A)** extracellular matrix structural constituents; **B)** extracellular matrix remodeling enzymes; **C)** cytoskeleton regulators; and **D)** growth factors, are shown. \*P < 0.05 and \*\*P < 0.01; unpaired t tests.

*The overall microbiome was not significantly altered by CTBp vaccination.*

With the changes observed in colon gene expression and immune cell populations, we speculated a possible change in the microbiome profile. Fecal samples were collected prior to initial dosing with PBS or CTBp and at the time of sacrifice and sequencing of the V4 region of 16S ribosomal RNA was performed on fecal DNA.

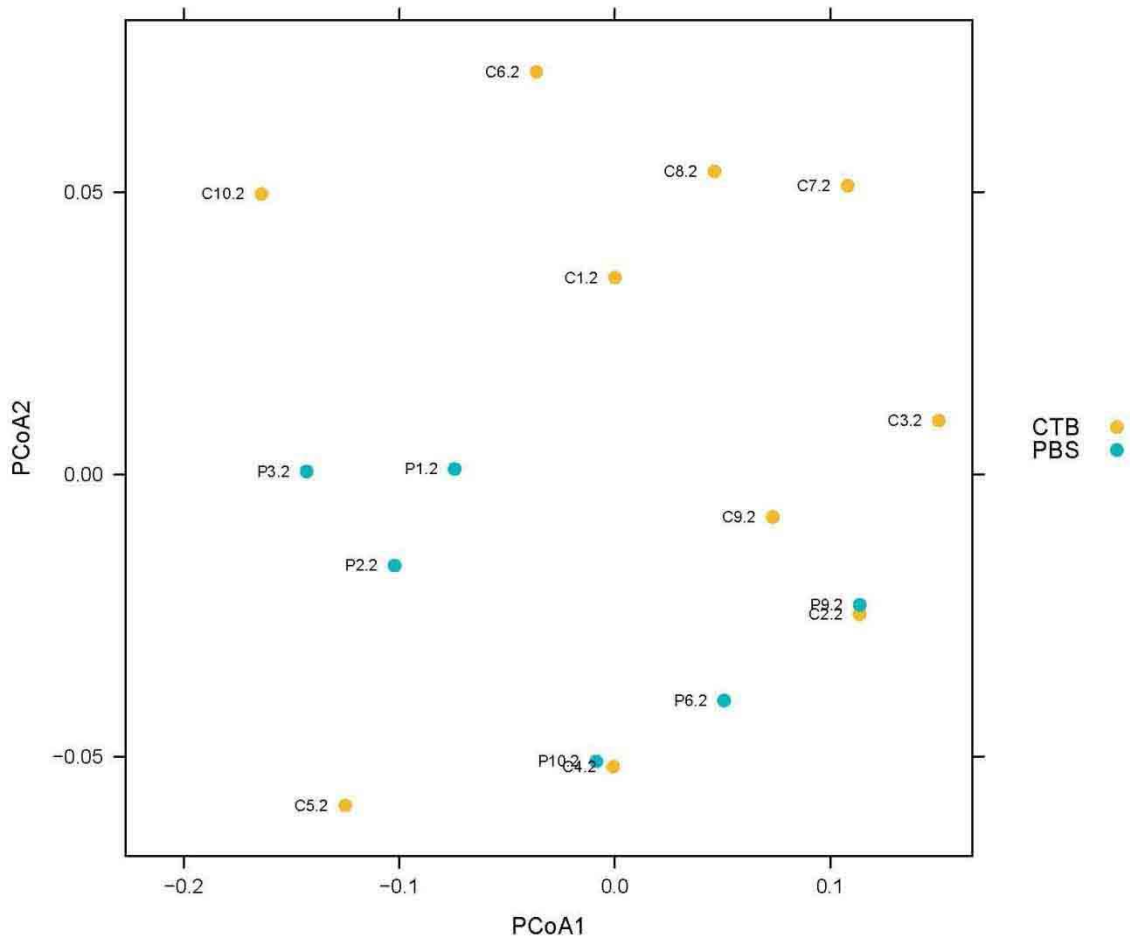


**Figure 2.11. No significant change in overall microbiome was observed two weeks following CTBp vaccination.**

Fecal samples were collected from each mouse 2 weeks after the final vaccination dose of PBS or CTBp. Following bacterial DNA isolation samples were analyzed. No significant alteration of overall microbiome was noted following CTBp administration. Weighted UniFrac metric was performed on 2,559 taxa followed by an Adonis test.

The overall microbiome profile was not significantly altered 2 weeks after CTBp oral administration (Fig 2.11). *Bacteroidetes* and *Firmicutes* spp. dominated at the phylum level which is typical for C57BL/6J mice (95, 96). Additionally, the six most common species were split evenly between *Bacteroidetes* and *Firmicutes* (Fig. 2.12A and B). However, there were minor subpopulations of the gut flora that were altered by CTBp; all belonging to the phylum *Firmicutes*. Of the 12 Operational Taxonomic Units (OTUs) significantly altered by CTBp, 11 were

significantly downregulated compared to the PBS colon samples (Fig. 2.12C). All 11 downregulated OTUs can be traced to the order *Clostridiales* of the *Firmicutes* phylum. The only induced OTU belonged to the order *Erysipelotrichales* also of the *Firmicutes* phylum.



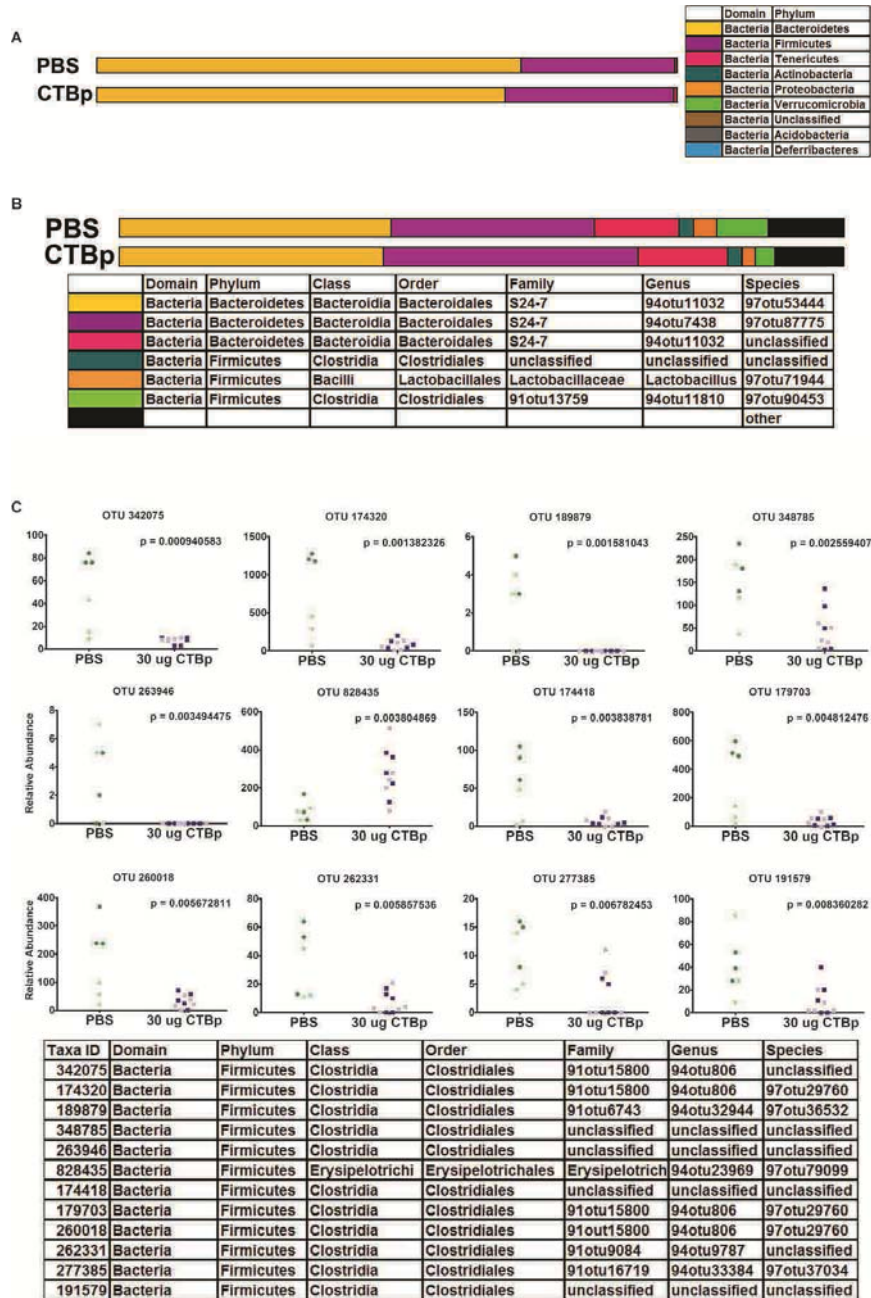


**Figure 2.12. CTBp does not significantly alter the microbiome at the Phylum level but several species were significantly altered in the Firmicutes Phylum..**

Fecal samples were collected from each mouse 2 weeks after the final vaccination dose of PBS or CTBp. Following bacterial DNA isolation samples were analyzed. **A)** Representative samples of Phylum level analysis. **B)** Representative samples of species level analysis and top 6 represented species in the samples. **C)** Operational Taxonomic Units representing the lowest p-values as determined by ANOVA.

## DISCUSSION

CTB's strong mucosal immunogenicity is well known; however, its detailed biological activities and impacts on the GI tract upon oral administration are not comprehensively described. Hence, our goal was to characterize CTBp's effect on the GI tract following oral administration using a systems biology approach; by profiling gene expression changes and characterizing lymphocyte populations in relevant immune compartments. We also attempted to link gene expression and immune cell population changes to the gut microbiota. To effectively reveal CTBp's impacts, we administered 30 µg CTBp twice over a two week interval to mice; since this dose induced the maximum antibody response that lasted over 6 months, as reported previously (76).

CTB is known to alter the immune cell profile when co-administered with an antigen (reviewed in (33, 59, 97)). Thus, we first focused on characterizing alteration of immune cell populations following CTBp oral administration. The most striking changes were noticed in the colon lamina propria two weeks after CTBp administration; while T cell profiles were not affected, other immune cell types were significantly altered in the colon (Fig. 2.5). CTBp binds to GM1-ganglioside on epithelial cells, but the receptor is also present on macrophages, dendritic cells and B cells, which might imply that the protein could impact the function of these immune cells (98). In fact, *in vitro*, studies have previously shown that CTB affects dendritic cell maturation (99) and diminishes the proinflammatory response of macrophages to lipopolysaccharide (100). Collectively, we postulate that the increased number of dendritic cells, natural

killer cells and macrophages in the colon lamina propria are likely a result of the immunomodulatory activity of CTBp.

The immunomodulatory activity of CTBp is often linked to TGF $\beta$  (60, 84). Previously, CTB was shown to induce *Tgfb1* expression in lymphoid cells in models of autoimmune diseases (101-103). Additionally, CTB was shown to induce IgA class-switching through *Tgf $\beta$ 1* stimulation (104).

TGF $\beta$  is a pleiotropic cytokine involved in various biological activities, which include important functions in fetal development and gut homeostasis (105). More specifically in the gut, TGF $\beta$  is an important modulator of the immune response and gut homeostasis (106). Maintenance of gut homeostasis by TGF $\beta$  requires tissue remodeling involving wound healing pathways (106-108). The gene expression microarray and pathway focused qPCR analysis revealed CTBp significantly upregulated genes associated with wound healing driven by *Tgf $\beta$ 1* (Fig. 2.7C). In a model of colonic anastomosis in rabbits, CT was previously shown to enhance wound healing by inducing *Tgf $\beta$*  (109). However, to our knowledge, our results are the first to show that CTB oral administration increased *Tgf $\beta$ 1* expression in the colon epithelium. Our data reveals a potential novel function of CTBp to enhance mucosal wound healing in the colon, apart from eliciting a strong humoral immune response, via its capacity to induce *Tgf $\beta$*  expression.

Despite the changes to gene expression and innate immune cell populations induced by CTBp in the colon, no overall change in the microbiome

of mice treated with CTBp was observed, indicating our findings are a direct result of the protein's impact on the colon (Fig. 2.11). Only a small number of OTU's were altered by CTBp administration; however, all of the downregulated OTU's belonged to the *Clostridiales* order, which constitutes a fraction of the overall gut microflora. An increase in *Clostridiales*, has previously been shown to enhance intestinal permeability and inflammation, suggesting that CTBp did not drive the microbiome to an inflammatory predisposition (110).

One of our most striking findings was that CTBp seemed to drastically affect the colon but little change was seen in the small intestine. One possibility to explain this is that epithelial turnover is slower in the colon than the small intestine (111). As a result, CTBp may remain in the colon longer than the small intestine after the GM-1-ganglioside-binding and internalization in epithelial cells. Additionally, intraepithelial lymphocytes differ significantly between the colon and small intestine (112). The report did not make functional observations but clear differences in immune cell populations would suggest different responses to an immunomodulatory molecule like CTBp. Lastly, the small intestine is the major site of absorption of nutrients and drugs; however, the colon is exposed to a larger population of microorganisms (113). This increased exposure to the commensal microbiota leads to constant immune surveillance and sampling of the colon microenvironment (114). This enhanced immune sampling may aid in inducing the stronger response to CTBp in the colon. Further investigation is required to elucidate the mechanism for CTBp's compartmentalized impacts on the GI tract.

In summary, this Chapter revealed previously undescribed impacts of orally administered CTB on the mucosal epithelia and immune cells in the distal part of the GI tract. Our data point to a potential utility of CTBp to enhance mucosal wound healing in the colon, extending its application beyond the original goal as an antigen for use in the oral cholera vaccine.

CHAPTER 3: CTB<sub>p</sub> PROTECTS AGAINST DSS-INDUCED ACUTE  
COLITIS

## INTRODUCTION

Our earlier findings pointed to a strong anti-inflammatory and wound healing potential, in the colon, for CTBp. To our knowledge, the wound healing potential of CTB is a novel finding.

As discussed in Chapter 1, CTB was shown to protect against trinitrobenzene sulfonic acid (TNBS)-induced colitis in mice and reduced inflammatory cytokine production in human Crohn's disease explants (72, 73). In the mouse model of Crohn's disease, the protein blunted T<sub>H</sub>1 cell signaling by inhibiting transcription factors (STAT-4, STAT-1, and T-bet) and cytokines associated with T<sub>H</sub>1 cells in the colon lamina propria (72, 73). Furthermore, Stal et al. showed in a small clinical trial that oral administration of CTB could reduce inflammation in Crohn's disease (74). However, the protein's potential to induce mucosal wound healing in the colon, which was suggested in Chapter 2, has not been previously reported. Our work, combined with the previous findings mentioned above, led us to hypothesize that CTBp could enhance wound healing and/or decrease inflammation in colonic injury and chronic inflammatory conditions including IBD.

IBD is composed of two main disease categories, Crohn's disease and ulcerative colitis, which have similarities pathologically but some important differences remain (see reviews (115-117)). Overall, differences exist in genetic susceptibility, environmental factors and T helper cell profiles. While the exact etiology of IBD remains elusive, Crohn's disease is generally accepted to be a

T<sub>H</sub>1-driven disease while ulcerative colitis is a T<sub>H</sub>2-dominated disease with T<sub>H</sub>17 cells having an apparent role in both IBD types (118, 119). Recently, Globig *et al.* found that a subset of T<sub>H</sub>17 cells that coproduce IFN $\gamma$  and IL-17 were specifically enriched in both active Crohn's disease and ulcerative colitis (120). As the disease progresses, it can lead to ulceration of the mucosal surface in the colon. As a result, mucosal wound healing plays a key role in resolving the inflammation and restoring gut homeostasis. In fact, failure to achieve mucosal wound healing in patients is associated with poor outcomes over the clinical course of the disease (121).

In this chapter, we used a modified model of intestinal wound healing using a human intestinal epithelial cell line, Caco2, (122) to evaluate the wound healing effect of CTBp. Next, we evaluated if CTBp could protect mice in the DSS colitis model, which is a well-established method for the study of ulcerative colitis and wound healing (123-125). The results in this chapter point to CTBp's potential therapeutic application in mucosal protection against colonic injury and colitis.



## **METHODS**

### *Animals*

8 week old C57BL/6J female mice were obtained from Jackson Laboratories (Bar Harbor, Maine) and allowed to acclimate for one week. Animals were housed according to the University of Louisville's Institutional Animal Care and Use Committee standards.

### *Caco2 wound healing assay*

The Caco2 wound healing assay was performed using a modified method (122). Briefly, Caco2 cells were seeded and grown to confluence in 6 well plates (Thermo Scientific™ Nunc™ Cell-Culture Treated). The culture medium was discarded, two 0.5-1.0 mm across linear wounds were made per well with a 200  $\mu$ L sterile beveled pipette tip (USA Scientific) and cells were washed with PBS to remove loose cells. PBS, CTBp (0.3-1  $\mu$ M), transforming growth factor- $\beta$  (TGF- $\beta$ ; .2 nM), and/or Anti-TGF $\beta$  antibody (3.85 nM; Abcam) were subsequently added in fresh serum-deprived medium to a total volume of 2 mL. Photomicrographs of the wounds were taken 0 and 24 H after the wounding at 4x magnification. Quantification of the remaining cell-free area to the initial wound area was measured using the public domain software Image J (<http://rsbweb.nih.gov>), and calculated as a mean percentage per well.

### *Animal study design and dosing regimen*

Animals were orally administered with PBS or 30  $\mu$ g plant-made cholera toxin B subunit (CTBp) twice at a 2-week interval as described above. DSS exposure

was initiated on the day of the second CTBp dosing (Fig. 3.2). The DSS exposure was slightly modified based on a previously published protocol (123). Body weights were measured just prior to the DSS exposure period as a baseline weight. Every morning during the study body weights were measured and percent change from baseline was determined. Animals were exposed to 4% DSS (product type and manufacturer information) in drinking water for up to 8 days and allowed up to a 7 day recovery period in which the animals received normal drinking water. Mice were sacrificed using carbon dioxide inhalation followed by thoracotomy. Serum and colon samples were taken for further analysis.

#### *Histology.*

Colons were removed and washed with PBS. A portion of the distal colon was fixed with paraformaldehyde overnight and stored in 70% Ethanol until paraffin embedding, sectioning and routine H&E staining. Inflammation scoring was performed using a scale that has been previously published (126). Sections were scanned using a Aperio ScanScope CS (Leica Biosystems) for grading. Tissue was scored based on a previously established protocol with minor modifications (126). Briefly, grades were assigned as follows: grade 0 = intact crypt, grade 1 = loss of bottom one third of the crypt, grade 2 = loss of bottom two thirds of the crypt, grade 3 = loss of entire crypt with the surface epithelium intact, and grade 4 = loss of the entire crypt and surface epithelium. Additionally this grade was assigned to percentages of the colon section based on 10% increments and averaged for each sections final score. Tissue sections from 8

mice were scored and averaged for each group. Statistics were performed comparing each group.

### *Immunohistochemistry*

Colons were removed and washed with PBS. A portion of the distal colon was fixed with paraformaldehyde overnight and stored in 70% Ethanol until paraffin embedding and sectioning. Sections were deparaffinized with Citrisolv and rehydrated through several ethanol washing steps ending with incubation in distilled water. Antigen retrieval was performed overnight with a 2100 Retriever (Electron Microscopy Sciences) using Buffer B designed specifically for the Retriever. Tissue sections were blocked for endogenous peroxidase, avidin, biotin, and serum from the animal in which the secondary antibody was raised. Primary antibody (F4/80; ab111101 or CD3; ab16669) was incubated with the tissue sections for 2 hours at room temperature. The Vectastain Elite ABC kit (rabbit anti-goat; Vector Labs) was used to label the primary antibody. F4/80+ and CD3+ cells were visualized with the ImmPACT DAB Substrate Kit (Vector Labs) and then dehydrated through an ethanol gradient and finally incubated with Citrisolv. Sections were scanned using a Aperio ScanScope CS (Leica Biosystems) and positive cells were counted in 10 representative sections (40x magnification) from each colon. The 10 sections were averaged and used as the score for each animal.

### *RNA Isolation*

Sections from the small intestine and distal colon were stored in RNA $later^{\text{TM}}$  (Qiagen, Valencia, CA) at -20°C until RNA was isolated. Colon tissue

(approximately 14 mg) was placed in QIAzol lysis reagent in a 2.0 mL conical bottom centrifuge tube with Zirconia/Silica beads. A Bead Bug™ (Catalog no. S8452-SK, Denville Scientific Inc., MA) was used to homogenize the tissue. An RNeasy® Microarray Tissue Kit from Qiagen (Catalog no. 73304) was used to purify the RNA from the tissue homogenate. RNA was stored at -80°C until use.

#### *Quantitative RT-PCR gene expression analysis*

Gene expression was carried out by qPCR using quality verified by Nanodrop 1000 (Thermo Scientific) RNA samples. First strand cDNA was obtained from reverse transcription of 150 ng RNA using a SUPERSCRIPT VILO cDNA synthesis kit (Life Technologies) according to the manufacturer's instructions. Template cDNA were added to a reaction mixture containing 10 µl of 2×TaqMan® Fast Advanced Master Mix (Life Technologies) and endonuclease free water to 20 µl and loaded in TaqMan® Array Standard 96 well Plates (Applied Biosystems). These plates contain pre-spotted individual TaqMan® Gene Expression probes for the detection of genes of interest as well as the house keeping genes *18S*, *β-actin* (*ACTB*), and *GAPDH* (Table 4.1). PCR amplification was carried out on a 7900HT Fast Real-Time PCR System (Applied Biosystems) with the following conditions: 95°C, 20 min; 40 cycles (95°C, 1 min); 20 min at 60°C. The 7500 Software v2.0.6 (Applied Biosystems) was used to determine the cycle threshold (Ct) for each reaction and derive the expression ratios relative to control. Wound healing pathway analysis was performed with a RT2 Profiler PCR Mouse Wound Healing Array (Cat. No. PAMM-121Z) (Qiagen) under the same conditions described above.

**Table 3.1. Gene Identity for qPCR analysis**

| Gene Name  | Gene ID | Entrez Gene ID |
|--|---------|----------------|
| Cathepsin K  | Ctsk    | 13038          |
| Collagen, type 1, alpha 1                            | Col1a1  | 12842          |
| Colony stimulating factor 2 (granulocyte-macrophage) | Csf2    | 12981          |
| Interleukin 1 beta                                   | Il1b    | 16176          |
| Interleukin 33                                       | Il33    | 77125          |
| NLR family, pyrin domain containing 3                | Nlrp3   | 216799         |
| Transforming growth factor, beta 1                   | Tgfb1   | 21803          |
| Tumor necrosis factor                                | Tnf     | 21926          |

### *Protein isolation*

Distal colon tissue isolated at sacrifice was snap frozen in liquid nitrogen and pulverized with a Bessman Tissue Pulverizer and placed in T-PER (Thermo Scientific) with a protease inhibitor cocktail (Sigma-Aldrich). Total protein was isolated by gravity centrifugation of tissue fragments followed by collection of the buffer containing isolated protein, and storage at -80°C until analysis.

### *Protein quantification*

Protein sample concentrations were determined using a Nanodrop 1000 (Thermo Scientific). Protein was normalized for all samples prior to loading on a Mouse Cytokine/Chemokine Magnetic Bead Panel (EMD Millipore). The panel was analyzed with a Milliplex MAP Kit on a MagPix with Luminex xMAP technology.

### *Statistics*

Graphs were prepared and analyzed using Graphpad Prism version 5.0 (Graphpad Software). To compare two data sets, we conducted an unpaired, two-tailed Student's *t* test. To compare three or more data sets, we conducted a one-way ANOVA with a Bonferroni post-test. For body weight and DAI results we conducted a Two-way ANOVA with a Bonferroni post-test.

## RESULTS

### *CTBp significantly enhances wound healing in human colonic epithelial cells*

To investigate the mucosal wound healing potential of CTBp suggested by the gene expression analysis, we employed the human colon epithelial cell line Caco2 wound healing model (122). In this assay, wound closure after 24 hours, in the presence of CTBp, TGF $\beta$  or PBS control, was measured.

As shown in Figure 3.1, CTBp (1.0 and 3.0  $\mu$ M) significantly enhanced wound healing compared to the PBS control, and was comparable to 0.2 nM TGF $\beta$ . Co-incubation of 3.0  $\mu$ M CTBp with an anti-TGF $\beta$  antibody (3.85 nM) completely blunted the wound healing, demonstrating that CTBp's effect is mediated by TGF $\beta$ .

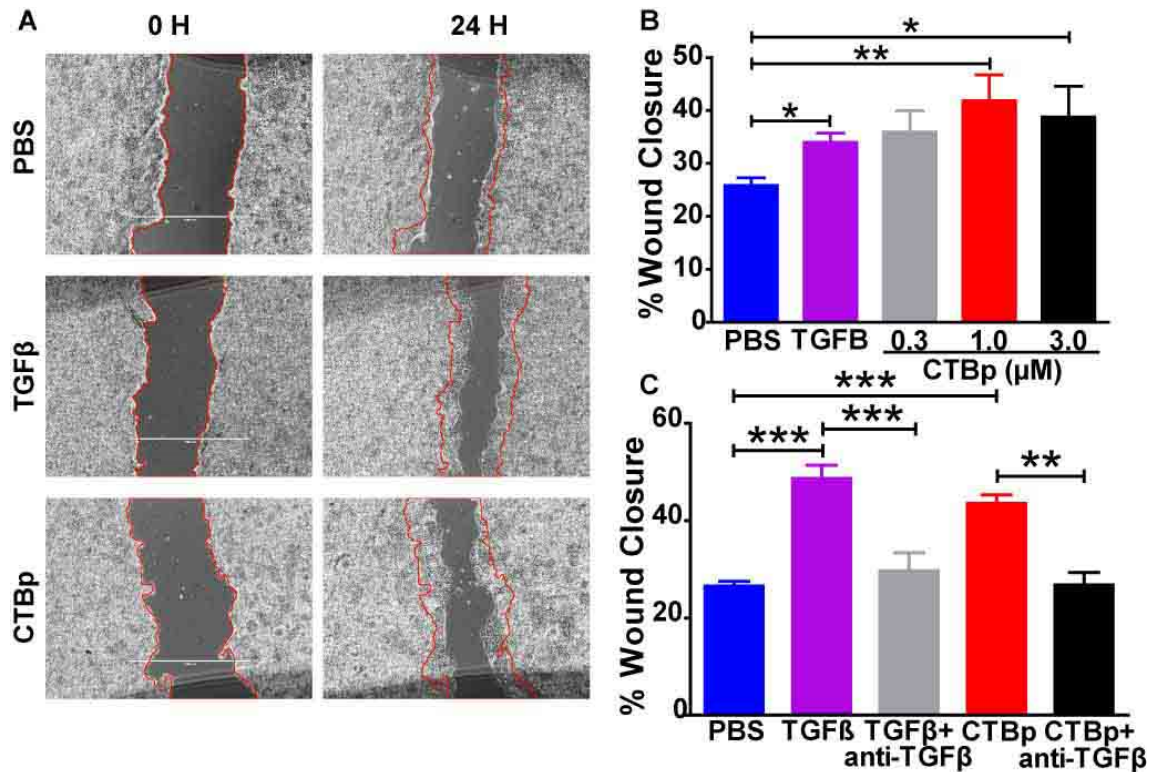


**Figure 3.1. CTBp enhanced wound healing in Caco2 cells.**

Caco2 cells were grown to confluence and scratched with a pipette tip. Cells were then incubated with PBS, TGFβ, Anti-TGFβ, and/or CTBp at indicated concentration. The *in vitro* wound closure was recorded over 24 H and 4x magnification images were acquired with a EVOS<sup>®</sup> by Advanced Microscopy Group and mean percentage closure was determined by Image J software. **(A)** Photomicrographs of wounded Caco2 cells. **(B)** Analysis of *in vitro* wound closure after 24 H by wound area measurement. Mean ± SEM is shown. N = 4 experimental replicates per group. \*\*  $P < 0.01$ , and \*\*\*  $P < 0.001$ ; one-way ANOVA with Bonferroni's multiple comparison tests. **(C)** Graphs represents percent wound closure after 24 H. Mean ± SEM is shown (N = 4, experimental replicates per group). \*  $P < 0.05$ , \*\*  $P < 0.01$ , and \*\*\*  $P < 0.001$ ; one-way ANOVA with Bonferroni's multiple comparison tests.

### *CTBp mitigates DSS-induced acute body weight loss and colon inflammation*

With the above data supporting the mucosal wound healing potential of CTBp, from both colon gene expression analysis and the human colon epithelial wound model, we next explored if this potential could be translated into a therapeutic effect *in vivo*. We employed a well-established mouse DSS colitis model, which induces injury and severe inflammation in the distal colon (123, 127). PBS or CTBp (30 or 100 μg per mouse) was orally administered twice at a 2 week interval to mice prior to DSS exposure and body weights were recorded daily (Fig

3.2). Distal colons were removed, paraffin embedded and stained with hematoxylin and eosin (H&E) for inflammation scoring.

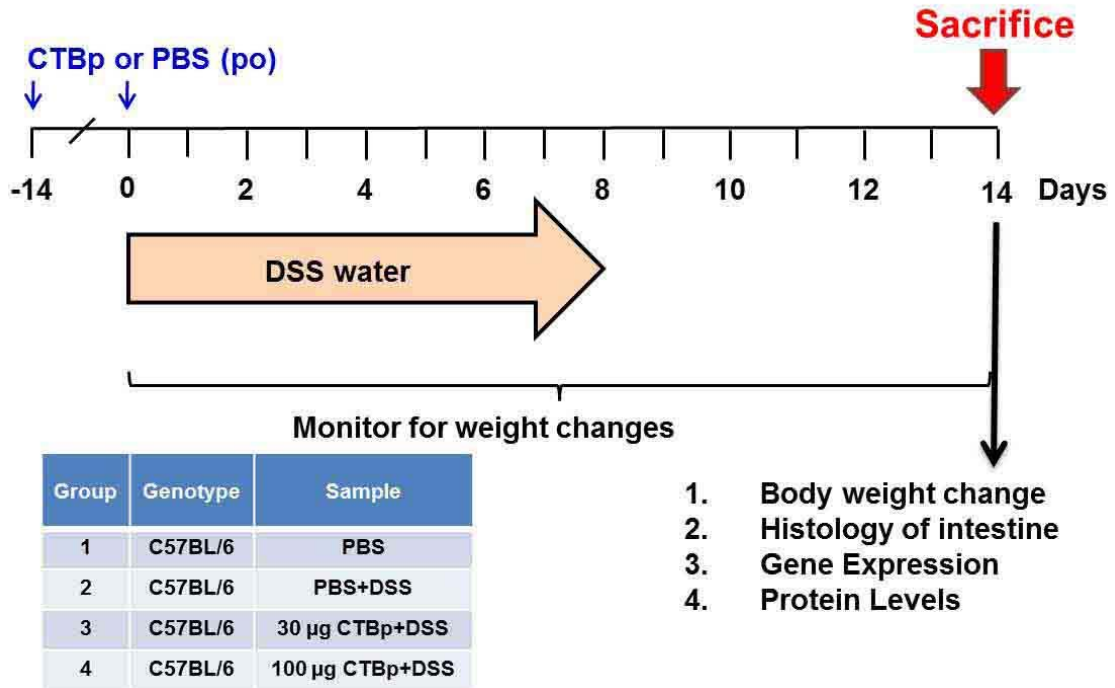


**Figure 3.2. Study design for recovery acute colitis experiment.** Mice were orally administered PBS or CTBp twice at a two-week interval. Immediately after the second administration DSS exposure began for 8 days. Animals were sacrificed either immediately after the DSS exposure period or after a 6 day recovery.

DSS exposure resulted in significant body weight loss, a strong indicator of disease severity, when compared to control animal's (Fig. 3.3). Notably, both 30 and 100 µg CTBp significantly blunted the weight loss by the end of the DSS exposure and through the early recovery period. It should be noted, however, no dose dependency was observed in CTBp-treated mice.



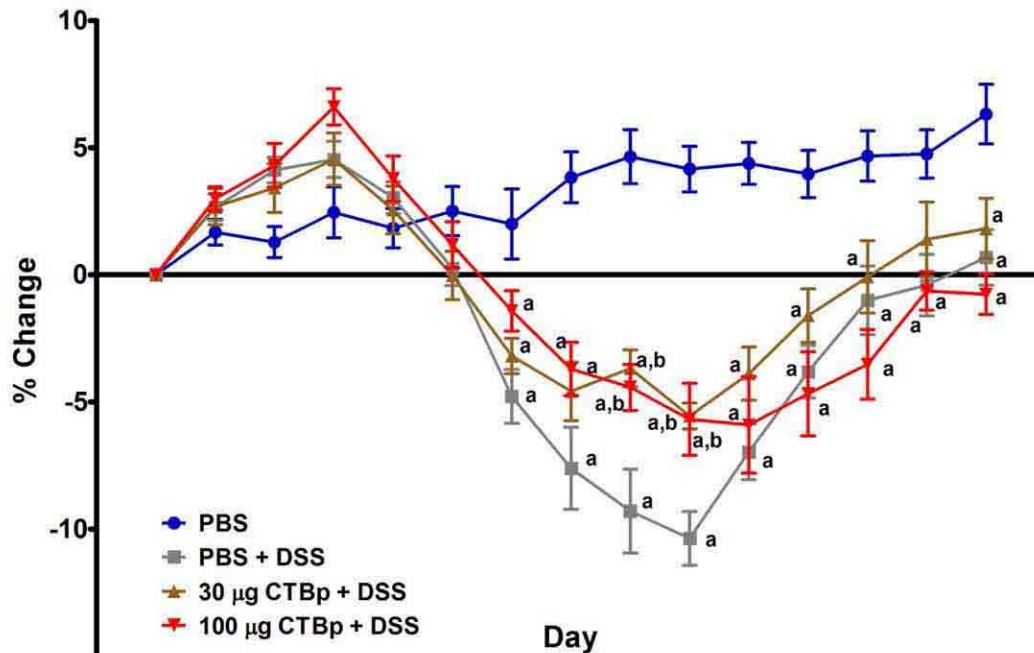


**Figure 3.3. CTBp blunts body weight loss from DSS exposure.**

Mice were exposed to 4% DSS in water ad libitum for 7 days and allowed to recover on normal drinking water an additional 7 days. Mean  $\pm$  SEM is shown. N = 6 for PBS and N = 8 for all DSS exposed groups. <sup>a</sup>  $P < 0.05$  compared to PBS, <sup>b</sup>  $P < 0.05$  compared to PBS+DSS; two-way ANOVA with Bonferroni's multiple comparison test.

Histopathological examination was performed on the H&E-stained colon tissue sections to assess disease severity after a one week recovery period. The analysis clearly showed that 30  $\mu$ g CTBp treatment prevented the aberrant loss of crypts and ulceration that were noted in the untreated control group; although shortening of basal crypts and mild inflammatory infiltrates were observed, the epithelial surface remained largely intact (Fig. 3.4A and B). Moreover, this dose of CTBp prevented fibrosis, evident in the PBS-treated group, in the colon according to Masson's trichrome stain (Fig. 3.5). By contrast, such a protective effect was not observed with 100  $\mu$ g CTBp.

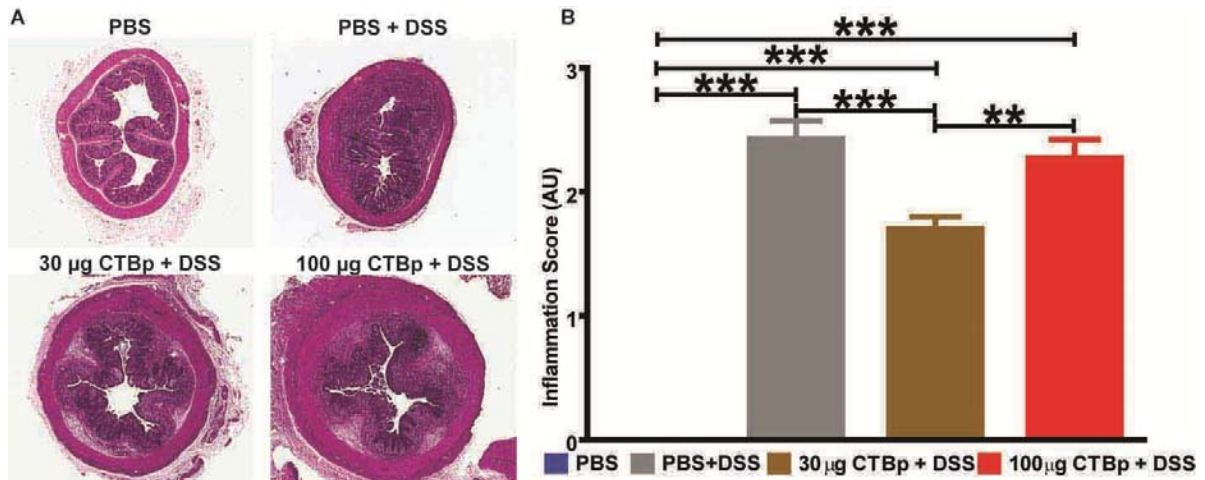


**Figure 3.4. Histopathological analysis of colon 1 week after DSS exposure.**

Colon inflammation scoring. Paraffin embedded tissue sections were scored after staining with Hematoxylin and Eosin (H&E). Scoring was based on a 0 to 4 scale. Mean  $\pm$  SEM is shown. **A)** Representative photomicrographs of colon sections. **B)** Inflammation scoring of tissue sections. Mean  $\pm$  SEM is shown. N = 6 for PBS and N = 8 for all DSS exposed groups. \*\*  $P < 0.01$  and \*\*\*  $P < 0.001$ ; one-way ANOVA Bonferroni's multiple comparison tests.

Given that 30  $\mu$ g CTBp significantly improved the recovery from DSS-induced acute injury and inflammation in the colon, we next investigated its effect at the maximum injury/inflammatory point immediately after DSS exposure using the same dosage of CTBp (Fig. 3.6). Oral administration of CTBp showed significant reduction of inflammation at this time point, as observed in the recovery phase; characterized by shortened yet visible basal crypts, relatively mild inflammatory infiltrates in the mucosa and submucosa, and retention of the epithelial cell surface unlike the PBS control group (Fig. 3.7). Meanwhile, daily oral administration of 100  $\mu$ g mesalamine (MES) during the DSS exposure, which simulates a current treatment for ulcerative colitis in humans (128), showed similar protection observed with the CTBp regimen employed here, demonstrating the effectiveness of CTBp against acute colonic injury and inflammation.

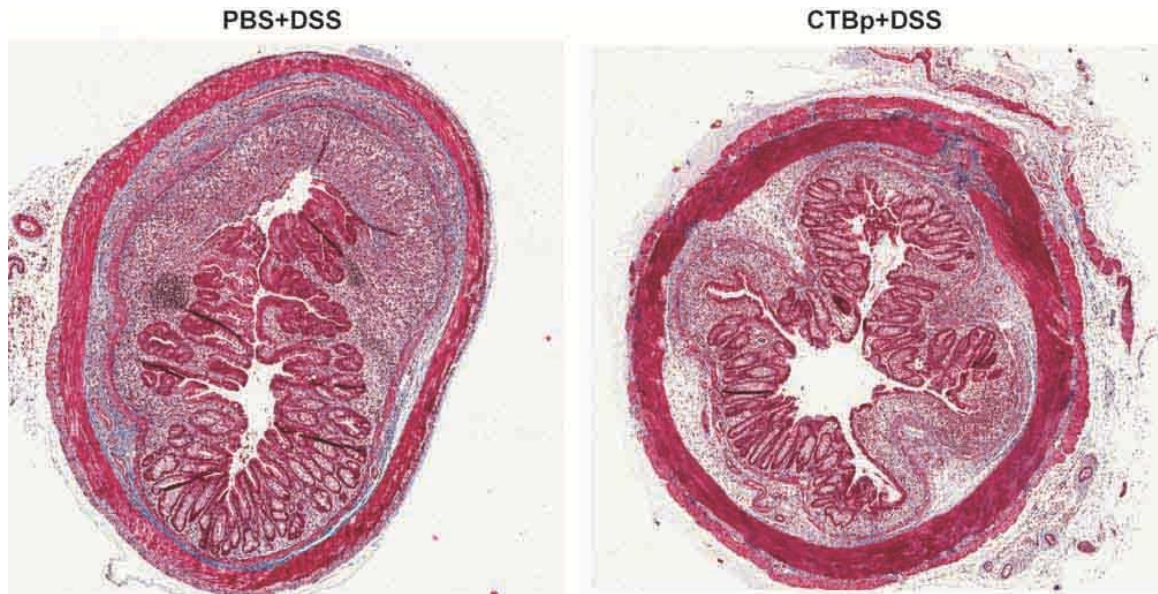


**Figure 3.5. Masson's trichrome stain of distal colon cross sections.**  
 Representative photomicrographs of collagen deposition in the submucosa and lamina propria of distal colons following a 1 week recovery (Fig. 16). Paraffin embedded sections were stained using Masson's Trichrome for Connective Tissue Kit #26367 (Electron Microscopy Sciences).

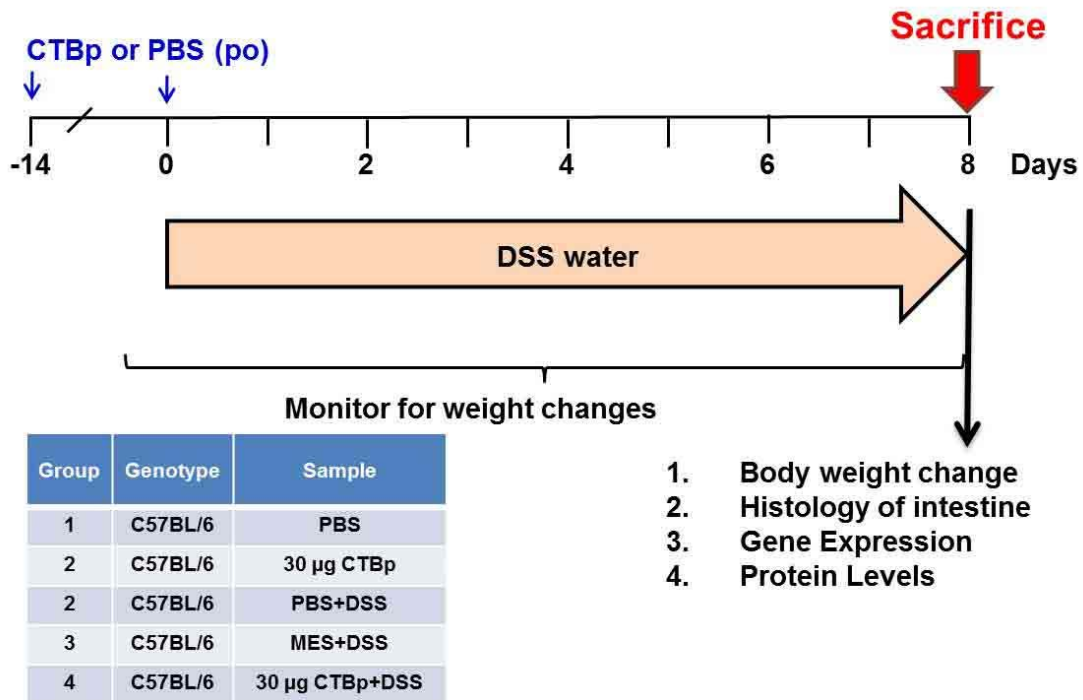


**Figure 3.6. Study design for recovery acute colitis experiment.**

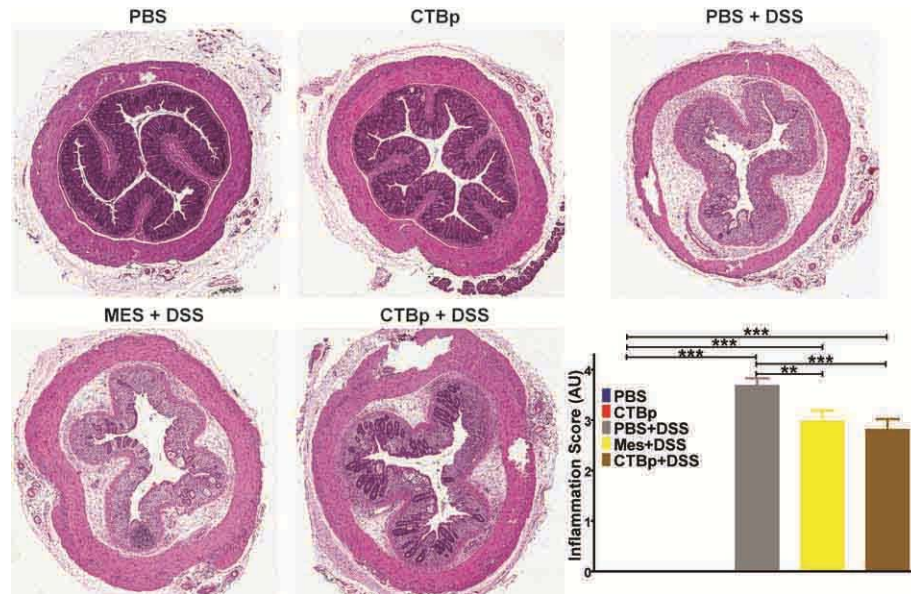


**Figure 3.7. CTBp blunts inflammation immediately after DSS exposure.**

Mice were exposed to DSS for 8 days and sacrificed immediately. Colons were isolated, paraffin embedded and stained with hematoxylin and eosin. Scoring was performed by a trained pathologist. Representative photomicrographs of colon sections. Inflammation scoring of tissue sections. Mean  $\pm$  SEM is shown. N = 5 for PBS and 30  $\mu$ g CTBp groups. N = 7 for PBS+DSS group. N = 8 for CTBp+DSS group. N = 9 for Mes+DSS group. \*\*  $P < 0.01$  and \*\*\*  $P < 0.001$ ; one-way ANOVA Bonferroni's multiple comparison tests.

CTBp's protective effect was further characterized at the gene expression level, by analyzing genes associated with ulcerative colitis by real-time qPCR analysis. While body weights had mostly recovered at one week after the end of DSS exposure, classic ulcerative colitis cytokines, including *Il1b*, *Tnfa*, and *Il33*, were still significantly increased at this time point in the PBS-treatment group

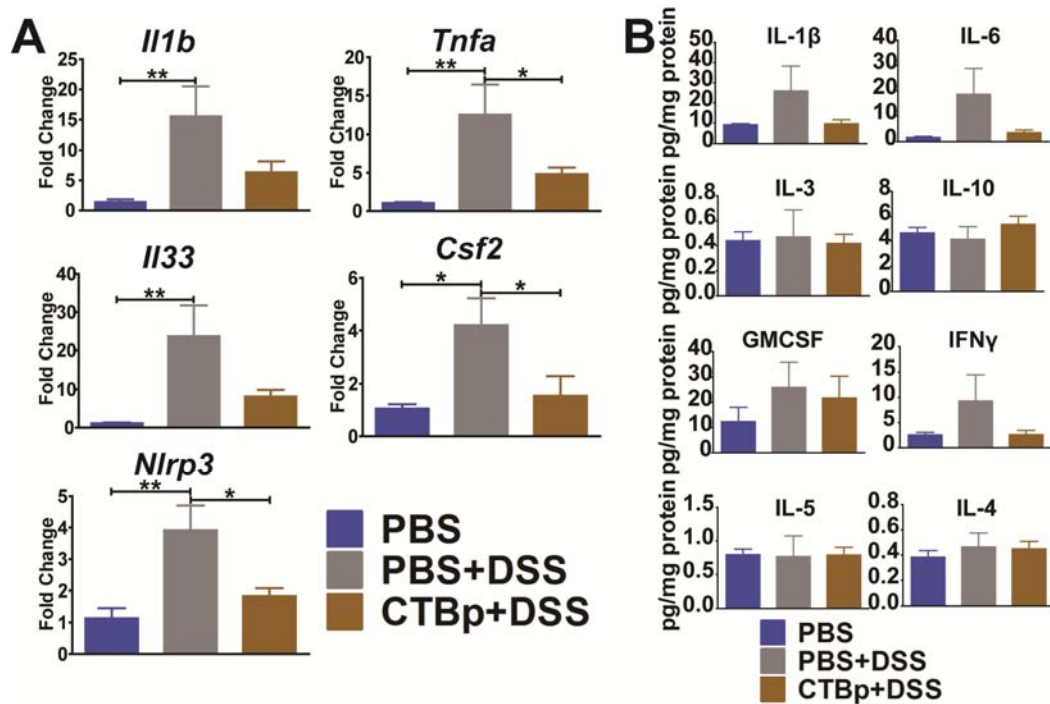


**Figure 3.8. CTBp blunts pro-inflammatory genes in DSS colitis after a 1 week recovery.** Mice were exposed to DSS for 8 days and sacrificed immediately. Colons were removed and RNA and Protein isolated. Gene expression was analyzed by qRT-PCR and protein levels were determined by Luminex. **A)** Gene expression in colon tissue from mice given PBS or CTBp and exposed to water or DSS containing drinking water. Mean  $\pm$  SEM is shown. N = 5 per group. \*  $P < 0.05$ , \*\*  $P < 0.01$  and \*\*\*  $P < 0.001$ ; one-way ANOVA Bonferroni's multiple comparison tests. **B)** Protein concentrations for cytokines detected colon tissue from mice given PBS or CTBp and exposed to water or DSS containing drinking water. Mean  $\pm$  SEM is shown. N = 5 per group. \*  $P < 0.05$ , \*\*  $P < 0.01$  and \*\*\*  $P < 0.001$ ; one-way ANOVA Bonferroni's multiple comparison tests.

(Fig. 3.8A) (129). CTBp blunted the expression of these genes to near baseline one week after the end of the DSS exposure (Fig. 3.8B). Additionally, the expression of *Nlrp3*, a crucial player in colitis inflammation (130), and *Csf2*, which induces a pro-inflammatory cytokine profile in M1 macrophages (131, 132), were also significantly reduced by CTBp treatment. Lastly, *Col1a1* and *Tgfb1*, pro-fibrotic cytokines, were significantly increased 1 week following the end of DSS exposure in PBS pretreated mice; CTBp on the other hand, reduced the gene expression to near baseline levels (Fig 3.9).

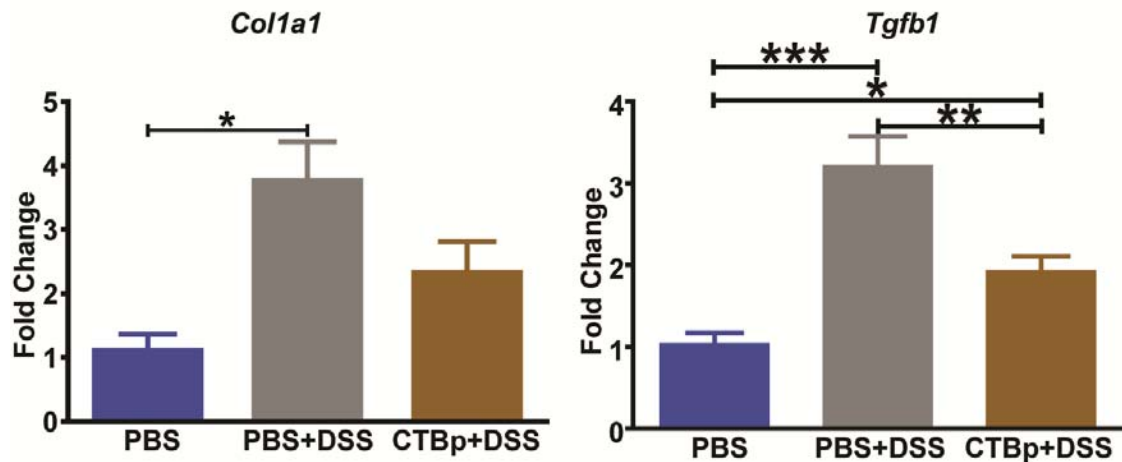


**Figure 3.9. Pro-fibrotic cytokine gene expression significantly elevated 1 week after DSS exposure with PBS but not CTBp.**

Mice were exposed to DSS for 8 days, allowed a 6 day recovery and sacrificed following the recovery. Gene expression in colon tissue from mice given PBS or CTBp and exposed to water or DSS containing drinking water. Mean  $\pm$  SEM is shown. N = 5 per group. \*  $P < 0.05$ , \*\*  $P < 0.01$ , and \*\*\*  $P < 0.001$ ; one-way ANOVA Bonferroni's multiple comparison tests.

Similar trends were also noted at the maximal inflammatory time point, i.e., immediately following the end of DSS exposure; CTBp significantly blunted the increase of *Il1b* and *Il33* induced by DSS exposure (Fig. 3.10A). Though not statistically significant, CTBp also alleviated the massive increase of *Nlrp3* and *Csf2*.

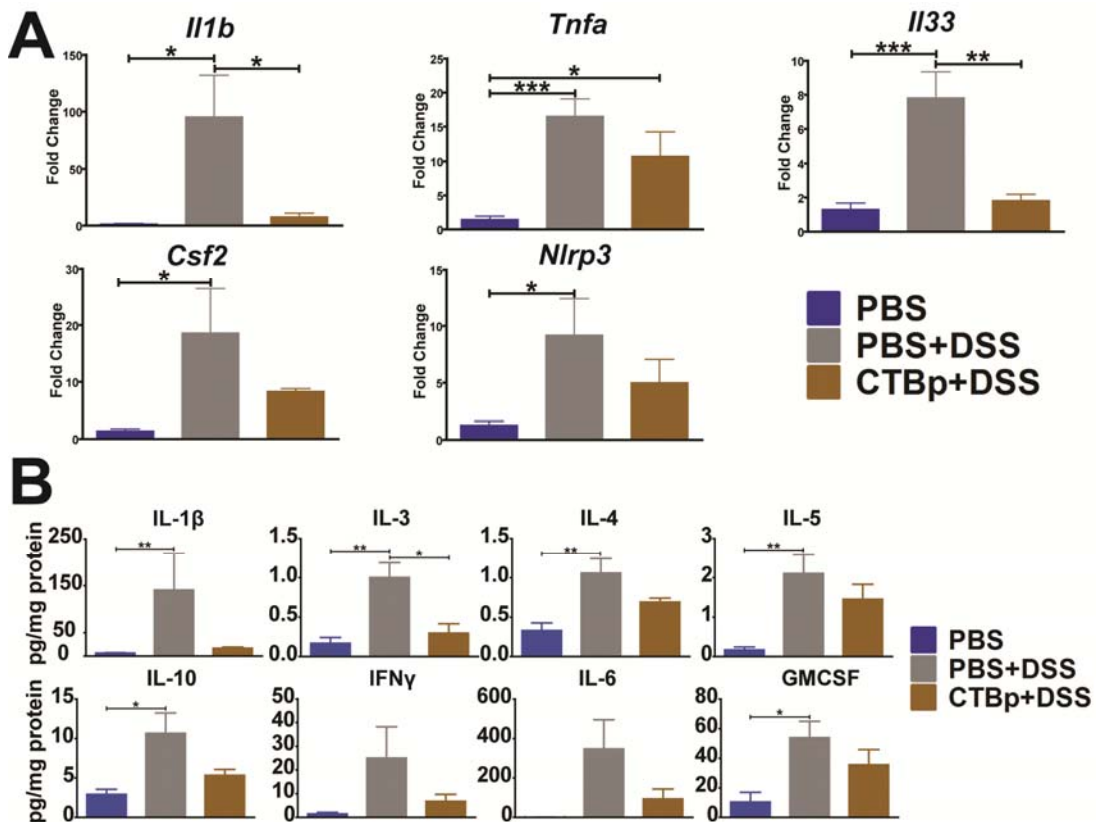


**Figure 3.10. 30  $\mu$ g CTBp blunts inflammatory gene expression and protein levels immediately after DSS exposure.**

Mice were exposed to DSS for 8 days and sacrificed immediately. Colons were removed and RNA and Protein isolated. Gene expression was analyzed by qRT-PCR and protein levels were determined by Luminex. **A)** Gene expression in colon tissue from mice given PBS or CTBp and exposed to water or DSS containing drinking water. Mean  $\pm$  SEM is shown. N = 5 per group. \*  $P < 0.05$ , \*\*  $P < 0.01$  and \*\*\*  $P < 0.001$ ; one-way ANOVA Bonferroni's multiple comparison tests. **B)** Protein concentrations for cytokines detected colon tissue from mice given PBS or CTBp and exposed to water or DSS containing drinking water. N = 5 per group. \*  $P < 0.05$ , \*\*  $P < 0.01$ ; one-way ANOVA Bonferroni's multiple comparison tests.

To further analyze inflammatory signals, we measured soluble inflammatory markers at the protein level in the distal colon. Immediately following the end of the DSS exposure period, CTBp significantly reduced IL-3

(Fig. 3.10B). Though not statistically significant, other major inflammatory proteins (IL-1 $\beta$ , IFN $\gamma$ , IL-4, IL-5, IL-6, and GM-CSF) were also relatively decreased. Interestingly, CTBp administration did not increase IL-10, suggesting that CTBp's anti-inflammatory activity is independent of this anti-inflammatory cytokine, despite that IL-10 has previously been linked to the potential anti-inflammatory activity of CTB and CT (133-135). By the end of the one week recovery, all the elevated inflammatory markers induced by DSS exposure had returned closer to the normal levels of the non DSS-exposed control group. Hence, there was no noticeable effect of CTBp at the protein level at this time point (Fig. 3.8B).

*CTBp did not alter macrophage counts following DSS exposure*

Our earlier findings suggested macrophages were significantly increased 2 weeks after CTBp oral administration in the colon lamina propria. Thus we performed an immunohistochemistry analysis to discern whether macrophages played a role in CTBp's anti-colitis activity. No difference was observed between mice exposed to DSS with and without CTBp; both groups showed a progressive increase in macrophages after DSS exposure (Fig 3.11).



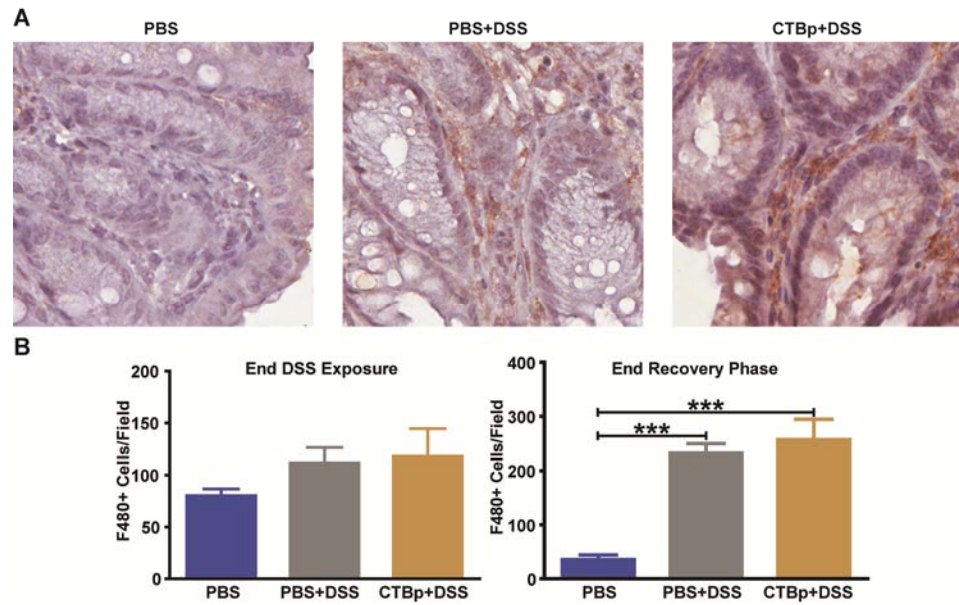


**Figure 3.11. Immunohistochemistry analysis of macrophages in distal colon sections.**

F4/80+ cells were counted in the distal colon. Mouse colons were removed at the time of sacrifice and washed with 1x PBS and formalin fixed. Paraffin embedded colon cross sections were incubated with F4/80 primary antibody (1:100 dilution) and a biotinylated secondary antibody. After addition of a HRP and DAB solution, positive cells were counted in 10 fields per section and averaged for each colon. A) Representative photomicrographs of colon sections. B) F4/80 scoring of tissue sections from each sacrifice after acute DSS exposure. Mean  $\pm$  SEM is shown ( $N \geq 5$  per group). \*\*\*  $P < 0.001$ ; one-way ANOVA with Bonferroni's multiple comparison tests.

## DISCUSSION

Our results in Chapter 2 alluded to a novel wound healing capacity for CTBp by inducing *Tgfβ*-driven pathways in the colon. CTB has been shown to induce *Tgfb1* expression in lymphoid cells in models of autoimmune diseases but a link to wound healing has not previously been explored (101-103). Consistent with the gene expression results, an *in vitro* wound healing assay using the Caco2 human colon epithelial cell line showed that CTBp could enhance TGFβ-mediated mucosal wound healing (Fig. 3.1).

These results led us to further explore CTBp's therapeutic potential *in vivo*, using the DSS model of acute colonic injury and colitis. We found hallmarks of decreased inflammation (decreased body weight loss and inflammation scoring) in the DSS colitis model noted after CTBp administration (Fig. 3.4 and 3.7). CTBp also blunted proteins associated with inflammation and eosinophil recruitment increased by DSS (i.e. IL-3, IL-5, and GM-CSF; Fig. 3.10B) (136). In addition to these anti-inflammatory effects, findings supporting enhanced mucosal wound healing were noted at both time points of sacrifice from the histological scoring of the colons. Mucosal healing is increasingly being targeted in the clinic because, when achieved, it leads to far better outcomes for patients (137). Although, the definition of mucosal healing is still debated, generally it implies the absence of ulceration (137, 138), as we noted with CTBp administration. Current therapeutic options (e.g. mesalamine, corticosteroids, infliximab, etc.) induce mucosal wound healing in approximately 50% of patients (138). Recombinant TGFβ has induced intestinal epithelial wound healing *in vitro*

as shown in Figure 3.1 and by others (139), leading some to speculate on the potential of using this cytokine as a therapy for ulcerative colitis (87). In fact, recombinant TGF $\beta$  has successfully been used to treat colitis in mice. However, its application in humans is complicated due to the pro-fibrogenic and carcinogenic effects of TGF $\beta$  (140). Giving recombinant TGF $\beta$  directly induces strong effects associated with the cytokine; however, by giving CTBp we may be stimulating the production of secreted TGF $\beta$  only to a level which is allowed by a stringent feedback control naturally equipped for the highly active cytokine (141). Because we did not see a classic dose response with CTBp in the Caco2 or colitis experiments, there appears to be a rate limiting step, perhaps by feedback inhibition of TGF $\beta$ .

Fibrosis results from excessive production, deposition and contraction of the extracellular matrix during wound healing to compensate for severe injury (106). Histological analysis of collagen deposition by Masson's trichrome stain revealed that CTBp blunted collagen deposition associated with fibrosis (Fig. 3.5) (142). Furthermore, after 1 week recovery from DSS exposure, genes associated with fibrosis were significantly blunted by CTBp administration (Fig. 3.8); *Tgf $\beta$ 1*, *Il-1 $\beta$*  and *Nlrp3* all play significant roles in promoting collagen deposition and therefore fibrosis (123, 142). Lastly, the reduction of *Col1a1* expression by CTBp, following recovery from DSS colitis, reveals that CTBp prevented prolonged expression of a major pro-fibrotic gene (143). These results revealed the therapeutic potential of CTBp to prevent fibrosis in colitis. Although the prevention of fibrosis by CTBp requires further investigation, our data suggest

that oral administration of CTBp can induce more regulated wound healing than direct administration of recombinant TGF $\beta$ , leading to superior mucosal protection.

In summary, the work in this chapter demonstrated that CTBp can promote mucosal wound healing *in vitro*, protect from chemically induced colonic injury and inflammation while preventing fibrosis. These findings strongly support the investigation of CTBp's potential therapeutic effect under clinically relevant conditions. In a clinical setting, a therapeutic intervention would be employed following diagnosis of ulcerative colitis and likely at a point when inflammation in the colon is present. Further work should therefore be performed to determine if CTBp can be given therapeutically and enhance recovery of mice from DSS colitis.

CHAPTER 4: EFFECTS OF A LONG-TERM ORAL CTB $\rho$   
ADMINISTRATION

## INTRODUCTION

Our work initially focused on the short-term effects of CTBp administration on the GI tract; however, the findings in the acute colitis model suggested a long-term treatment regimen using CTBp may have clinical relevance in chronic intestinal inflammation. Our goal in this chapter is to determine toxicity and immunological impacts resulting from a long-term oral administration of CTBp.

Human studies have evaluated long-term antibody response and clinical responses after the standard oral dosing regimen (2 times over 2 weeks or 3 times over 18 weeks) of a cholera vaccine containing CTB (23, 24, 27). However, to our knowledge, no study has addressed potential physiological changes upon long-term oral dosing of CTB. As a result, physiological changes from long-term CTB dosing remain a clear gap in the knowledge base.

Our short-term experiment (2 doses over 2 weeks) in mice revealed significant changes in immune cell populations and gene expression in the colon two weeks after the second administration, but there was no major change in the overall gut microbiome (Chapter 2). One of the most profound findings from this work was the upregulation of *Tgf $\beta$*  pathways in the colon by CTBp oral administration as revealed by microarray gene expression analysis, which subsequently lead us to discover the protein's mucosal wound healing potential in Chapter 3. The results from the mouse acute colitis studies discussed in Chapter 3 demonstrated that CTBp could protect against DSS-induced colon inflammation and enhance recovery from the mucosal injury.

However, increased *Tgfβ* expression raised a potential concern that CTBp may have a deleterious effect over long-term dosing. For instance, increased TGFβ1 has been linked to fibrosis following wounding of the skin (144). TGFβ1 is a key player in the induction of the epithelial to mesenchymal transition (EMT) process (145), and resveratrol-induced reduction of TGFβ1 levels blunted fibrosis and EMT in a mouse model of pulmonary fibrosis (146). These results suggest that increasing *Tgfβ* expression in the colon epithelium over the long term, under stress, could lead to enhanced fibrosis. Additionally, TGFβ is a cytokine with multifaceted functions that has diverse impacts on multiple cell types including epithelial cells, macrophages and T cells (106). This leads us to speculate that long-term administration of CTBp may impact the homeostasis in the gut, and possibly in the systemic compartment as well.

In this chapter, we performed a preliminary examination of changes in the immune cell population and gut microbiota, as well as general toxicity in healthy adult mice orally administered with 3 μg CTBp biweekly four times over the nine-week experimental period. Overall, the results revealed that the CTBp dosing regimen induced no major toxicity but did appear to have some impacts on circulating immune cells and soluble factors indicative of systemic immune modulation.

## **METHODS**

### *Animals*

8 week old C57BL/6J female mice were obtained from Jackson Laboratories (Bar Harbor, Maine) and allowed to acclimate for one week. Animals were housed according to the University of Louisville's Institutional Animal Care and Use Committee standards.

### *Study Design and Dosing Regimen*

Animals were vaccinated with PBS or 30 µg plant-made cholera toxin B subunit (CTBp) and subsequent doses were given every 2 weeks for a total of 4 doses. After a two week recovery period, mice were sacrificed using Carbon Dioxide inhalation followed by a thoracotomy. Whole blood, serum, feces, small intestine, colon, mesenteric lymph nodes, and spleens were taken for further analysis.

### *Immune Cell Isolation*

One or two weeks following the second vaccination with PBS or CTBp the animals were sacrificed. Colons, small intestines, mesenteric lymph nodes (MLN), and spleens were removed for T cell isolations. Peyers patches (PP) were removed from the small intestines. Lamina propria leukocytes (LPLs) were isolated from the small intestine and colons by using a series of washing steps and collagenase steps. Epithelial cells, mucus and fat tissue were removed by incubating with EDTA at 37°C. The colon and small intestine were cut into small pieces and incubated with collagenase at 37°C. Cell suspensions were filtered



through a 100 and 40  $\mu\text{m}$  filters sequentially. Filtered Cells were counted in a hemocytometer and  $1 \times 10^6$  cells were put into flow cytometry tubes for staining. Mesenteric lymph node immune cell populations were isolated by mincing the Mesenteric lymph nodes and using a syringe plunger to squeeze the cells from the tissue. Cell suspensions were run through a 100 and 40  $\mu\text{m}$  filter sequentially and immune cells were isolated. Filtered Cells were counted in a hemocytometer and  $1 \times 10^6$  cells were put into flow cytometry tubes for staining. Splenocytes were isolate by crushing the spleens on metal mesh and separating the supernatant from any debris. ACK buffer was used to lyse red blood cells and following several washes the cells were filtered through a 70  $\mu\text{m}$  cell strainer. Splenocytes were counted on a hemocytometer and  $1 \times 10^6$  cells were put into flow cytometry tubes for staining. Peyer's patch lymphocytes were isolated by chopping up the Peyer's patches with fine surgical scissors and incubating the pieces in collagenase at 37°C. After allowing the suspension to settle, the supernatant was removed and saved for lymphocyte isolation. The collagenase step was repeated and the second suspension was isolated. The suspensions were centrifuged and supernatants were discarded. After a second wash the cells were combined and filtered through a 70  $\mu\text{m}$  cell strainer. Cells were counted in a hemocytometer and  $1 \times 10^6$  cells were put into flow cytometry tubes for staining.

### *Flow Cytometry*

Cells were stained using antibodies and a Cell staining kit from eBiosciences, Inc. (San Diego, CA). Briefly, tubes containing  $1 \times 10^6$  cells were washed with

flow cytometry staining buffer 2 times. Fc Block was added to each tube in flow cytometry staining buffer for 10 minutes. Surface staining antibodies were then added to each tube (CD3-FITC, CD4-APC-Cy7, CD25-PerCP) and allowed to incubate at 4°C for 30 minutes. After removing surface antibodies, fixation/permeabilization buffer was added to the tubes and incubated overnight. The following morning the tubes were washed with permeabilization buffer 2 times and again incubated for 10 minutes with Fc block. Internal cell antibodies (Gata3-PE, T-Bet-PE-Cy7, FoxP3-APC, IL-17-eFlour450) were added to each tube and incubated for 30 minutes at 4°C. The tubes were washed 2 times with permeabilization buffer and finally cells were suspended in flow cytometry staining buffer. Events (1 x 10<sup>5</sup>) were counted on a BD FACSCanto™ II and analyzed with the BD FACSDiva Software v6.1.3.

#### *Complete blood cell count*

Blood was collected from the inferior vena cava was collected in a BD Microtainer® (Becton, Dickinson and Company) containing EDTA and stored at 4°C until analysis. The analysis was performed on a Hemavet 950FS (Drew Scientific Inc.) and results were graphed in Graphpad Prism version 5.0 (Graphpad Software).

#### *Serum chemistry analysis*

Serum samples were collected from the inferior vena cava. Whole blood samples were collected in a BD Microtainer® (Becton, Dickinson and Company) containing a serum separator. Samples were spun at 6,000 rcf at 4°C for 5

minutes in an Eppendorf centrifuge 5430 R (Eppendorf) and serum was removed from the tubes and stored at -20°C until analysis. Samples were analyzed by the University of Louisville Research Services Diagnostic Lab and results were graphed with Graphpad Prism version 5.0 (Graphpad Software).

#### *Serum protein analysis*

Serum samples were collected from the inferior vena cava. Whole blood samples were collected in a BD Microtainer® (Becton, Dickinson and Company) containing a serum separator. Samples were spun at 6,000 rcf at 4°C for 5 minutes in an Eppendorf centrifuge 5430 R (Eppendorf) and serum was removed from the tubes and stored at -20°C until analysis.

#### *Microbiome analysis*

Fecal samples were collected at the end of the acclimation period and at the time of study termination. Bacterial DNA was isolated using the PowerFecal® DNA Isolation Kit (Mo Bio Laboratories, Inc.). Briefly, fecal samples were added to a bead tube with solution and lysed with a bead beater. Through a series of centrifugation and elution steps Fecal DNA was isolated. DNA concentration was determined using the Quant-iT dsDNA Broad-Range Kit (Life Technologies). Samples were then sent to Second Genome, Inc. for analysis. Upon arrival, samples were enriched for bacterial 16S V4 rDNA region by utilizing fusion primers designed against conserved regions and tailed with sequences to incorporate Illumina flow cell adapters and indexing barcodes. Amplified products were concentrated using a solid-phase reversible immobilization method and

quantified by electrophoresis using an Agilent 2100 Bioanalyzer®. Samples were loaded into a MiSeq® reagent cartridge and then loaded into the instrument. Amplicons were sequenced for 250 cycles with the MiSeq instrument. Second Genome's PhyCA-Stats™ analysis software package was used to analyze the results.

A secondary endpoint of the microbiome analysis was to evaluate if any cage effect existed in our experiment. Previously, Hufeldt and colleagues found that sex, same room single housing, and separate room housing had no effect on ceecal V3 16S rDNA microbiome content in C57BL/6 mice (147). However, this has been challenged by V3-V5 16S rDNA analysis which showed a significant cage effect at the phylum level (148). Additionally, it was determined that fecal and cecal samples do not have similar profiles; thus leaving the question open if fecal samples have a cage effect (149). To that end we evaluated fecal samples from 3 separate cages per dosing group at the end of acclimation and at the end of the study.

### *Statistics*

Graphs were prepared and analyzed using Graphpad Prism version 5.0 (Graphpad Software). We conducted an unpaired, two-tailed Student's *t* test on the results.

## RESULTS

### *Immune cell populations are significantly altered by a long-term CTBp oral administration*

Immune cell profiles in various lymphatic tissues were determined one week after four biweekly oral administrations of 3  $\mu$ g CTBp, based on the methods previously established for the acute dosing time points (See Chapter 2). The lamina propria cells in the small intestine showed no significant changes in any cell types analyzed following long-term oral CTBp administration. However several populations of immune cells in the other compartments were significantly altered (Figure 4.1 and 4.2).

The proportion of T<sub>H</sub>17 cells among CD4<sup>+</sup> T cell populations was significantly lower in the mesenteric lymph nodes and Peyer's patches following long-term oral CTBp administration. Spleen and colon lamina propria both showed a significant reduction in the proportion of CD25<sup>+</sup>FoxP3<sup>+</sup> regulatory T cells (T<sub>REG</sub>) cells but diverged on other T helper (T<sub>H</sub>) cell profiles. In the colon lamina propria, the proportion of T<sub>H</sub>1 cells was significantly decreased, while T<sub>H</sub>2 cells were significantly decreased in the spleen (Figure 4.1). Additionally, in the spleen, a marginal yet significant increase in the B cell proportion among CD45<sup>+</sup> cells was noted (Fig 4.2).

For CD45<sup>+</sup> innate immune cells analyzed (i.e., macrophages, natural killer cells and dendritic cells), the only significant changes induced by the long-term

oral CTBp administration were the increase of macrophages in the mesenteric lymph node and the reduction of dendritic cells in the spleen (Fig 4.2).

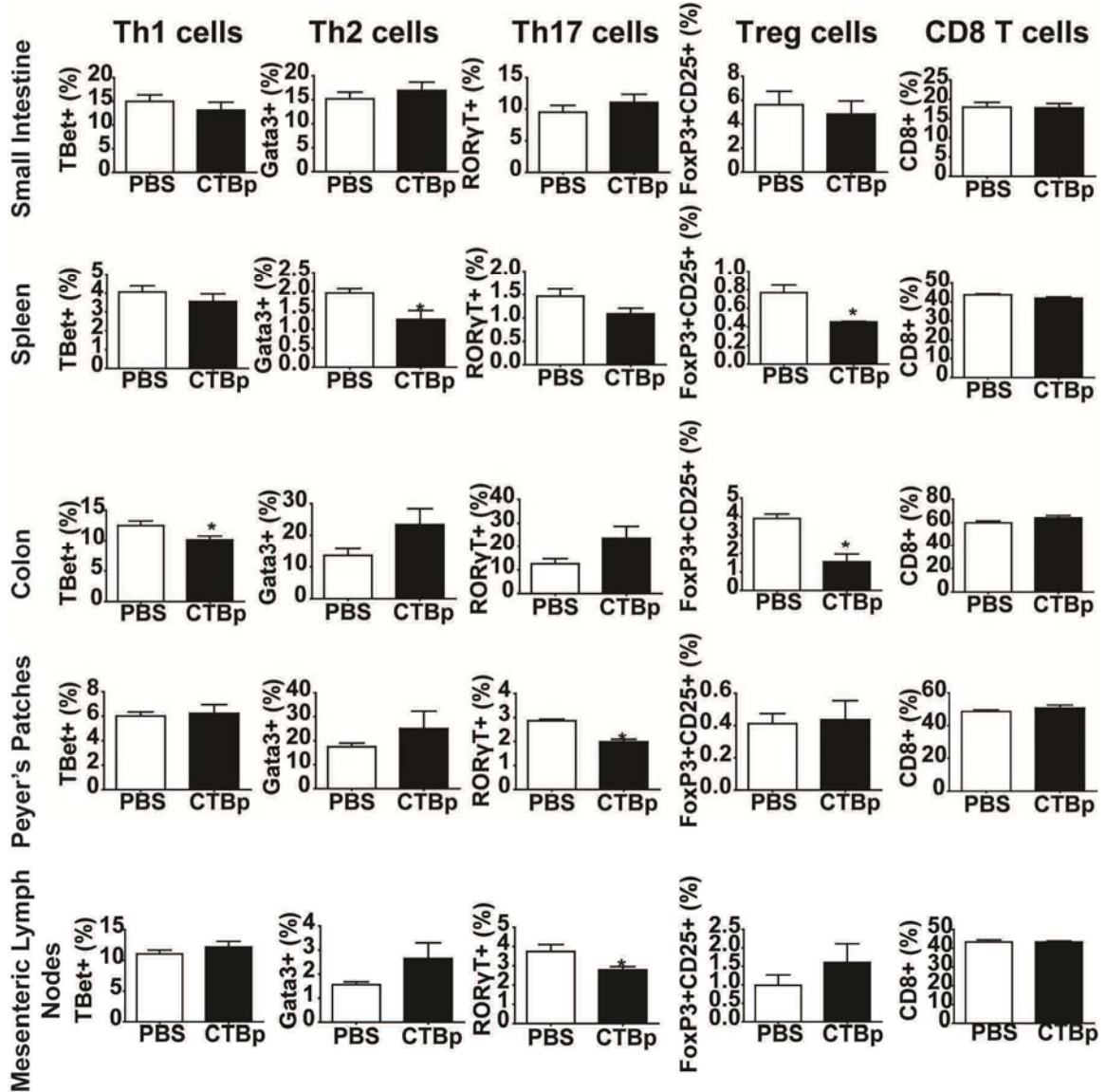


**Figure 4.1. Chronic administration of CTBp significantly alters T cell populations.**

Animals were given PBS or CTBp every 2 weeks a total of four doses and 1 week later the mice were sacrificed. Small intestine and Colon lamina propria, spleen, Peyer's Patches and Mesenteric lymph node lymphocytes were isolated and stained for surface and internal markers specific for immune cell subtypes. CD4+ and CD8+ cells gated on T lymphocyte subpopulation (CD3+). Data are presented as mean  $\pm$  standard error of the mean (SEM) of at least 4 biological replicates comprised of 2 pooled mice each. \*  $P < 0.05$  compared to PBS group; Unpaired  $t$  test was performed.

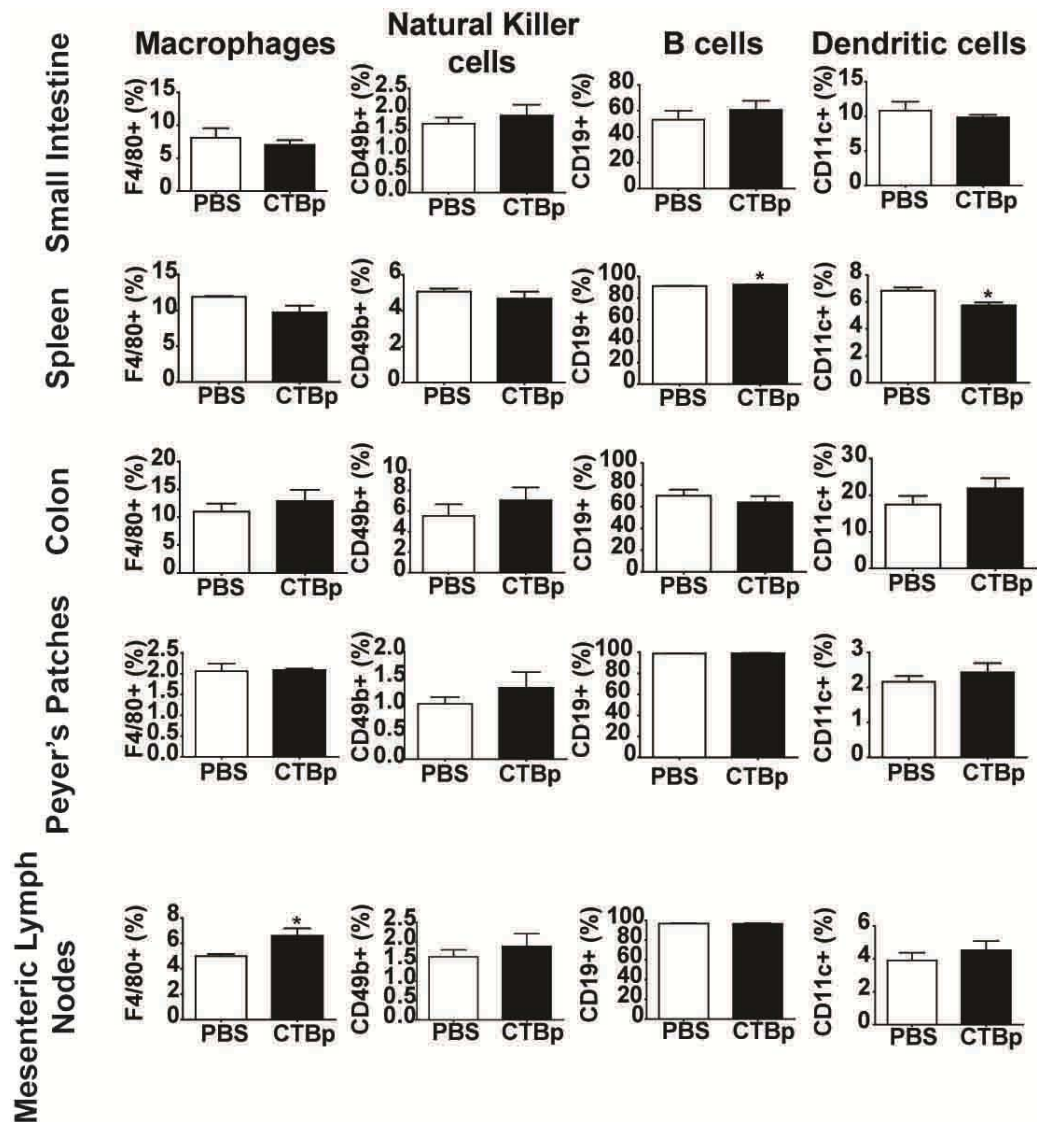


**Figure 4.2. Chronic administration of CTBp significantly alters CD45+ cell populations.** Animals were given PBS or CTBp every 2 weeks a total of four doses and 1 week later the mice were sacrificed. Small intestine and Colon lamina propria, spleen, Peyer's Patches and Mesenteric lymph node lymphocytes were isolated and stained for surface and internal markers specific for immune cell subtypes. CD45+ cells were further divided into B (CD19+), Macrophage (F4/80+), Dendritic (CD11c+) and Natural Killer (CD49b+) subpopulations. Dot plots are representative samples taken from each group. Data are presented as mean  $\pm$  standard error of the mean (SEM) of at least 4 biological replicates comprised of 2 pooled mice each. \* P < 0.05 compared to PBS group; Unpaired t test was performed.

*Total white blood cells were significantly increased by long-term CTBp treatment*

The long-term oral administration of CTBp significantly increased total white blood cells by approximately 1.5 fold in the complete blood count analysis.

This significant increase was seen across multiple subcategories of white blood cells, including neutrophils, lymphocytes, monocytes, and eosinophils (Fig. 4.3A). Interestingly, the ratio of these cell types within total white blood cells remained the same between CTBp and PBS-administered animals, indicating that the entire white blood cells uniformly increased by the long-term oral CTBp administration (Fig. 4.3B).



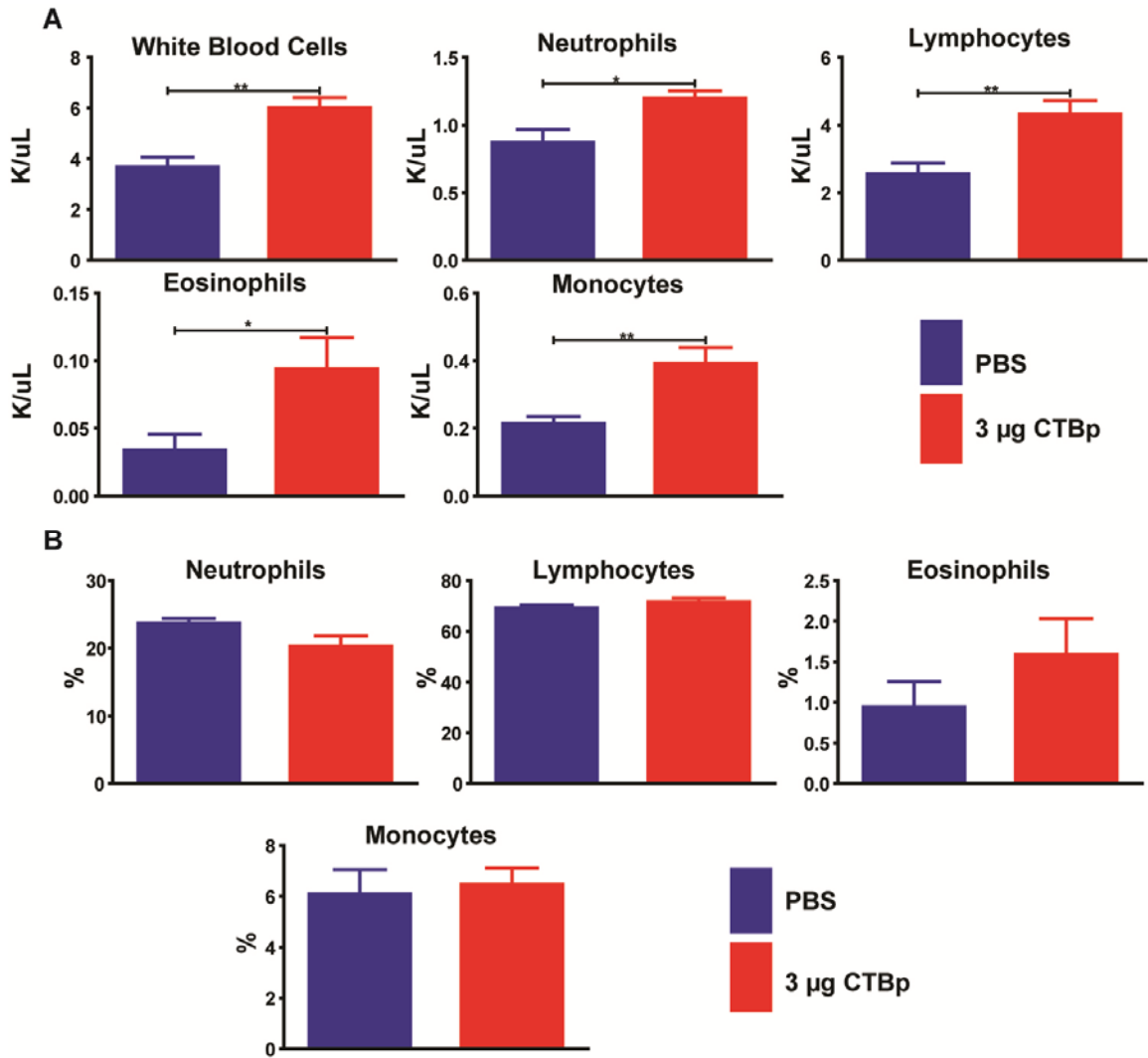


**Figure 4.3. CTBp increased immune cell populations proportionally to the total population, as well as the total white blood cell population.** Mice were orally administered PBS or 3 µg CTBp biweekly 4 times and 1 week after the final dose the mice were sacrificed. Blood was drawn from the inferior vena cava. Complete blood count was determined with a Hemavet 950FS. **A)** White blood cell counts for white blood cells and immune cell populations. **B)** Immune cell populations as a percentage of the entire population. N = 5 per group. \* P < 0.05 and \*\* P < 0.01; Unpaired t test was performed.

*The serum chemistry profile was unchanged*

Serum albumin, alkaline phosphatase, alanine aminotransferase and total bilirubin were not altered by long-term oral CTBp administration, indicating no liver toxicity (Fig. 4.4). Additionally, blood urea nitrogen and creatinine, indicative of kidney toxicity, was unchanged by CTBp administration. Amylase, associated

with pancreatitis, was also unchanged by CTBp administration. Lastly, CTBp administration did not significantly alter the profile of several nutrients: calcium, glucose and phosphorus. Serum globulins were unchanged with long term CTBp administration, despite that CTBp clearly induced a significant level of CTBp-specific immunoglobulins at the dose used (76).

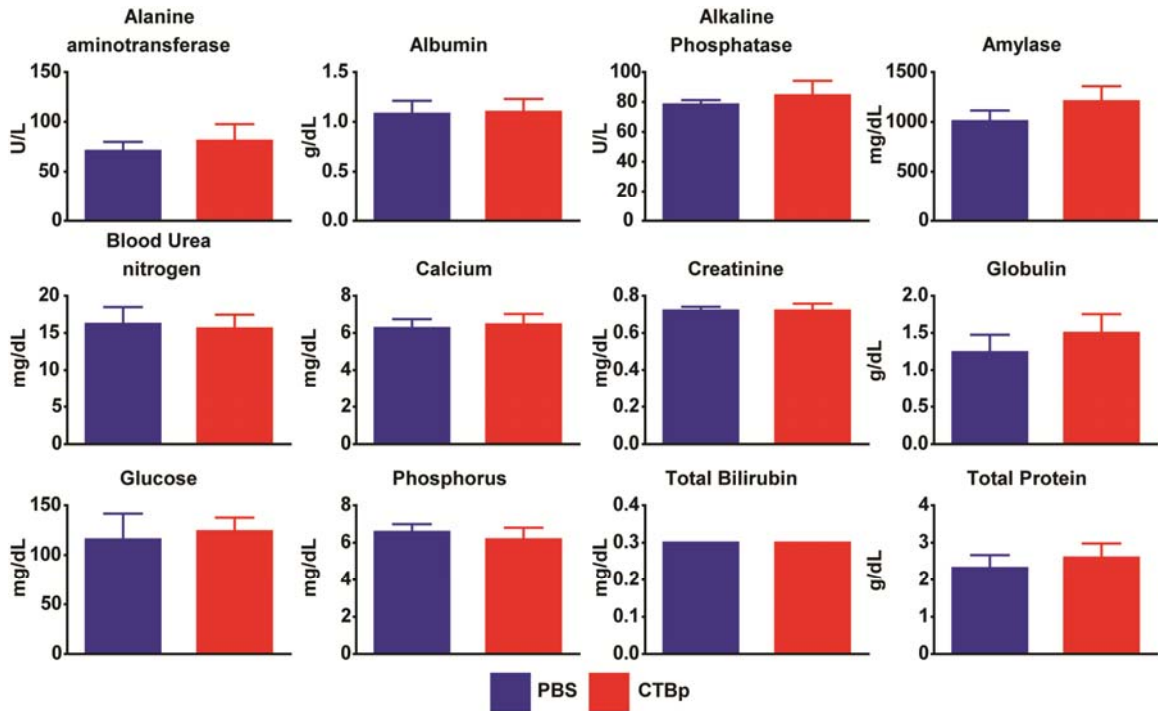


**Figure 4.4. No changes in serum chemistry were noted following CTBp administration.** Animals were given PBS or CTBp every 2 weeks a total of four doses and 1 week later the mice were sacrificed. Whole blood samples were taken from the inferior vena cava and spun in a centrifuge to isolate serum. Serum samples were analyzed by the University of Louisville Research Services Diagnostic Lab. Unpaired *t* test was performed. *N* ≥ 4 per group.

*Serum Interferon  $\gamma$  (IFN $\gamma$ ) was significantly decreased*

We used a Luminex inflammatory cytokine panel to evaluate any changes in serum inflammatory proteins. The only cytokine that was significantly altered was IFN $\gamma$  which was decreased by chronic CTBp administration (Fig. 4.5).

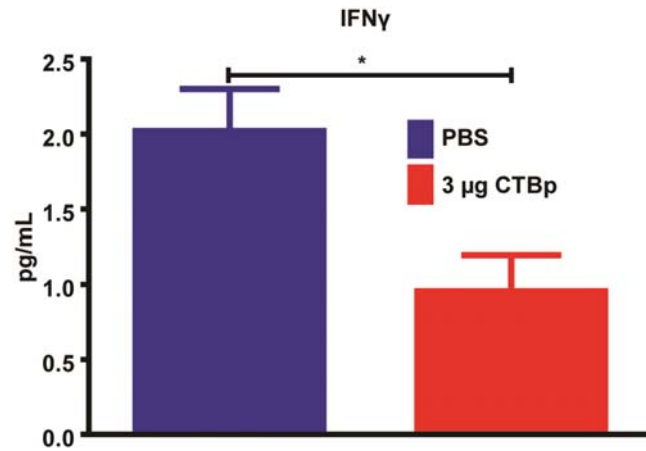


**Figure 4.5. Serum IFN $\gamma$  was significantly decreased by the long-term CTBp administration.** Mice were orally administered PBS or 3  $\mu$ g CTBp biweekly four times and one week after the final dose the mice were sacrificed. Blood was drawn from the inferior vena cava and serum was obtained. Protein levels were determined by Luminex. Protein concentrations for IFN $\gamma$  detected in serum from mice given PBS or CTB. N = 9 per group. \*  $P < 0.05$ ; Unpaired  $t$  test was performed.

*The overall gut microbiome was unaffected*

Fecal samples collected before and after the long-term oral administration with PBS or CTBp, were analyzed for the gut microbial composition.

There were no overall changes in the microbiota after the long-term oral dosing with CTBp (Fig. 4.6). No cage effect was noted over the long-term dosing period in either dosing group. At the Operational Taxonomic Unit (OTU) level, there were eight significantly decreased bacteria with six belonging to the *Firmicutes* phylum and the other two belonging to the *Bacteroidetes* phylum (Fig. 4.7).

However, the overall compositions of the microbiomes remained unchanged, as these are minor bacterial subpopulations.

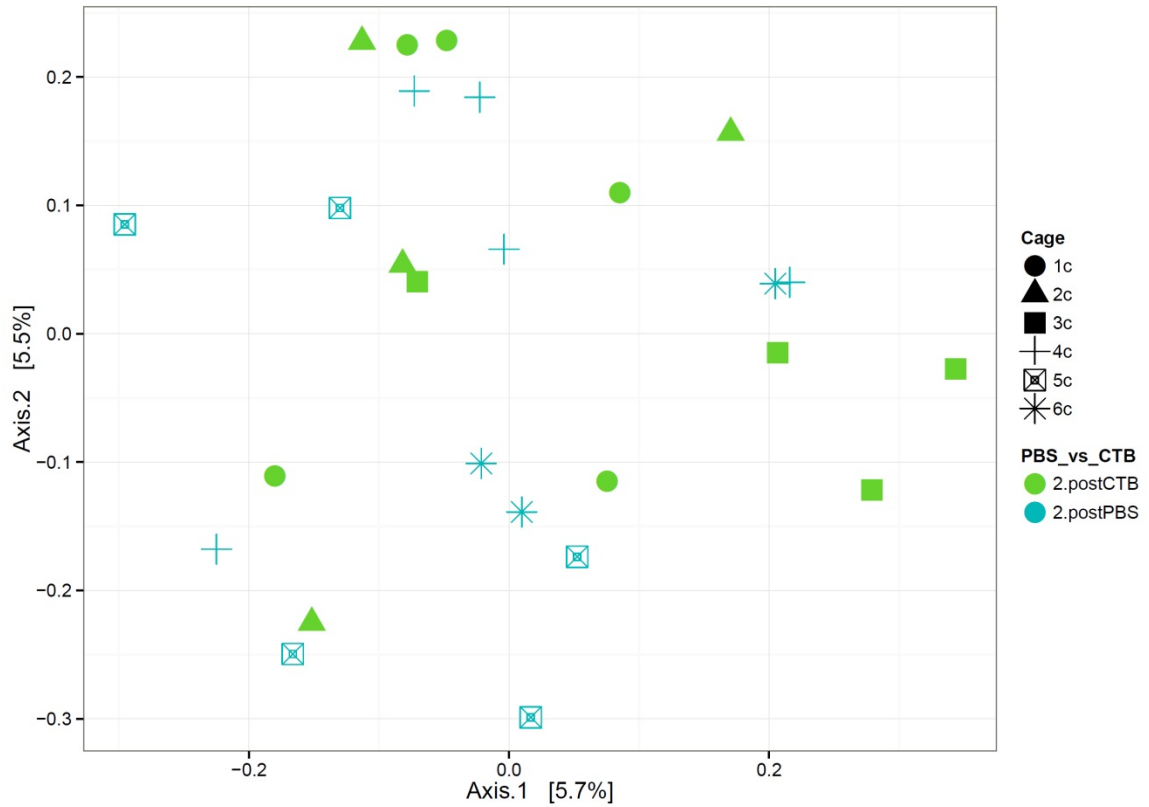


**Figure 4.6. Treatment with CTBp and cage did not significantly alter the overall microbiome.** Mice were orally administered PBS or 3  $\mu$ g CTBp biweekly four times and one week after the final dose the mice were sacrificed. Following bacterial DNA isolation samples were analyzed. No significant alteration of overall microbiome was noted following CTBp administration. Dimensional reduction of the Jaccard distance on the OTU table, using the Principle Coordinate Analysis ordination method.

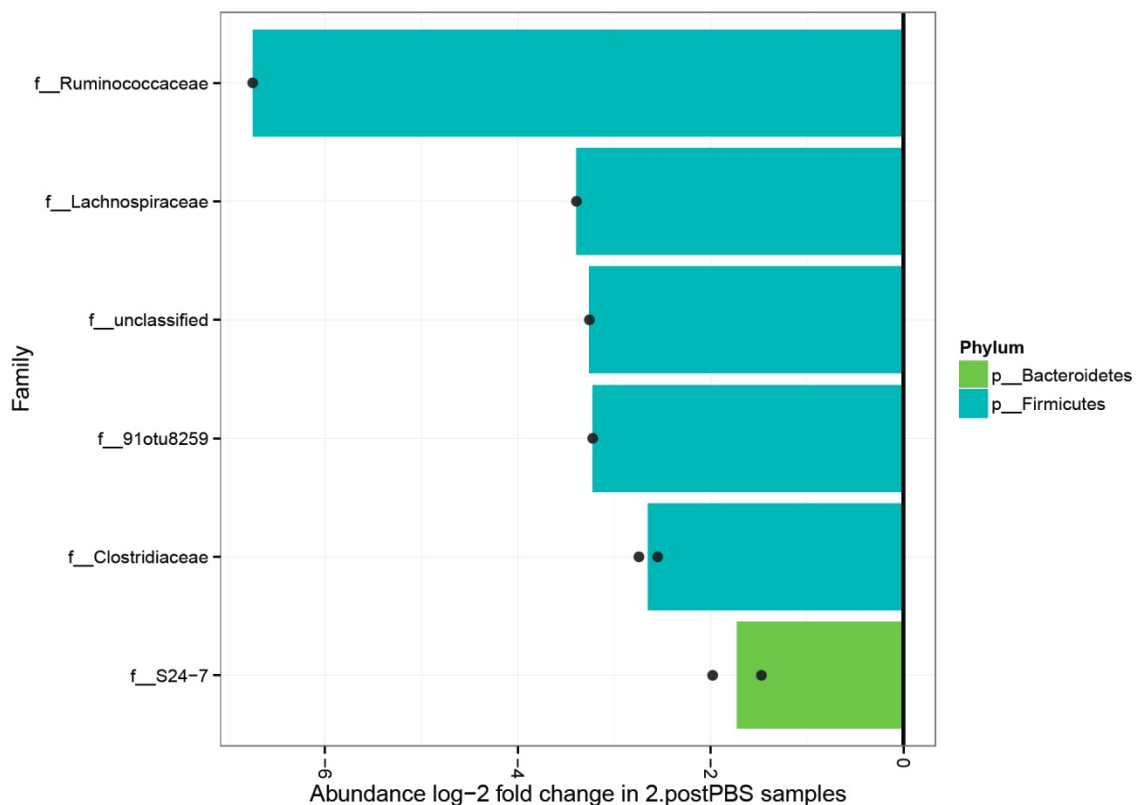


**Figure 4.7. OTU's significantly decreased by CTBp oral administration.**

Mice were orally administered PBS or 3  $\mu$ g CTBp biweekly four times and one week after the final dose the mice were sacrificed. Following bacterial DNA isolation samples were analyzed. The *Bacteroidetes* and *Firmicutes* Phylum had significantly decreased OTU's following CTBp administration. Bars represent median value of each Family and points are OTU's belonging to that family. Features were significant if their False Discovery Rate-corrected p-value was less than or equal to 0.05 and the absolute value of their Log-2 fold change was greater than or equal to 1.

## DISCUSSION

Our work in previous chapters indicated therapeutic potential of orally administered CTBp in colon injury resulting from colitis. Given this, the goal in this chapter was to preliminarily examine the safety of long-term oral CTBp administration. We employed a dosing regimen in which 3 µg CTBp in a total volume of 300 µl (i.e., 10 µg/ml) was orally administered four times biweekly, given that a similar concentration of CTB (1 mg in 75 – 150 ml, or 6.7 – 13.3 µg/ml) is orally administered for Dukoral® vaccines. The protein is active in the lumen, as demonstrated in the epithelial wound healing study in Chapter 3. Hence, luminal concentration was considered more relevant than typical body weight-based dose administration.

Flow cytometry analysis revealed that immune cell profiles in diverse lymphoid tissues were significantly altered by CTBp over the long-term dosing schedule (Fig. 4.1 and 4.2), with the exception of small intestine lamina propria, similar to the short-term study in Chapter 2. By contrast, other lymphoid organs in the GI tract and spleen were significantly affected by long-term CTBp administration. Notably, T<sub>H</sub>17 cells were significantly blunted in Peyer's patches and mesenteric lymph nodes which could implicate a unique anti-inflammatory function of CTBp because T<sub>H</sub>17 cells are generally considered to play an inflammatory role in multiple autoimmune diseases (*e.g.* rheumatoid arthritis, psoriasis, and Crohn's disease)(150). In this regard, a recent study in a rat model of rheumatoid arthritis showed that oral administration of Norisoboldine significantly reduced arthritis, which was associated with a decrease in T<sub>H</sub>17 cells

in the mesenteric lymph nodes and Peyer's patches (151). Furthermore, the anti-inflammatory effect of Norisoboldine was gut dependent as it could not be reproduced though intraperitoneal injection. Meanwhile, the spleen and colon had a reduction in T<sub>REG</sub> cells when CTBp was given chronically. T<sub>REG</sub> cells are generally considered to be anti-inflammatory (152, 153); however, there are pro-inflammatory characteristics of these cells (154, 155). These pro-inflammatory T<sub>REG</sub> cells appear to differentiate in the periphery, suggesting a specific cytokine profile plays a key role in their development (156). Further analysis of T<sub>REG</sub> subsets following CTBp administration may be warranted based on our results to determine their phenotype.

Interestingly, complete blood count indicated that overall white blood cell populations are significantly increased by CTBp (Fig. 4.3). Leukocytosis, increased white blood cell counts, is a common finding that encompasses both benign and malignant conditions, which can be caused by infection, inflammation, allergic reaction, cancer, hereditary disorders, etc. (157). Since CTBp is a potent mucosal immunogen, it is likely that the protein's immunogenicity had been transduced into the systemic immune system upon repeated oral administration. Our data showed that CTBp boosted the entire immune cell population without causing an imbalance of overall cell types or any discernible impact on the animal health. However, the flow cytometry analysis indicated some compartmentalized changes in the subpopulations, suggesting that there is an immunological consequence upon a long-term oral CTBp administration that could not be identified in the present study. Hence, additional

studies using a longer-term dosing strategy and varying dose amounts are warranted to reveal clinical and safety implications of the systemic immune modulation induced by long-term oral CTBp dosing.

Despite the significant changes in the systemic immune cell profile, no apparent organ toxicity was found based on results from the serum chemistry (Fig. 4.4), indicating the general safety of CTBp in our dosing scheme. Similar to what was seen in the short-term dosing study in Chapter 2, the overall microbiome did not appear to be effected by CTBp administration and there was no cage effect in our experimental design (Fig. 4.6).

In summary, we demonstrated that a long-term biweekly oral administration of CTBp, as a dosage similar to that used in an internationally licensed oral cholera vaccine, does not have any discernible organ toxicity but it did induce compartmentalized changes in immune cell populations in both gut and systemic immune systems. The effect of these immune cell changes on immune competency needs to be further investigated. However, our results justify the use of long-term administration of 3  $\mu$ g CTBp for studying its effects on chronic inflammation in the colon.



## CHAPTER 5: CTBp MITIGATES CHRONIC COLITIS

## INTRODUCTION

CTBp is a functional, non-glycosylated variant of CTB that can be rapidly and efficiently manufactured in *Nicotiana benthamiana* plants (76). In Chapters 2 and 3, our data suggested that CTBp was able to enhance mucosal wound healing mediated by activation of TGF $\beta$  signaling in the colon epithelia. We explored CTBp's potential as a therapy in ulcerative colitis and showed that oral administration of CTBp blunted inflammation and weight loss, which was associated with reduced inflammatory cytokines at gene expression and protein levels, in mice exposed to dextran sulfate sodium (DSS) over 1 week. Subsequently, in Chapter 4 we determined that four biweekly administrations of 3  $\mu$ g CTBp did not lead to any apparent toxicity in mice, indicating CTBp may be applicable for long-term treatment in ulcerative colitis patients.

Ulcerative colitis has become a growing concern in the developed world and leads to an enhanced risk of developing colon cancer (158, 159). Colon cancer is the 2<sup>nd</sup> leading cause of cancer-related death in the United States (160). Extent and duration of inflammation in the colon plays a clear role in the development of colorectal cancer, which suggests that, by controlling the inflammation, we can decrease the incidence of colorectal cancer. Our results from Chapter 3 revealed that, in the acute colitis setting, orally administered CTBp was able to protect against the inflammation associated with DSS-induced colitis and injury in the colonic mucosa. Additionally, Granulocyte macrophage colony-stimulating factor (GM-CSF), which has previously been shown to enhance tumorigenesis in the colon (161), was blunted by CTBp administration

(Fig. 3.8 and 3.10). These findings lead us to postulate that there is potential for CTBp to mitigate chronic colitis and reduce the risk of tumor formation in the colon under chronic inflammatory conditions.

A potential concern from our earlier finding, in Chapter 2, is that CTBp appeared to induce epithelial to mesenchymal transition (EMT) in the colon epithelia, according to gene expression microarray analysis, because EMT is associated with increased invasion and metastases in colorectal cancer (CRC) (162, 163). Although, obtained under basal conditions and not in a model of injury, the results from the CTBp oral administration study and the Caco2 wound healing experiment may point to a potential side effect of CTBp that could enhance tumorigenesis in a chronic colitis model via TGF $\beta$  driven EMT.

As a counter argument to this concern, in the DSS colitis model, we found that colonic inflammation was reduced by oral administration of CTBp, in which TGF $\beta$ 1 actually returned to baseline faster than with PBS pretreatment during the recovery phase (Fig 3.9). Additionally, fibrosis was prevented by CTBp in the acute colitis model, which indicates that the protein did not cause aberrant stimulation of TGF $\beta$  signaling (106). All the above results point to the importance of investigating CTBp's impacts on the development of colon cancer in chronic colitis.

To address the above issue, we employed the azoxymethane/DSS model of ulcerative colitis in this chapter so that we could build on our earlier findings in the acute DSS model of colitis and explore CTBp's protective effect under

chronic inflammation. In this model, we employed a dosing regimen used in Chapter 4, in which CTBp was orally administered biweekly while inducing chronic inflammation in the colon. Our results provide important implications towards the therapeutic use of CTBp for patients who have already presented with inflammation from ulcerative colitis.

## **METHODS**

### *Animals*

8 week old C57BL/6J female mice were obtained from Jackson Laboratories (Bar Harbor, Maine) and allowed to acclimate for one week. Animals were housed according to the University of Louisville's Institutional Animal Care and Use Committee standards.

### *Colon cancer model*

Azoxymethane (AOM; 10 mg/kg) was administered by intraperitoneal injection to the mice (Fig. 24). Body weights were measured just prior to the DSS exposure period as a baseline weight. Every morning during the study, body weights were measured and percent change from baseline was determined. DSS exposure (2%) was initiated 1 week after the AOM injection for 7 days and allowed to recover for 14 days following the DSS exposure period. The DSS exposure and recovery cycle was repeated 3 times and mice were sacrificed by Carbon Dioxide inhalation followed by thoracotomy following the 3<sup>rd</sup> cycle. This method is slightly modified from the published protocol (123). Colons were excised for further analysis.

### *Disease activity index*

Animals were scored on a daily basis which consisted of the following scoring rubric adapted from the literature (123, 164). Weight loss: 0 for no weight loss, 1 for 1 to 5% weight loss, 2 for 6 to 10% weight loss, 3 for 11 to 15% weight loss and 4 for greater than 15% weight loss. Stool consistency: 0 for normal stools, 2

for loose stools and 4 for diarrhea. Occult blood: 0 for no blood, 1 for some occult blood, 2 for heavy positive occult blood, 3 for visible blood in stool with no anus clotting, or 4 for gross anus bleeding and clotting present.

### *Tumor scoring*

Tumors were scoring via endoscopic analysis of the full length of the colon.

Tumor scoring was based on the following rubric: 0 for no tumor, 1 is a very small but detectable tumor, 2 the tumor covers up to 1/8 colon circumference, 3 tumor covers 1/4 of colon circumference, 4 tumor covers up to 1/2 of colon, and 5 tumor covers more than 1/2 of colon.

### *Histology.*

Colons were removed and washed with PBS and cut into thirds longitudinally. A portion of the colon was fixed with paraformaldehyde overnight and stored in 70% Ethanol until paraffin embedding, sectioning and routine H&E staining.

Inflammation scoring was performed using a scale that has been previously published (126). Sections were scanned using an Aperio ScanScope CS (Leica Biosystems) for grading. Tissue was scored based on a previously established protocol with minor modifications (126). The colon was scored based on proximal, middle and distal sections determined by histological evaluation.

Briefly, grades were assigned as follows: grade 0 = intact crypt, grade 1 = loss of bottom one third of the crypt, grade 2 = loss of bottom two thirds of the crypt, grade 3 = loss of entire crypt with the surface epithelium intact, and grade 4 = loss of the entire crypt and surface epithelium. Additionally this grade was

assigned to percentages of the colon section based on 10% increments and averaged for each sections final score. Tissue sections from 8 mice were scored and averaged for each group. Statistics were performed comparing each group.

#### *RNA Isolation*

Sections from the distal colon were stored in RNA*later*<sup>™</sup> (Qiagen, Valencia, CA) at -20°C until RNA was isolated. Colon Tissue (approximately 14 mg) were placed in QIAzol lysis reagent in a 2.0 mL conical bottom centrifuge tube with Zirconia/Silica beads. A Bead Beater was used to homogenize the tissue. An RNease Microarray Tissue Kit from Qiagen was used to purify the RNA from the tissue homogenate. RNA was stored at -80°C until use.

#### *Quantitative RT-PCR gene expression analysis*

Gene expression was carried out by quantitative RT-PCR using quality verified RNA samples obtained previously. First strand cDNA was obtained from reverse transcription of 150 ng RNA using a SUPERSRIPT VILO cDNA synthesis kit (Life Technologies) according to the manufacturer's instructions. Optimal amounts of template cDNA were added to a reaction mixture containing 10 µl of 2×TaqMan® Fast Advanced Master Mix (Life Technologies) and endonuclease free water to 20 µl and loaded in TaqMan® Array Standard 96 well Plates (Applied Biosystems). These plates contain pre-spotted individual TaqMan® Gene Expression probes for detection of genes of interest (Table 5.1) as well as the house keeping genes 18 S, beta actin (ACTB), and GAPDH (Table Sup). PCR amplification was carried out using a 7900HT Fast Real-Time PCR System

(Applied Biosystems) in the following conditions: 95°C, 20 min; 40 cycles (95°C, 1 min); 20 min at 60°C. The 7500 Software v2.0.6 (Applied Biosystems) was used to determine the cycle threshold (Ct) for each reaction and derive the expression ratios.

**Table 5.1. Gene Identity for Chronic qPCR analysis**

| <b>Gene Name</b>                                     | <b>Gene ID</b> | <b>Entrez Gene ID</b> |
|--|----------------|-----------------------|
| Colony stimulating factor 2 (granulocyte-macrophage) | Csf2           | 12981                 |
| NLR family, pyrin domain containing 3                | Nlrp3          | 216799                |
| Transforming growth factor, beta 1                   | Tgfb1          | 21803                 |
| Interleukin 18                                       | Il18           | 16173                 |
| Interferon gamma                                     | Ifny           | 15978                 |
| Forkhead box P3                                      | Foxp3          | 20371                 |

### *Protein isolation*

Distal colon sections were isolated at sacrifice and stored at -80°C until the protein was isolated and analyzed. Briefly, tissue was frozen in liquid nitrogen and pulverized with a Bessman Tissue Pulverizer and placed in T-PER (Thermo Scientific) with a protease inhibitor cocktail (Sigma-Aldrich). Protein was isolated by gravity centrifugation of tissue fragments, removing the buffer containing isolated protein, and storing at -80°C until analysis.

### *Protein quantification*

Protein sample concentrations were determined using a Nanodrop 1000 (Thermo Scientific). Protein was normalized for all samples prior to loading on a Mouse Cytokine/Chemokine Magnetic Bead Panel (EMD Millipore). The panel was analyzed with a Milliplex MAP Kit on a MagPix with Luminex xMAP technology.

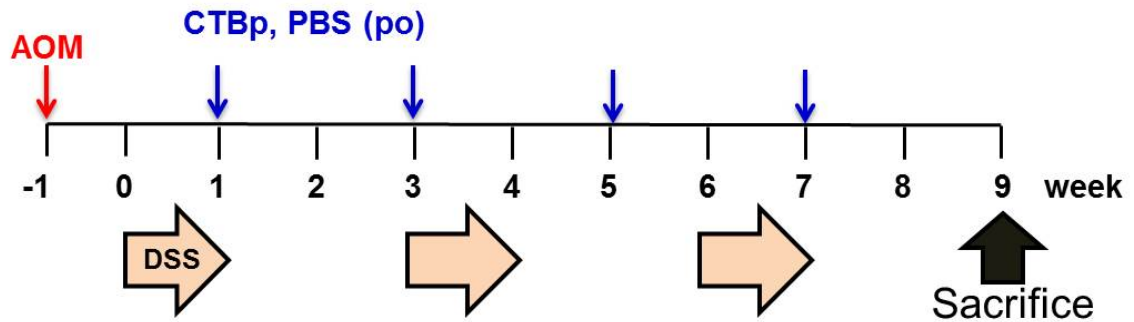
### *Statistics*



Graphs were prepared and analyzed using Graphpad Prism version 5.0 (Graphpad Software). To compare two data sets, we conducted an unpaired, two-tailed Student's *t* test. To compare three or more data sets, we conducted a one-way ANOVA with a Bonferroni post-test. For body weight and DAI results we conducted a Two-way ANOVA with a Bonferroni post-test.

## RESULTS

*CTBp oral administration protected against colon cancer development in an AOM/DSS colitis model*



| Group | Genotype | Sample             |
|-------|----------|--------------------|
| 1     | C57BL/6  | PBS                |
| 2     | C57BL/6  | 10 µg CTBp+AOM     |
| 3     | C57BL/6  | PBS+AOM+DSS        |
| 4     | C57BL/6  | 3 µg CTBp+AOM+DSS  |
| 5     | C57BL/6  | 10 µg CTBp+AOM+DSS |

Figure 5.1. Study design for chronic colitis and colon cancer model.

The significant protection seen in the acute colitis/colon injury model (Chapter 3) prompted us to investigate if CTBp could also protect in a colitis-associated colon cancer model using AOM intraperitoneal injection followed by three cycles of DSS exposure/recovery (Fig. 5.1). CTBp was given at the end of the first DSS exposure period followed by three additional doses every two weeks for a total of four doses, the same dosing schedule used in a long-term CTB administration study in Chapter 4; combined with a preliminary study assessing therapeutic dosing (data not shown), we decided to test 3 and 10 µg CTBp in the chronic DSS experiment.

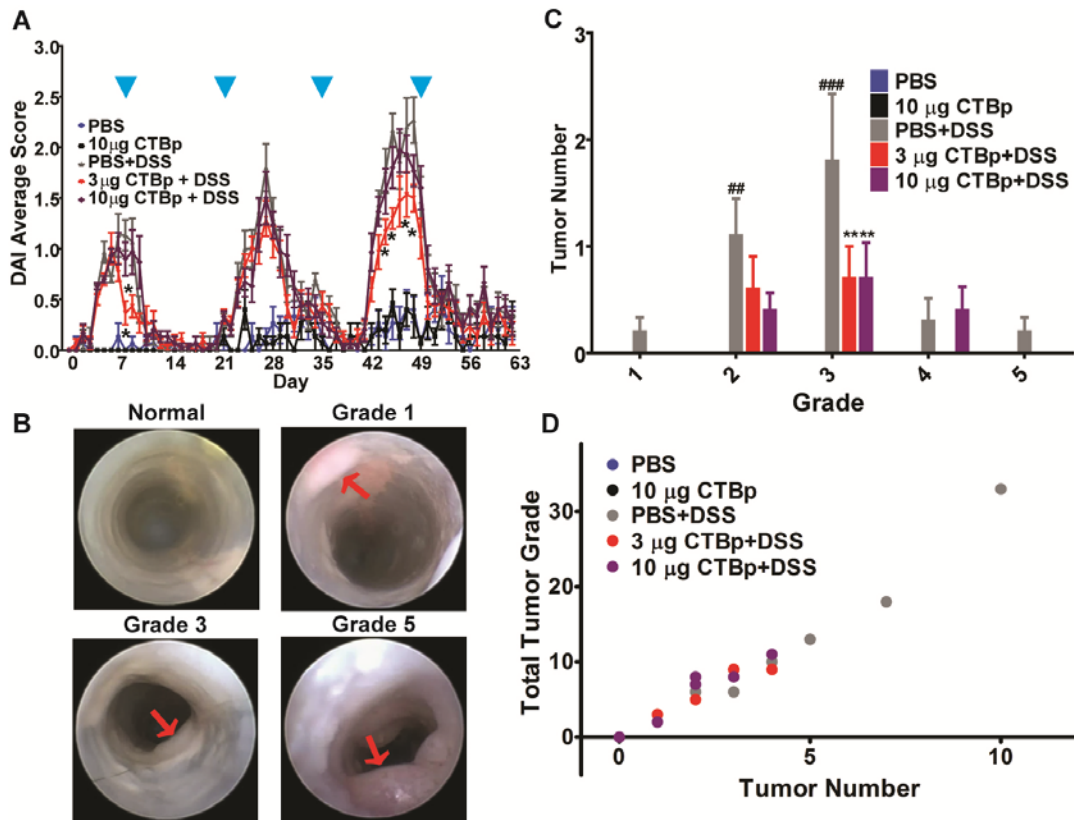


**Figure 5.2. CTBp protects against colitis associated colon cancer.**

Mice received azoxymethane (AOM) i.p. one week prior to DSS exposure. Mice were given water or 2% DSS water for seven days followed by water for two weeks; the cycle was repeated two additional times. Mice were dosed orally with PBS, 3 μg CTBp or 10 μg CTBp on days 7, 21, 35, and 49 (Blue arrows). **A)** Disease Activity Index (DAI). Body weights, fecal consistency and occult blood were scored daily. **B)** Representative tumor scoring. Tumors were scored from 0 to 5 with 0 being normal tissue and 5 being greater than 50% of colon circumference tumor invasion. Red arrows indicate representative tumors. **C)** Tumor scoring results. Tumors were scored based on the scale in B. **D)** Tumor score vs tumor number. Total tumor number is the X axis and total tumor grade is the Y axis. A dot represent each mouse. Mice with no tumors are at the axis intersection. Mean ± SEM is shown (n = 5 for PBS and 10 μg CTBp groups and all other groups n = 10). A repeated-measures ANOVA with Bonferroni Correction was performed for A and C. For A, \*  $P < 0.05$  compared to PBS+DSS group. For C: ###  $P < 0.01$  and ####  $P < 0.001$  compared to PBS and \*\*  $P < 0.01$  compared to PBS+DSS.

As shown in Figure 27, CTBp administration (3 μg dose) significantly decreased the disease activity index (DAI) score immediately following the first dose of CTBp and more dramatically during the 3<sup>rd</sup> DSS exposure period (Fig. 5.2A). Such a clear effect was not observed with the higher dose (10 μg) of CTBp. However, DSS exposed mice developed, on average, 4 tumors per colon over the length of the study, which was reduced by CTBp administration at both dose levels to approximately 1 – 2 tumors per colon (Fig. 5.2C). Additionally, tumor

growth was significantly limited by CTBp, as indicated by the decreased number of grade 3 – 5 tumors (Fig. 5.2C) and total tumor grade (Fig. 5.2D) in CTBp-administered groups. Of note, CTBp administration (10 µg) without DSS exposure did not induce any sign of intestinal inflammation (Fig. 5.2A) or tumor growth (Fig. 5.2C, D), suggesting the proteins lack of adverse effect at this dose level.

*CTBp significantly altered colon cancer associated genes*

In order to further characterize the protection of CTBp in colon cancer we evaluated genes associated with colon cancer development and progression. CTBp administration resulted in significantly increased expression of *Tgfβ1*, *Foxp3*, *Ifny*, *Csf2* and *Nlrp3* while downregulating the expression of *Il-18* two weeks following the final DSS exposure (Fig. 5.3). These results reveal significant upregulation of early-stage tumor suppressing genes by CTBp (i.e. *Ifny*, *Csf2* and *Tgfβ1*) (165-167).

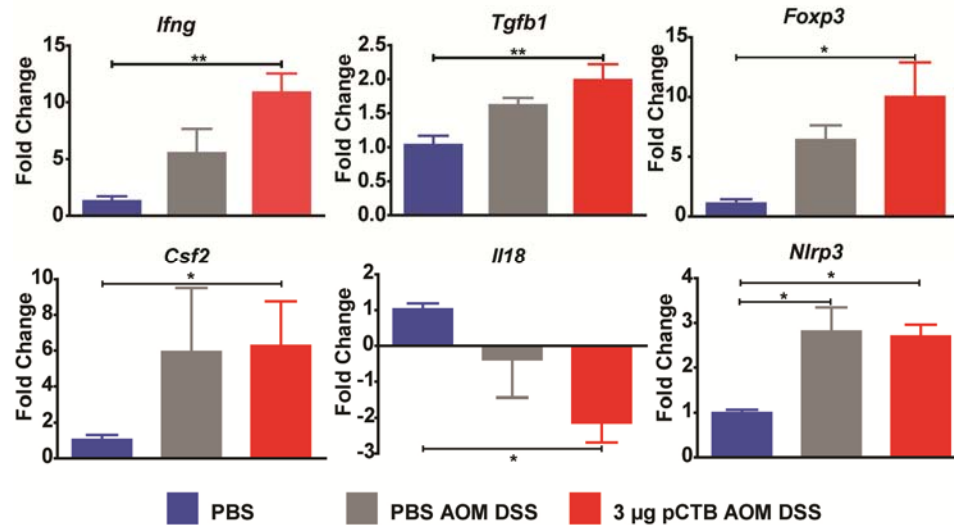


**Figure 5.3. CTBp significantly enhances genes related to suppression of tumor development.** Mice were injected with AOM one week prior to the first round of DSS exposure. The one week DSS exposure was followed by a two week recovery period, which was repeated two additional times. The mice were sacrificed immediately after completion of the final round of DSS exposure/recovery. Colons were removed and RNA isolated. Gene expression was analyzed by qRT-PCR. Graphs are gene expression in colon tissue from mice given PBS or CTBp and exposed to water or DSS containing drinking water. Mean  $\pm$  SEM is shown. N = 5 per group. \*  $P < 0.05$  and \*\*  $P < 0.01$ ; one-way ANOVA Bonferroni's multiple comparisons test.

*CTBp significantly decreases inflammatory proteins and significantly increases anti-tumor proteins in distal colon tissue*

While PBS administered animals had elevated pro-inflammatory cytokines after the induction of chronic colitis, CTBp treated animals completely blunted the significant inflammatory cytokine responses. For example, GM-CSF, IL-1 $\alpha$ , and MIP-2 were significantly blunted by CTBp compared to PBS (Fig. 5.4).

Additionally, several inflammatory cytokines (KC, M-CSF, TNF $\alpha$ , and MIG CXCL9) appeared to be blunted by CTBp. In sharp contrast, IFN $\gamma$  and IL-2 were significantly increased by CTBp treatment.

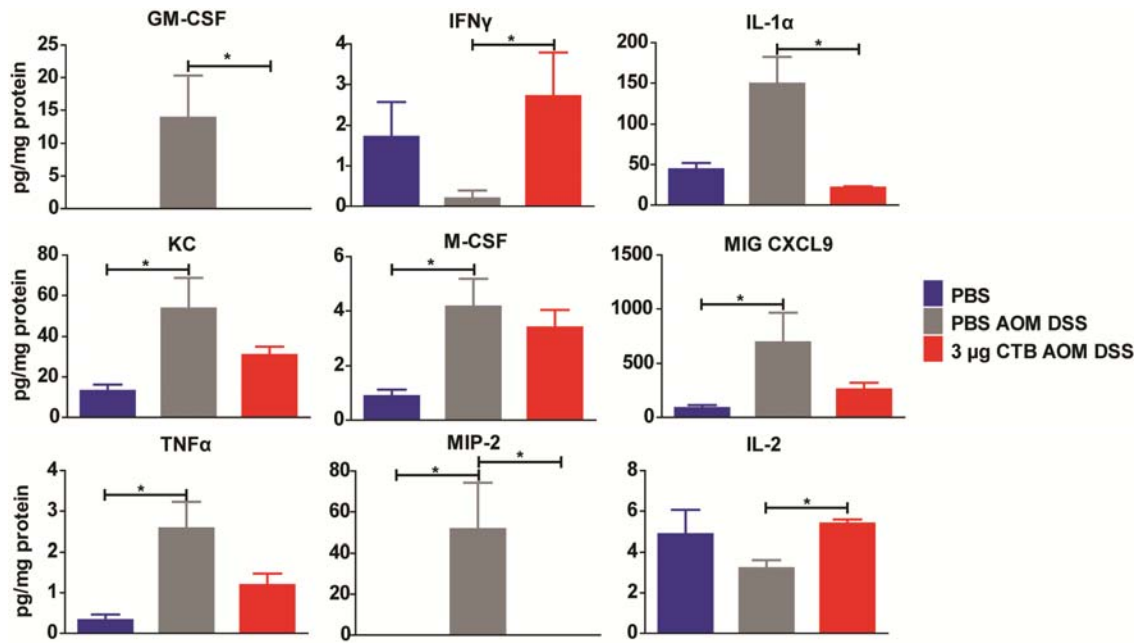


**Figure 5.4. CTBp treatment blunted tissue inflammatory cytokine protein levels.**

Mice were injected with AOM one week prior to the first round of DSS exposure. The one week DSS exposure was followed by a two week recovery period, which was repeated two additional times. The mice were sacrificed immediately after completion of the final round of DSS exposure/recovery. Colons were removed and Protein isolated. Protein levels were determined by Luminex. Graphs are protein concentrations for cytokines detected colon tissue from mice injected with AOM or PBS, given PBS or CTBp and exposed to water or DSS containing drinking water. N = 5 per group. \*  $P < 0.05$ , \*\*  $P < 0.01$ ; one-way ANOVA Bonferroni's multiple comparisons test

## DISCUSSION

Our previous findings indicated that CTBp was a potential therapy for ulcerative colitis in an acute colitis study. Long-term dosing with CTBp in healthy animals did not reveal any major toxicity, leading us to analyze if the long-term administration of CTBp could be protective in a chronic model of ulcerative colitis (AOM/DSS colon cancer model).

In the AOM/DSS colon cancer model, the DAI revealed significant protection by CTBp immediately following dosing and during the third cycle of DSS exposure (Fig. 5.2A). Notably, biweekly oral administration of CTBp during the induction of chronic colitis resulted in a significant decrease in the tumor number and grade at the end of the study (Fig 5.2C and D). These findings illustrate that CTBp's protection against inflammation also slows the development of colon tumors. In support of these results, microarray analysis of colon gene expression in healthy mice (Fig. 2.5) previously revealed that *Hspa5*, *Hspa8* and *Hsp90aa1* were significantly suppressed by CTBp administration; increased expression of these stress proteins has been associated with poor outcomes in colon cancer (90). Consequently, there may be an additional mechanism for CTBp to slow the growth of tumors in colorectal cancer adding to the anti-inflammatory and wound healing potential observed *in vivo* and *in vitro*, respectively.

The results from the DAI and tumor scoring suggested that 3  $\mu\text{g}$  CTBp was superior to 10  $\mu\text{g}$  CTBp (Fig 5.2), which was similar to what occurred with the acute colitis work in Chapter 3. This suggests the protection by CTBp may

reach saturation in which higher doses no longer provide added benefit. Current immune therapies in IBD have similar features, whereby higher doses do not increase efficacy and can even lead to deleterious effects (168). This suggests that different doses of CTBp should be evaluated to establish a therapeutic window. Nevertheless, the current results aid in deciphering the protection from chronic colitis by CTBp at the molecular level.

Our results from oral administration of CTBp in healthy mice (Chapter 2) suggested there was an upregulation of TGF $\beta$ -driven wound healing pathways. In the present AOM/DSS study, we again observed that CTBp significantly induced gene expression of *Tgfb1* in the colon (Fig. 5.3). As previously established, aside from its anti-inflammatory potential, TGF $\beta$  can be tumor promoting. However, in early stages of cancer, this cytokine has been shown to suppress tumor development (reviewed in (167)). Tumor promoting functions of TGF $\beta$  occur later in the progression of cancer when mutations in TGF $\beta$ RII and *SMAD4* occur after transition from an adenoma to carcinoma and allow for tumor progression (169). Additionally, once tumors developed, TGF $\beta$  can aid in invasion by facilitating EMT, blunting the immune response and eventually leading to metastasis (170). Another dual-role gene we found significantly increased by CTBp administration was *Foxp3*, commonly associated with blunting inflammation and immune cell response but can lead to cancer progression (171). Recently, Pastille et al. found that by ablating regulatory T cells, the antitumor immune response could be enhanced in the AOM/DSS model (172). On the contrary, increased Foxp3<sup>+</sup> Treg cells in CRC did not alter patient



survival and other studies revealed that a high frequency of tumor infiltrating Foxp3<sup>+</sup> Treg cells leads to a favorable prognosis for CRC patients (173). Collectively, the above results may indicate that CTBp-induced *Tgfb1* and *Foxp3* in the AOM/DSS model played a role at an early stage, and as a result, did not promote the tumor development.

Other cytokines essential to the inhibition of tumor growth were also altered by CTBp administration. For example, IFN $\gamma$ , IL-2 and GM-CSF have been shown to suppress colon cancer progression (165, 166, 174, 175) and the two former cytokines were significantly induced while the latter was reduced by CTBp administration compared to PBS control in AOM/DSS-exposed mice. These results point to a potential inhibition of tumor progression by CTBp administration; however, our results were from a single time point and therefore leave unanswered questions. Further experiments must be performed to address the potential effects of CTBp in tumor progression. Nevertheless, the data did point to CTBp's strong anti-inflammatory effect in the colon in the chronic colitis model similar to what was observed in the acute colitis study. In fact, multiple pro-inflammatory cytokines were blunted to near baseline by 3  $\mu$ g CTBp two weeks after the final DSS exposure period. TNF $\alpha$  and IL-1 $\alpha$  are both involved in epithelial breakdown in ulcerative colitis (176, 177). IL-1 $\alpha$  is an alarmin that is released from intestinal epithelial cells which initiates the inflammation in the colon. GM-CSF and M-CSF both play a role in macrophage polarization to either the M1 (proinflammatory) or M2 (anti-inflammatory) subtypes, respectively (178). CTBp did not significantly elevate either of these

proteins, similar to the TNF $\alpha$  and IL-1 $\alpha$  results, indicating that inflammation was decreased by CTBp. This is further confirmed by Kc and MIG CXCL9 protein levels, a proinflammatory cytokine and chemokine, respectively, which are present in more severe ulcerative colitis (179, 180).

Recently, the whole CT molecule (not CTB) has been shown to protect against colon carcinogenesis in the DSS colitis model employing Balb/c mice (134). In that study, 10  $\mu$ g of CT was orally administered at the first day of each of the three cycles of DSS exposure. However, we were able to achieve a similar endpoint with four biweekly doses of 3  $\mu$ g of CTBp, thus reducing the total amount of protein required for protection by sixty percent. Additionally, CTBp was administered on a scheduled basis similar to current therapies, while the CT was dosed at the initiation of DSS exposure. The major discrepancy between the seemingly similar effects obtained by CT and CTB is manifested by the cytokine profiles in the colon; CT significantly increased the anti-inflammatory cytokine IL-10, whereas we did not see any change in this cytokine (data not shown). As a result, the authors of the CT study attributed the protective mechanism to increased IL-10 and colon T<sub>REG</sub> cells. In contrast, we postulate CTBp-mediated protection was conferred in part through enhanced mucosal healing based on TGF $\beta$  signaling in the colon epithelia along with anti-inflammatory activity.

In summary, this chapter demonstrated the potential of CTBp to mitigate chronic colitis in an animal model. Our data additionally point to an appropriate therapeutic window for CTBp to decrease inflammation in the colon and protect

against tumor development. These results provide a basis to further investigate CTBp for a potential therapeutic option in ulcerative colitis treatment.

CHAPTER 6: SUMMARY OF CTBp RESEARCH AND  
IMPLICATIONS FOR FUTURE DIRECTIONS

## SUMMARY OF THE PRESENT CTBp STUDIES

Oral administration of CTB leads to a robust antibody response and an anti-inflammatory effect (60, 76, 181, 182). The former represents the protein's most well-known biological activity, which has been exploited in cholera prevention (as a component of Dukoral® vaccine) and vaccine development for decades. On the other hand, the utilization of CTB's immunomodulatory activity in the treatment of inflammatory diseases is yet to be achieved, in part due to its obscure underlying mechanisms. Thus, in the present studies we initially attempted to comprehensively unveil the impacts of orally administered CTBp on the GI tract; the use of CTBp is justified because it retains key molecular features of CTB and an efficient manufacturing method has been established (76). Global analysis tools based on flow cytometry and gene expression microarray revealed that oral administration of CTBp exhibits previously unidentified impacts on the distal part of the GI tract; recruitment of macrophages, dendritic cells and natural killer cells into the colon lamina propria and upregulation of TGF $\beta$  signaling pathways in the colon (Fig. 2.3, 2.5). These data subsequently lead us to demonstrate that CTBp promotes wound healing in the colonic mucosa *in vitro* (Chapter 3). Although CTB was previously shown to upregulate TGF $\beta$  expression in B cells for IgA class switching (104) and induce *Tgfb1* expression in lymphoid cells in models of autoimmune diseases (101-103), the present study showed for the first time that CTB can exert TGF $\beta$ -driven mucosal healing in the colon epithelia.

TGF $\beta$  is a key cytokine that has multifaceted functions including pivotal roles in gut homeostasis and intestinal wound healing (106, 140). A recent study by Oshima et al. has shown that the suppression of TGF $\beta$  signaling in an injured and inflamed mucosa leads to invasive tumor development in the colon, showing that TGF $\beta$ -mediated mucosal repair plays a key role in colitis-associated colon tumor prevention (183). This is in line with our findings in the chronic DSS study, whereby bi-weekly oral administration of CTBp reduced DAI and colon tumor development (Chapter 4). However, it is also known that TGF $\beta$ 1 is elevated in collagenous colitis and connected to increased collagen deposition and fibrosis, indicating the dual nature of this cytokine in mucosal remodeling (184, 185). In this regard, the fact that CTBp administration prevented fibrosis formation in the acute DSS colitis study (Fig. 3.5, 3.9) suggests that the CTBp dosing regimen used here did not overstimulate TGF $\beta$  signaling to a level causing adverse effects. Additionally, this may in turn explain why the higher dose of CTBp was not as effective as the lower dose in the acute and chronic DSS studies (Fig. 3.3 and 5.2). However, the reduced wounding in the colon evident following CTBp administration in both acute and chronic DSS colitis studies, may also have prevented fibrosis seen in control samples. Thus, detailed investigation into CTBp's dose-effect relationship is warranted to define a therapeutic window for optimal protection in ulcerative colitis.

It is of interest to note that CTBp-induced TGF $\beta$  activation in the colon epithelium was accompanied by a significant increase of several innate immune cells in the same mucosa (Fig. 2.1, 2.3). CTB is known to alter the T cell profile

under various conditions (reviewed in (33, 59, 97)), and *in vitro*, the protein affected dendritic cell maturation (99) and diminished the proinflammatory response of macrophages to lipopolysaccharide (100). However, the protein's impacts on immune cells in different regions of the GI tract, as shown in Chapter 2, are unprecedented. At this point, the mechanism by which CTBp induced such compartmentalized effects on GI tract immune cells is not clear, which therefore represents a limitation of the present work. We speculated on a possible change in the gut microbiota. However, the overall fecal microbiome profile was not significantly altered at the point when colon gene expression and immune cell profile changes were observed (Fig. 2.9 and 2.10A). *Bacteroidetes* and *Firmicutes* spp. dominated at the phylum level (Fig. 2.10B), which is typical for C57BL/6J mice (95, 96). We also speculated that chronic CTBp dosing may affect the gut microbiota; however, a chronic administration of CTBp in Chapter 4 did not alter the overall fecal microbiome profile. Both short-term and long-term experiments yielded a small number of significantly altered operational taxonomic units (OTUs), heavily populated by the *Firmicutes* phylum, however no OTUs were significant in both experiments.

There still remains much work to be done in regard to the possible impacts of CTBp on gut microbiota. Because CTBp is administered orally, there may be changes in the microbiota present in the upper intestinal tract of the mice, which could not be revealed in the fecal analysis we performed. The gut microbiota varies throughout the GI tract, therefore fecal samples may not be representative of the microbiota in the proximal intestinal tract (186). As an example, Pang et

al. found that caecal and fecal microbiota samples do not cluster together from the same mouse (149). More recently it has been shown that in C57BL/6 mice the colon and fecal samples are similar in comparison to gastric and small intestinal samples (187). Additionally, changes at the species level in the gut microbiota can alter energy and lipid metabolism; indicating that a shift at the Phylum level is not necessary for a metabolic shift in the gut (188). Our analysis did reveal changes at the species level in fecal microbiota but any effect on metabolism could not be determined in the current work. Lastly, the gut microbiota play a role in the development of DSS colitis (189) and we did not evaluate the microbiota in our colitis models. Exploration of the microbiome under the inflammatory conditions of the DSS colitis model may reveal possible changes in the microbiota resulting from CTBp administration.

Meanwhile, the observation that CTBp concomitantly stimulated the activation of TGF $\beta$  signaling and the increase of macrophages, dendritic cells and natural killer cells in the colon leads us to postulate that the latter effect might also play a role in the protein's mucosal healing effects. For example, macrophages can remove bacteria that penetrate the epithelium and damaged tissue (190) and play an important role in enhancing late phase wound healing (191). Lamina propria-resident dendritic cells were previously shown to suppress the severity of DSS colitis (192). Natural killer cells play a major role in tissue remodeling by clearing dead or dying cells (193). Accordingly, studies are currently underway to elucidate the mechanism and the potential contribution of CTBp-induced colonic immune cell profile in the context of mucosal healing.



While CTB's mucosal healing potential has not been previously reported, past studies have shown that the protein can blunt intestinal inflammation of Crohn's disease in a mouse model and in a small-scale clinical trial (73, 74). In the mouse model, CTB inhibited the production of IFN $\gamma$  and IL-12 in colon lamina propria mononuclear cells, which was reproduced in human Crohn's disease explant tissues (73). In the present study, hallmarks of anti-inflammatory effects (decreased body weight loss, inflammation scores and inflammatory cytokine mRNA/protein levels) were noted in the DSS colitis model after CTBp administration (Chapter 3); similar to the findings from the Crohn's disease experiments. Since DSS colitis is pathologically similar to ulcerative colitis in humans (194), our data extend the previous findings in Crohn's disease and now suggest that the protein is also effective against ulcerative colitis, another major form of IBD. At present, there is no cure available for ulcerative colitis; current therapies aim to induce and maintain remission. Aminosalicylates such as mesalamine, which need to be taken daily, are the primary choice for treatment of mild to moderate ulcerative colitis (121). For more severe symptoms, steroids and biologics targeting TNF $\alpha$  (infliximab and adalimumab) are used, but these agents may cause severe side effects associated with immunosuppression (121, 195). Our data suggest that CTB may provide a new therapeutic option that blunts inflammation and enhances wound healing; which has recently become an important target for ulcerative colitis therapy because it is associated with improved clinical outcomes (138, 140, 195). Of note, only two low oral doses of CTBp were as effective as mesalamine dosed daily during the 8-day DSS

exposure in the acute colitis model (Chapter 3), and biweekly dosing of CTBp also proved to be effective against chronic colitis (Chapter 4), highlighting the protein's remarkable therapeutic potential in ulcerative colitis.

In summary, our work revealed a novel function of CTBp to enhance mucosal protection in the colon. Although further investigations are required to carefully define the dose-effect relationship in mucosal remodeling and efficacy in other clinically relevant conditions such as Smad7 overexpression (140), CTB's proven anti-inflammatory effects in Crohn's disease and Bechet's disease in humans strongly support its therapeutic potential in different inflammatory conditions. Hence, we propose that CTBp is a new oral immunotherapy candidate against ulcerative colitis.

## PERSPECTIVES

To develop CTBp as an anti-colitis agent, one of the most important questions that need to be addressed is if the mucosal protection activity of CTBp can translate to human patients. In this document we found that TGF $\beta$ -driven wound healing pathways may play a role in protecting against DSS induced colitis inflammation. TGF $\beta$  signaling occurs through a canonical pathway (SMAD pathway) and multiple non-SMAD pathways. In the canonical pathway, TGF $\beta$  binds to the type 2 TGF $\beta$  receptor which complexes with the type 1 TGF $\beta$  receptor which phosphorylates SMAD2 and SMAD3. These activated SMAD proteins disassociate from the SMAD anchor for receptor activation (SARA) and form a complex with SMAD4 which then translocate to the nucleus where the complex interacts with a plethora of transcriptional factors to mediate gene expression and repression (196). SMAD7 inhibits the TGF $\beta$  signaling by preventing SMAD phosphorylation and promoting polyubiquitination and degradation of the activated receptor complexes (197). This pathway has become a target of IBD therapy because defects in it have been linked to the disease (198, 199). SMAD7 has previously been shown to be elevated in Inflammatory Bowel Disease patients that may counteract the protective effect of CTBp (140).

We are currently investigating if the overexpression of SMAD7 can be overcome by CTBp. In final preparation for the human clinical trial, work should be performed on biopsies from human patients presenting with ulcerative colitis. Dionne *et al.* has previously developed a protocol to culture human biopsies from

the lesions of actively colitic patients (200). This work will allow us to correlate SMAD7 expression with CTBp dose levels to elucidate a dosing strategy in the human clinical trial. In this design, samples are incubated for 4 or 18 H after isolation and the media is collected for cytokine analysis. These time points will allow us to further clarify the inflammatory cytokine profile resulting from CTBp exposure.

Additionally, sex differences in incidence, severity and mortality have been suggested in IBD and this has also been demonstrated with the DSS colitis model (201). Female mice were found to be less susceptible to DSS exposure compared to male mice in the study. Since all of our work was performed in female mice, further work should be done to confirm CTBp's protective effect in colitis in male mice.

Altering the route of administration may be another study that is warranted to establish an appropriate use of CTBp against ulcerative colitis; oral administration of CTBp requires sodium bicarbonate to survive the acidic environment of the stomach. Our research indicates that the colon is the site most impacted by oral CTBp administration. Rectal administration of CTBp may allow for a lower dose of CTBp and eliminate the sodium bicarbonate co-administration. A short DSS experiment (7 day DSS exposure followed by a 7 day recovery) to judge if rectal administration is more efficient (e.g. lower dose) incorporating our previously established methods of evaluating acute colitis injury will tell us if this method is indeed an improvement on oral administration.

In Chapter 2, we described that CTBp contains a C-terminal KDEL sequence for Endoplasmic reticulum (ER) retention for enhanced *N. benthamiana* production, which is not present in native (*E.coli* produced) CTB. The KDEL receptor is widely conserved in eukaryotic cells, raising a possibility that CTBp may exhibit altered intracellular localization compared to the native protein upon internalization by mucosal epithelial cells. We have therefore begun to explore the possibility that the KDEL sequence might play a role in CTBp's wound healing and anti-inflammatory activity. A preliminary experiment (Fig. 6.1) revealed that CTBp was much more effective at wound healing than native CTB. The mechanism for this interesting discrepancy is not clear at this point. However, a recent study has shown that mild ER stress can enhance wound healing in the presence of TGF $\beta$  in fibroblasts (202). Hence, we speculate that KDEL-mediated targeting of CTB to the ER of intestinal epithelial cells may somehow induce a mild ER stress response, leading to enhanced wound healing in the colon.

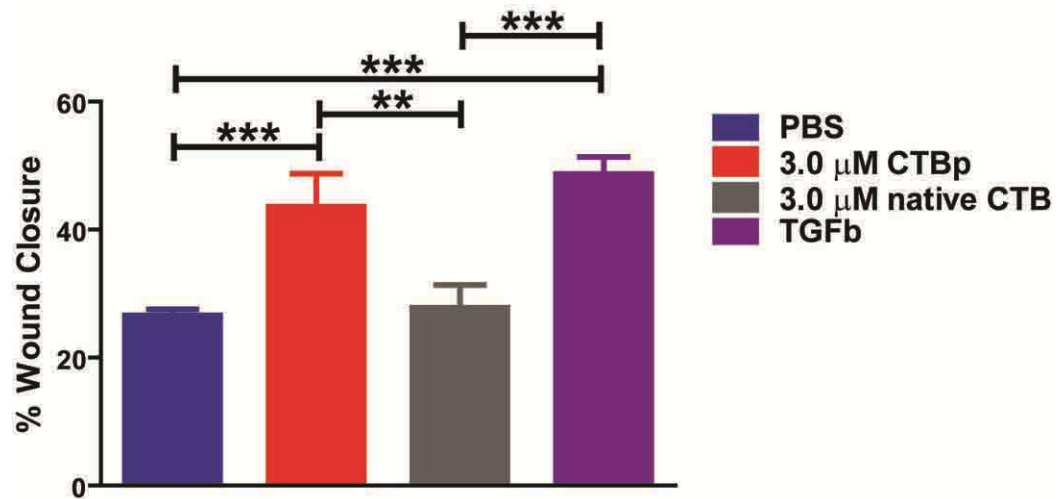


**Figure 6.1. CTBp significantly enhances wound healing compared to native CTB.**

Caco2 cells were grown to confluence and scratched with a pipette tip. Cells were then incubated with PBS, TGFβ, CTBp, or native CTB at the indicated concentration. The *in vitro* wound closure was recorded over 24 H and 4x magnification images were acquired with a EVOS<sup>®</sup> by Advanced Microscopy Group and mean percentage closure was determined by Image J software. Mean ± SEM is shown. N = 4 experimental replicates per group. \*\* P < 0.01, and \*\*\* P < 0.001; one-way ANOVA with Bonferroni's multiple comparison tests.

To address the above finding, one of the logical next steps should be to determine if CTBp remains in the cell and localized to the ER longer than native CTB. There are several techniques available to visualize the ER under the microscope (203). For example, by tagging CTBp with a fluorescent marker we can visualize where CTBp accumulates in the cell over a period of time in a confocal microscope equipped with at least a 60x objective capable of fluorescence imaging. ER localization work has previously been done in Caco2 cells would be an appropriate cell type to evaluate the compartmentalization of CTBp in (204). Next, we should evaluate CTBp's ability to modulate ER stress by analyzing ER stress markers previously established in Caco2 cells, such as X-box binding protein-1 (EBP1) and 78 kDa glucose-regulated protein (GRP78) following incubation with *E. coli* produced CTB or CTBp (205). By comparing CTBp to *E. coli* produced CTB under these conditions we should be able to

establish if CTBp a) is able traffic to and remain in the ER longer and b) enhance mucosal wound repair by modulating ER stress. Collectively, this work will help to determine if the KDEL is a necessary component to CTBp's wound healing and anti-inflammatory potential.

Additionally, the KDEL may play a role in the retention of CTBp in the GI tract. CTB is often used as a neurotracer to monitor neuronal processes (206). However, biodistribution and retention of CTB following oral administration is less well studied. We may be able to fill this gap in our knowledge by using immunohistochemistry of colon tissues, similar to work previously performed using CTB to label neurons (207). Additionally, we can quantify CTBp in organ tissue lysates using an ELISA to determine its biodistribution profile. An alternative method to explore the biodistribution of CTBp, may be linking CTBp to a fluorescent probe that can be imaged *in vivo* and revealing the distribution of CTBp following oral administration (208). These experiments will help us to investigate pharmacodynamics and safety of orally administered CTBp.

Additional work must be performed to clarify CTBp's TGF $\beta$  driven wound healing activity *in vivo*, while our DSS colitis work suggests a potential role for TGF $\beta$ -driven wound healing in the protection, a possible approach includes a previously established method using an endoscope and forceps to wound the colon epithelium and analyze the healing every two days following the injury in mice (209). Another possible approach is employing FITC-dextran, which measures intestinal permeability by moving into the serum following oral

administration and can be used to determine colon wound severity in DSS exposed mice (210).

TGF $\beta$  is considered to be beneficial to wound healing, but negative effects can also occur. For example, TGF $\beta$ 1 can be pro-fibrogenic and has been shown to be increased in the colonic mucosa of patients with collagenous colitis (184, 199). As briefly discussed in Chapter 5, upregulation of TGF $\beta$  can lead to increased epithelial to mesenchymal transition (EMT) leading to colon cancer progression and resistance to treatment. E-cadherin is decreased and vimentin is increased in EMT (211). As these markers can be detected in paraffin embedded tissue sections by IHC, future work should include it as a study endpoint in the chronic colitis/colon cancer model to determine if CTBp facilitates EMT and colon cancer progression.

The theoretical concerns described above strongly suggest the need to evaluate a therapeutic window of CTBp dosing. We have already established high dose levels that do not enhance wound healing but we have yet to establish if there is a detrimental dose of CTBp that may increase the injury to the colon. This work can be accomplished in the short-term DSS exposure study, which will allow us to determine if there is a threshold in which CTBp increases colon injury. Additionally, in our long-term CTBp dosing experiment we noted a possible sign of leukocytosis. There is a paucity of experimental data examining long-term effects of leukocytosis. In monoclonal B lymphocytosis, a subcategory of leukocytosis, the clinical course is asymptomatic with a very small number of cases progressing to chronic lymphocytic leukemia (CLL) (212). More work



should be done to determine if there is an enhanced risk of developing leukemia from long-term CTBp administration but most cases of leukocytosis are found to be benign. Alternatively, we speculate that increased blood leukocytes induced by oral CTBp administration could be exploited in immunocompromised conditions (e.g. aging and chemotherapy). In this regard, long-term dosing studies using various disease models might reveal a potential new application of CTBp.

This document shows the potential of CTBp to protect against colitis-associated colon cancer; however, the exact mechanism by which CTBp slows the development of colon cancer remains to be determined. Inflammation is a major player in the development of colorectal cancer and we have shown that CTBp can reduce colonic inflammation (213). Our results showed increased *Ifny* gene expression and IFN $\gamma$  protein levels (Fig. 5.3 and 5.4), which is considered an anti-tumor cytokine while helping to maintain the intestinal epithelial barrier (165). Additionally, CTBp decreased tumor number but within this tumor number we also significantly decreased tumor size. These results strongly point to CTBps potential to slow tumor progression; however, a definitive answer can be achieved. This can be done by evaluating tumors at various stages of the chronic colitis study via colonoscopy which is a well-established procedure (214). Previously, it has been shown that once weekly endoscopic evaluation under anesthesia can be successfully performed on mice (215). When using the established procedure mentioned above, biopsies should be taken from tumors as they develop in the mice which could be tested for gene expression and

protein analysis. This would allow us to get detailed information on the development of the tumors over time at a gross level of evaluation, gene expression, and inflammatory proteins thus answering the question regarding tumor progression.

The work presented in this document has helped to elucidate the effects of oral CTBp administration on the GI tract in both acute and chronic dosing regimens. We found that short-term dosing significantly altered the epithelial and immune cell profiles in the colon, while chronic administration appears to have additional impacts on the whole-body immune system. We uncovered a previously unreported potential of CTBp to enhance mucosal wound healing through TGF $\beta$  driven pathways. Lastly and most significantly, we found that CTBp may provide a potential therapeutic option for ulcerative colitis patients based on our acute colitis and colon cancer dosing experiments. From this work, it is clear that a protein originally characterized in 1973 (216) and heavily studied since, still has some new tricks to teach immunologists.

## REFERENCES

1. C. Lutz, M. Erken, P. Noorian, S. Sun, D. McDougald. Environmental reservoirs and mechanisms of persistence of *Vibrio cholerae*. *Frontiers in microbiology* **4**. 375 (2013).
2. S. Chatterjee, K. Ghosh, A. Raychoudhuri, A. Pan, M. K. Bhattacharya, A. K. Mukhopadhyay, T. Ramamurthy, S. K. Bhattacharya, R. K. Nandy. Phenotypic and genotypic traits and epidemiological implication of *Vibrio cholerae* O1 and O139 strains in India during 2003. *Journal of medical microbiology* **56**. 824-832 (2007).
3. J. B. Harris, R. C. LaRocque, F. Qadri, E. T. Ryan, S. B. Calderwood. Cholera. *Lancet* **379**. 2466-2476 (2012).
4. D. S. Merrell, S. M. Butler, F. Qadri, N. A. Dolganov, A. Alam, M. B. Cohen, S. B. Calderwood, G. K. Schoolnik, A. Camilli. Host-induced epidemic spread of the cholera bacterium. *Nature* **417**. 642-645 (2002).
5. O. C. Stine, J. G. Morris, Jr. Circulation and transmission of clones of *Vibrio cholerae* during cholera outbreaks. *Current topics in microbiology and immunology* **379**. 181-193 (2014).
6. D. T. Leung, F. Chowdhury, S. B. Calderwood, F. Qadri, E. T. Ryan. Immune responses to cholera in children. *Expert review of anti-infective therapy* **10**. 435-444 (2012).
7. R. Piarroux, B. Faucher. Cholera epidemics in 2010: respective roles of environment, strain changes, and human-driven dissemination. *Clinical microbiology and infection : the official publication of the European Society of Clinical Microbiology and Infectious Diseases* **18**. 231-238 (2012).
8. F. D. Orata, P. S. Keim, Y. Boucher. The 2010 cholera outbreak in Haiti: how science solved a controversy. *PLoS pathogens* **10**. e1003967 (2014).
9. WHO. Cholera 2012. *Wkly Epidemiol Rec* **88**. 321-336 (2013).
10. Cholera vaccines: WHO position paper. *Wkly Epidemiol Rec* **85**. 117-128 (2010).
11. A. K. Siddique, G. B. Nair, M. Alam, D. A. Sack, A. Huq, A. Nizam, I. M. Longini, Jr., F. Qadri, S. M. Faruque, R. R. Colwell, S. Ahmed, A. Iqbal, N. A. Bhuiyan, R. B. Sack. El Tor cholera with severe disease: a new threat to Asia and beyond. *Epidemiology and infection* **138**. 347-352 (2010).
12. N. L. Wernick, D. J. Chinnapen, J. A. Cho, W. I. Lencer. Cholera toxin: an intracellular journey into the cytosol by way of the endoplasmic reticulum. *Toxins* **2**. 310-325 (2010).
13. W. I. Lencer, B. Tsai. The intracellular voyage of cholera toxin: going retro. *Trends in biochemical sciences* **28**. 639-645 (2003).
14. D. J. Chinnapen, H. Chinnapen, D. Saslowsky, W. I. Lencer. Rafting with cholera toxin: endocytosis and trafficking from plasma membrane to ER. *FEMS microbiology letters* **266**. 129-137 (2007).
15. J. Sanchez, J. Holmgren. Cholera toxin structure, gene regulation and pathophysiological and immunological aspects. *Cell Mol Life Sci* **65**. 1347-1360 (2008).
16. R. G. Zhang, D. L. Scott, M. L. Westbrook, S. Nance, B. D. Spangler, G. G. Shipley, E. M. Westbrook. The three-dimensional crystal structure of cholera toxin. *Journal of molecular biology* **251**. 563-573 (1995).

17. J. Sanchez, J. Holmgren. Cholera toxin - a foe & a friend. *The Indian journal of medical research* **133**. 153-163 (2011).
18. I. Basu, C. Mukhopadhyay. Insights into Binding of Cholera Toxin to GM1 Containing Membrane. *Langmuir : the ACS journal of surfaces and colloids* **30**. 15244-15252 (2014).
19. D. E. Saslowsky, Y. M. te Welscher, D. J. Chinnapen, J. S. Wagner, J. Wan, E. Kern, W. I. Lencer. Ganglioside GM1-mediated transcytosis of cholera toxin bypasses the retrograde pathway and depends on the structure of the ceramide domain. *The Journal of biological chemistry* **288**. 25804-25809 (2013).
20. R. C. Charles, I. J. Hilaire, L. M. Mayo-Smith, J. E. Teng, J. G. Jerome, M. F. Franke, A. Saha, Y. Yu, P. Kovac, S. B. Calderwood, E. T. Ryan, R. C. LaRocque, C. P. Almazor, F. Qadri, L. C. Ivers, J. B. Harris. Immunogenicity of a killed bivalent (O1 and O139) whole cell oral cholera vaccine, Shanchol, in Haiti. *PLoS neglected tropical diseases* **8**. e2828 (2014).
21. C. Schaetti, M. G. Weiss, S. M. Ali, C. L. Chaignat, A. M. Khatib, R. Reyburn, R. J. Duintjer Tebbens, R. Hutubessy. Costs of illness due to cholera, costs of immunization and cost-effectiveness of an oral cholera mass vaccination campaign in Zanzibar. *PLoS neglected tropical diseases* **6**. e1844 (2012).
22. A. Lajoinie, E. Henin, B. Kassai, D. Terry. Solid oral forms availability in children: a cost saving investigation. *British journal of clinical pharmacology* **78**. 1080-1089 (2014).
23. J. D. Clemens, D. A. Sack, J. R. Harris, J. Chakraborty, M. R. Khan, B. F. Stanton, B. A. Kay, M. U. Khan, M. Yunus, W. Atkinson, et al. Field trial of oral cholera vaccines in Bangladesh. *Lancet* **2**. 124-127 (1986).
24. J. D. Clemens, D. A. Sack, J. R. Harris, F. Van Loon, J. Chakraborty, F. Ahmed, M. R. Rao, M. R. Khan, M. Yunus, N. Huda, et al. Field trial of oral cholera vaccines in Bangladesh: results from three-year follow-up. *Lancet* **335**. 270-273 (1990).
25. M. M. Alam, D. T. Leung, M. Akhtar, M. Nazim, S. Akter, T. Uddin, F. Khanam, D. A. Mahbuba, S. M. Ahmad, T. R. Bhuiyan, S. B. Calderwood, E. T. Ryan, F. Qadri. Antibody avidity in humoral immune responses in Bangladeshi children and adults following administration of an oral killed cholera vaccine. *Clinical and vaccine immunology : CVI* **20**. 1541-1548 (2013).
26. M. E. Lucas, J. L. Deen, L. von Seidlein, X. Y. Wang, J. Ampuero, M. Puri, M. Ali, M. Ansaruzzaman, J. Amos, A. Macuamule, P. Cavailler, P. J. Guerin, C. Mahoudeau, P. Kahozzi-Sangwa, C. L. Chaignat, A. Barreto, F. F. Songane, J. D. Clemens. Effectiveness of mass oral cholera vaccination in Beira, Mozambique. *The New England journal of medicine* **352**. 757-767 (2005).
27. D. N. Taylor, V. Cardenas, J. L. Sanchez, R. E. Begue, R. Gilman, C. Bautista, J. Perez, R. Puga, A. Gaillour, R. Meza, P. Echeverria, J. Sadoff. Two-year study of the protective efficacy of the oral whole cell plus recombinant B subunit cholera vaccine in Peru. *The Journal of infectious diseases* **181**. 1667-1673 (2000).
28. J. D. Clemens, M. Jertborn, D. Sack, B. Stanton, J. Holmgren, M. R. Khan, S. Huda. Effect of neutralization of gastric acid on immune responses to an oral B subunit, killed whole-cell cholera vaccine. *The Journal of infectious diseases* **154**. 175-178 (1986).
29. A. Saha, M. I. Chowdhury, F. Khanam, M. S. Bhuiyan, F. Chowdhury, A. I. Khan, I. A. Khan, J. Clemens, M. Ali, A. Cravioto, F. Qadri. Safety and immunogenicity study of a killed bivalent (O1 and O139) whole-cell oral cholera vaccine Shanchol, in Bangladeshi adults and children as young as 1 year of age. *Vaccine* **29**. 8285-8292 (2011).
30. F. J. Luquero, L. Grout, I. Ciglencecki, K. Sakoba, B. Traore, M. Heile, A. A. Diallo, C. Itama, A. L. Page, M. L. Quilici, M. A. Mengel, J. M. Eiros, M. Serafini, D. Legros, R. F. Grais. Use

- of *Vibrio cholerae* vaccine in an outbreak in Guinea. *The New England journal of medicine* **370**. 2111-2120 (2014).
31. S. S. Kang, J. S. Yang, K. W. Kim, C. H. Yun, J. Holmgren, C. Czerkinsky, S. H. Han. Anti-bacterial and anti-toxic immunity induced by a killed whole-cell-cholera toxin B subunit cholera vaccine is essential for protection against lethal bacterial infection in mouse pulmonary cholera model. *Mucosal Immunol* **6**. 826-837 (2013).
  32. J. Holmgren, J. Adamsson, F. Anjuere, J. Clemens, C. Czerkinsky, K. Eriksson, C. F. Flach, A. George-Chandy, A. M. Harandi, M. Lebens, T. Lehner, M. Lindblad, E. Nygren, S. Raghavan, J. Sanchez, M. Stanford, J. B. Sun, A. M. Svennerholm, S. Tengvall. Mucosal adjuvants and anti-infection and anti-immunopathology vaccines based on cholera toxin, cholera toxin B subunit and CpG DNA. *Immunology letters* **97**. 181-188 (2005).
  33. N. A. Williams, T. R. Hirst, T. O. Nashar. Immune modulation by the cholera-like enterotoxins: from adjuvant to therapeutic. *Immunology today* **20**. 95-101 (1999).
  34. K. Bharati, N. K. Ganguly. Cholera toxin: a paradigm of a multifunctional protein. *The Indian journal of medical research* **133**. 179-187 (2011).
  35. J. Holmgren, N. Lycke, C. Czerkinsky. Cholera toxin and cholera B subunit as oral-mucosal adjuvant and antigen vector systems. *Vaccine* **11**. 1179-1184 (1993).
  36. C. C. Bowman, M. K. Selgrade. Utility of rodent models for evaluating protein allergenicity. *Regulatory toxicology and pharmacology : RTP* **54**. S58-61 (2009).
  37. M. K. Oyoshi, H. C. Oettgen, T. A. Chatila, R. S. Geha, P. J. Bryce. Food allergy: Insights into etiology, prevention, and treatment provided by murine models. *The Journal of allergy and clinical immunology* **133**. 309-317 (2014).
  38. C. O. Elson, W. Ealding. Generalized systemic and mucosal immunity in mice after mucosal stimulation with cholera toxin. *J Immunol* **132**. 2736-2741 (1984).
  39. R. J. Jackson, K. Fujihashi, J. Xu-Amano, H. Kiyono, C. O. Elson, J. R. McGhee. Optimizing oral vaccines: induction of systemic and mucosal B-cell and antibody responses to tetanus toxoid by use of cholera toxin as an adjuvant. *Infection and immunity* **61**. 4272-4279 (1993).
  40. I. Bourguin, T. Chardes, D. Bout. Oral immunization with *Toxoplasma gondii* antigens in association with cholera toxin induces enhanced protective and cell-mediated immunity in C57BL/6 mice. *Infection and immunity* **61**. 2082-2088 (1993).
  41. J. Holmgren, C. Czerkinsky, N. Lycke, A. M. Svennerholm. Strategies for the induction of immune responses at mucosal surfaces making use of cholera toxin B subunit as immunogen, carrier, and adjuvant. *The American journal of tropical medicine and hygiene* **50**. 42-54 (1994).
  42. T. G. Blanchard, N. Lycke, S. J. Czinn, J. G. Nedrud. Recombinant cholera toxin B subunit is not an effective mucosal adjuvant for oral immunization of mice against *Helicobacter felis*. *Immunology* **94**. 22-27 (1998).
  43. E. Kubota, T. Joh, S. Tanida, M. Sasaki, H. Kataoka, K. Watanabe, K. Itoh, T. Oshima, N. Ogasawara, S. Togawa, T. Wada, T. Yamada, Y. Mori, F. Fujita, T. Shimura, H. Ohara, M. Isaka, Y. Yasuda, M. Itoh. Oral vaccination against *Helicobacter pylori* with recombinant cholera toxin B-subunit. *Helicobacter* **10**. 345-352 (2005).
  44. M. Mutsch, W. Zhou, P. Rhodes, M. Bopp, R. T. Chen, T. Linder, C. Spyr, R. Steffen. Use of the inactivated intranasal influenza vaccine and the risk of Bell's palsy in Switzerland. *The New England journal of medicine* **350**. 896-903 (2004).
  45. R. B. Couch. Nasal vaccination, *Escherichia coli* enterotoxin, and Bell's palsy. *The New England journal of medicine* **350**. 860-861 (2004).

46. B. Rath, T. Linder, D. Cornblath, M. Hudson, R. Fernandopulle, K. Hartmann, U. Heininger, H. Izurieta, L. Killion, P. Kokotis, J. Oleske, M. Vajdy, V. Wong, G. Brighton Collaboration Bell's Palsy Working. All that palsies is not Bell's -the need to define Bell's palsy as an adverse event following immunization. *Vaccine* **26**. 1-14 (2007).
47. L. Guo, K. Liu, G. Xu, X. Li, J. Tu, F. Tang, Y. Xing, T. Xi. Prophylactic and therapeutic efficacy of the epitope vaccine CTB-UA against *Helicobacter pylori* infection in a BALB/c mice model. *Applied microbiology and biotechnology* **95**. 1437-1444 (2012).
48. E. D. de Geus, D. A. van Haarlem, O. N. Poetri, J. J. de Wit, L. Vervelde. A lack of antibody formation against inactivated influenza virus after aerosol vaccination in presence or absence of adjuvantia. *Veterinary immunology and immunopathology* **143**. 143-147 (2011).
49. M. Boustanshenas, B. Bakhshi, M. Ghorbani. Investigation into immunological responses against a native recombinant CTB whole-cell *Vibrio cholerae* vaccine in a rabbit model. *Journal of applied microbiology* **114**. 509-515 (2013).
50. A. A. Baptista, T. C. Donato, K. C. Garcia, G. A. Goncalves, M. P. Coppola, A. S. Okamoto, J. L. Sequeira, R. L. Andreatti Filho. Immune response of broiler chickens immunized orally with the recombinant proteins flagellin and the subunit B of cholera toxin associated with *Lactobacillus* spp. *Poultry science* **93**. 39-45 (2014).
51. L. Guo, R. Yin, K. Liu, X. Lv, Y. Li, X. Duan, Y. Chu, T. Xi, Y. Xing. Immunological features and efficacy of a multi-epitope vaccine CTB-UE against *H. pylori* in BALB/c mice model. *Applied microbiology and biotechnology* **98**. 3495-3507 (2014).
52. J. K. Tinker, J. Yan, R. J. Knippel, P. Panayiotou, K. A. Cornell. Immunogenicity of a West Nile virus DIII-cholera toxin A2/B chimera after intranasal delivery. *Toxins* **6**. 1397-1418 (2014).
53. C. Czerkinsky, J. B. Sun, M. Lebens, B. L. Li, C. Rask, M. Lindblad, J. Holmgren. Cholera toxin B subunit as transmucosal carrier-delivery and immunomodulating system for induction of antiinfectious and antipathological immunity. *Annals of the New York Academy of Sciences* **778**. 185-193 (1996).
54. B. A. Martell, F. M. Orson, J. Poling, E. Mitchell, R. D. Rossen, T. Gardner, T. R. Kosten. Cocaine vaccine for the treatment of cocaine dependence in methadone-maintained patients: a randomized, double-blind, placebo-controlled efficacy trial. *Archives of general psychiatry* **66**. 1116-1123 (2009).
55. F. M. Orson, R. D. Rossen, X. Shen, A. Y. Lopez, Y. Wu, T. R. Kosten. Spontaneous development of IgM anti-cocaine antibodies in habitual cocaine users: effect on IgG antibody responses to a cocaine cholera toxin B conjugate vaccine. *The American journal on addictions / American Academy of Psychiatrists in Alcoholism and Addictions* **22**. 169-174 (2013).
56. E. Harokopakis, G. Hajishengallis, T. E. Greenway, M. W. Russell, S. M. Michalek. Mucosal immunogenicity of a recombinant *Salmonella typhimurium*-cloned heterologous antigen in the absence or presence of coexpressed cholera toxin A2 and B subunits. *Infection and immunity* **65**. 1445-1454 (1997).
57. M. Martin, G. Hajishengallis, D. J. Metzger, S. M. Michalek, T. D. Connell, M. W. Russell. Recombinant antigen-enterotoxin A2/B chimeric mucosal immunogens differentially enhance antibody responses and B7-dependent costimulation of CD4(+) T cells. *Infection and immunity* **69**. 252-261 (2001).
58. M. Lebens, J. Holmgren. Mucosal vaccines based on the use of cholera toxin B subunit as immunogen and antigen carrier. *Developments in biological standardization* **82**. 215-227 (1994).

59. J. B. Sun, C. Czerkinsky, J. Holmgren. Mucosally induced immunological tolerance, regulatory T cells and the adjuvant effect by cholera toxin B subunit. *Scand J Immunol* **71**. 1-11 (2010).
60. H. H. Smits, A. K. Gloudemans, M. van Nimwegen, M. A. Willart, T. Soullie, F. Muskens, E. C. de Jong, L. Boon, C. Pilette, F. E. Johansen, H. C. Hoogsteden, H. Hammad, B. N. Lambrecht. Cholera toxin B suppresses allergic inflammation through induction of secretory IgA. *Mucosal Immunol* **2**. 331-339 (2009).
61. M. Stanford, T. Whittall, L. A. Bergmeier, M. Lindblad, S. Lundin, T. Shinnick, Y. Mizushima, J. Holmgren, T. Lehner. Oral tolerization with peptide 336-351 linked to cholera toxin B subunit in preventing relapses of uveitis in Behcet's disease. *Clin Exp Immunol* **137**. 201-208 (2004).
62. P. Libby, D. M. Nathan, K. Abraham, J. D. Brunzell, J. E. Fradkin, S. M. Haffner, W. Hsueh, M. Rewers, B. T. Roberts, P. J. Savage, S. Skarlatos, M. Wassef, C. Rabadan-Diehl, L. National Heart, I. Blood, D. National Institute of, Digestive, M. Kidney Diseases Working Group on Cardiovascular Complications of Type 1 Diabetes. Report of the National Heart, Lung, and Blood Institute-National Institute of Diabetes and Digestive and Kidney Diseases Working Group on Cardiovascular Complications of Type 1 Diabetes Mellitus. *Circulation* **111**. 3489-3493 (2005).
63. O. Odumosu, D. Nicholas, K. Payne, W. Langridge. Cholera toxin B subunit linked to glutamic acid decarboxylase suppresses dendritic cell maturation and function. *Vaccine* **29**. 8451-8458 (2011).
64. B. Denes, I. Fodor, W. H. Langridge. Persistent suppression of type 1 diabetes by a multicomponent vaccine containing a cholera toxin B subunit-autoantigen fusion protein and complete Freund's adjuvant. *Clinical & developmental immunology* **2013**. 578786 (2013).
65. P. K. Shil, K. C. Kwon, P. Zhu, A. Verma, H. Daniell, Q. Li. Oral Delivery of ACE2/Ang-(1-7) Bioencapsulated in Plant Cells Protects against Experimental Uveitis and Autoimmune Uveoretinitis. *Molecular therapy : the journal of the American Society of Gene Therapy* **22**. 2069-2082 (2014).
66. Q. Xiong, J. Li, L. Jin, J. Liu, T. Li. Nasal immunization with heat shock protein 65 attenuates atherosclerosis and reduces serum lipids in cholesterol-fed wild-type rabbits probably through different mechanisms. *Immunology letters* **125**. 40-45 (2009).
67. R. Klingenberg, M. Lebens, A. Hermansson, G. N. Fredrikson, D. Strodthoff, M. Rudling, D. F. Ketelhuth, N. Gerdes, J. Holmgren, J. Nilsson, G. K. Hansson. Intranasal immunization with an apolipoprotein B-100 fusion protein induces antigen-specific regulatory T cells and reduces atherosclerosis. *Arteriosclerosis, thrombosis, and vascular biology* **30**. 946-952 (2010).
68. J. A. Salazar-Gonzalez, S. Rosales-Mendoza, A. Romero-Maldonado, E. Monreal-Escalante, E. E. Uresti-Rivera, B. Banuelos-Hernandez. Production of a Plant-Derived Immunogenic Protein Targeting ApoB100 and CETP: Toward a Plant-Based Atherosclerosis Vaccine. *Molecular biotechnology* **56**. 1133-1142 (2014).
69. H. L. Weiner. The mucosal milieu creates tolerogenic dendritic cells and T(R)1 and T(H)3 regulatory cells. *Nature immunology* **2**. 671-672 (2001).
70. H. J. Hernandez, L. I. Rutitzky, M. Lebens, J. Holmgren, M. J. Stadecker. Diminished immunopathology in *Schistosoma mansoni* infection following intranasal administration of cholera toxin B-immunodominant peptide conjugate correlates with enhanced transforming growth factor-beta production by CD4 T cells. *Parasite immunology* **24**. 423-427 (2002).

71. X. Yu, B. Song, C. Huang, Y. Xiao, M. Fang, J. Feng, P. Wang, G. Zhang. Prolonged survival time of allografts by the oral administration of RDP58 linked to the cholera toxin B subunit. *Transplant immunology* **27**. 122-127 (2012).
72. M. Boirivant, I. J. Fuss, L. Ferroni, M. De Pascale, W. Strober. Oral administration of recombinant cholera toxin subunit B inhibits IL-12-mediated murine experimental (trinitrobenzene sulfonic acid) colitis. *J Immunol* **166**. 3522-3532 (2001).
73. E. M. Coccia, M. E. Remoli, C. Di Giacinto, B. Del Zotto, E. Giacomini, G. Monteleone, M. Boirivant. Cholera toxin subunit B inhibits IL-12 and IFN- $\gamma$  production and signaling in experimental colitis and Crohn's disease. *Gut* **54**. 1558-1564 (2005).
74. P. Stal, R. Befrits, A. Ronnblom, A. Danielsson, O. Suhr, D. Stahlberg, A. Brinkberg Lapidus, R. Lofberg. Clinical trial: the safety and short-term efficacy of recombinant cholera toxin B subunit in the treatment of active Crohn's disease. *Aliment Pharmacol Ther* **31**. 387-395 (2010).
75. S. Tamura, A. Yamanaka, M. Shimohara, T. Tomita, K. Komase, Y. Tsuda, Y. Suzuki, T. Nagamine, K. Kawahara, H. Danbara, et al. Synergistic action of cholera toxin B subunit (and Escherichia coli heat-labile toxin B subunit) and a trace amount of cholera whole toxin as an adjuvant for nasal influenza vaccine. *Vaccine* **12**. 419-426 (1994).
76. K. T. Hamorsky, J. C. Kouokam, L. J. Bennett, K. J. Baldauf, H. Kajiura, K. Fujiyama, N. Matoba. Rapid and scalable plant-based production of a cholera toxin B subunit variant to aid in mass vaccination against cholera outbreaks. *PLoS neglected tropical diseases* **7**. e2046 (2013).
77. R. G. Zhang, M. L. Westbrook, E. M. Westbrook, D. L. Scott, Z. Otwinowski, P. R. Maulik, R. A. Reed, G. G. Shipley. The 2.4 Å crystal structure of cholera toxin B subunit pentamer: cholera toxin B subunit. *Journal of molecular biology* **251**. 550-562 (1995).
78. T. Jelinek, H. Kollaritsch. Vaccination with Dukoral against travelers' diarrhea (ETEC) and cholera. *Expert Rev Vaccines* **7**. 561-567 (2008).
79. J. Clemens, S. Shin, D. Sur, G. B. Nair, J. Holmgren. New-generation vaccines against cholera. *Nature reviews. Gastroenterology & hepatology* **8**. 701-710 (2011).
80. S. Karaman, J. Cunnick, K. Wang. Expression of the cholera toxin B subunit (CT-B) in maize seeds and a combined mucosal treatment against cholera and traveler's diarrhea. *Plant cell reports* **31**. 527-537 (2012).
81. L. Wassen, M. Jertborn. Kinetics of local and systemic immune responses after vaginal immunization with recombinant cholera toxin B subunit in humans. *Clin Diagn Lab Immunol* **12**. 447-452 (2005).
82. H. S. Kim, J. H. Jeon, K. J. Lee, K. Ko. N-glycosylation modification of plant-derived virus-like particles: an application in vaccines. *BioMed research international* **2014**. 249519 (2014).
83. R. A. Irizarry, B. Hobbs, F. Collin, Y. D. Beazer-Barclay, K. J. Antonellis, U. Scherf, T. P. Speed. Exploration, normalization, and summaries of high density oligonucleotide array probe level data. *Biostatistics* **4**. 249-264 (2003).
84. A. K. Gloudemans, M. Plantinga, M. Guilliams, M. A. Willart, A. Ozir-Fazalalikhani, A. van der Ham, L. Boon, N. L. Harris, H. Hammad, H. C. Hoogsteden, M. Yazdanbakhsh, R. W. Hendriks, B. N. Lambrecht, H. H. Smits. The mucosal adjuvant cholera toxin B instructs non-mucosal dendritic cells to promote IgA production via retinoic acid and TGF- $\beta$ . *PLoS One* **8**. e59822 (2013).
85. L. J. Bayne, R. H. Vonderheide. Multicolor flow cytometric analysis of immune cell subsets in tumor-bearing mice. *Cold Spring Harb Protoc* **2013**. 955-960 (2013).



86. S. Eyerich, C. E. Zielinski. Defining Th-cell subsets in a classical and tissue-specific manner: Examples from the skin. *Eur J Immunol* **44**. 3475-3483 (2014).
87. A. Sturm, A. U. Dignass. Epithelial restitution and wound healing in inflammatory bowel disease. *World J Gastroenterol* **14**. 348-353 (2008).
88. P. Balogh, S. Katz, A. L. Kiss. The role of endocytic pathways in TGF-beta signaling. *Pathol Oncol Res* **19**. 141-148 (2013).
89. G. Jego, A. Hazoume, R. Seigneuric, C. Garrido. Targeting heat shock proteins in cancer. *Cancer Lett* **332**. 275-285 (2013).
90. G. D. Lianos, G. A. Alexiou, A. Mangano, A. Mangano, S. Rausei, L. Boni, G. Dionigi, D. H. Roukos. The role of heat shock proteins in cancer. *Cancer Lett* **360**. 114-118 (2015).
91. T. Kayashima, K. Tanaka, Y. Okazaki, K. Matsubara, N. Yanaka, N. Kato. Consumption of vitamin B6 reduces colonic damage and protein expression of HSP70 and HO-1, the anti-tumor targets, in rats exposed to 1,2-dimethylhydrazine. *Oncol Lett* **2**. 1243-1246 (2011).
92. V. Khattar, J. Fried, B. Xu, J. V. Thottassery. Cks1 proteasomal degradation is induced by inhibiting Hsp90-mediated chaperoning in cancer cells. *Cancer Chemother Pharmacol* **75**. 411-420 (2015).
93. J. S. Chen, Y. M. Hsu, C. C. Chen, L. L. Chen, C. C. Lee, T. S. Huang. Secreted heat shock protein 90alpha induces colorectal cancer cell invasion through CD91/LRP-1 and NF-kappaB-mediated integrin alphaV expression. *The Journal of biological chemistry* **285**. 25458-25466 (2010).
94. S. Baidur-Hudson, A. L. Edkins, G. L. Blatch. Hsp70/Hsp90 organising protein (hop): beyond interactions with chaperones and prion proteins. *Subcell Biochem* **78**. 69-90 (2015).
95. F. F. Anhe, D. Roy, G. Pilon, S. Dudonne, S. Matamoros, T. V. Varin, C. Garofalo, Q. Moine, Y. Desjardins, E. Levy, A. Marette. A polyphenol-rich cranberry extract protects from diet-induced obesity, insulin resistance and intestinal inflammation in association with increased Akkermansia spp. population in the gut microbiota of mice. *Gut* **64**. 872-883 (2015).
96. F. Gutierrez-Orozco, J. M. Thomas-Ahner, J. D. Galley, M. T. Bailey, S. K. Clinton, G. B. Lesinski, M. L. Failla. Intestinal microbial dysbiosis and colonic epithelial cell hyperproliferation by dietary alpha-mangostin is independent of mouse strain. *Nutrients* **7**. 764-784 (2015).
97. N. A. Williams. Immune modulation by the cholera-like enterotoxin B-subunits: from adjuvant to immunotherapeutic. *International journal of medical microbiology : IJMM* **290**. 447-453 (2000).
98. T. Stratmann. Cholera Toxin Subunit B as Adjuvant--An Accelerator in Protective Immunity and a Break in Autoimmunity. *Vaccines (Basel)* **3**. 579-596 (2015).
99. A. D'Ambrosio, M. Colucci, O. Pugliese, F. Quintieri, M. Boirivant. Cholera toxin B subunit promotes the induction of regulatory T cells by preventing human dendritic cell maturation. *J Leukoc Biol* **84**. 661-668 (2008).
100. V. Burkart, Y. E. Kim, B. Hartmann, I. Ghiea, U. Syldath, M. Kauer, W. Fingberg, P. Hanifi-Moghaddam, S. Muller, H. Kolb. Cholera toxin B pretreatment of macrophages and monocytes diminishes their proinflammatory responsiveness to lipopolysaccharide. *J Immunol* **168**. 1730-1737 (2002).
101. J. B. Sun, B. G. Xiao, M. Lindblad, B. L. Li, H. Link, C. Czerkinsky, J. Holmgren. Oral administration of cholera toxin B subunit conjugated to myelin basic protein protects against experimental autoimmune encephalomyelitis by inducing transforming growth

- factor-beta-secreting cells and suppressing chemokine expression. *Int Immunol* **12**. 1449-1457 (2000).
102. J. B. Sun, B. L. Li, C. Czerkinsky, J. Holmgren. Enhanced immunological tolerance against allograft rejection by oral administration of allogeneic antigen linked to cholera toxin B subunit. *Clin Immunol* **97**. 130-139 (2000).
  103. C. Aspod, C. Thivolet. Nasal administration of CTB-insulin induces active tolerance against autoimmune diabetes in non-obese diabetic (NOD) mice. *Clin Exp Immunol* **130**. 204-211 (2002).
  104. P. H. Kim, L. Eckmann, W. J. Lee, W. Han, M. F. Kagnoff. Cholera toxin and cholera toxin B subunit induce IgA switching through the action of TGF-beta 1. *J Immunol* **160**. 1198-1203 (1998).
  105. P. ten Dijke, C. S. Hill. New insights into TGF-beta-Smad signalling. *Trends in biochemical sciences* **29**. 265-273 (2004).
  106. P. Biancheri, P. Giuffrida, G. H. Docena, T. T. MacDonald, G. R. Corazza, A. Di Sabatino. The role of transforming growth factor (TGF)-beta in modulating the immune response and fibrogenesis in the gut. *Cytokine Growth Factor Rev* **25**. 45-55 (2014).
  107. A. Hameedaldien, J. Liu, A. Batres, G. S. Graves, D. T. Graves. FOXO1, TGF-beta regulation and wound healing. *International journal of molecular sciences* **15**. 16257-16269 (2014).
  108. D. M. Gonzalez, D. Medici. Signaling mechanisms of the epithelial-mesenchymal transition. *Science signaling* **7**. re8 (2014).
  109. M. Kaplan, B. B. Menten, E. Tatlicioglu, B. Kayhan, C. Aybay. Effect of mucosal immunomodulation with fed cholera toxin on healing of experimental colonic anastomosis. *Diseases of the colon and rectum* **45**. 819-825 (2002).
  110. C. B. de La Serre, C. L. Ellis, J. Lee, A. L. Hartman, J. C. Rutledge, H. E. Raybould. Propensity to high-fat diet-induced obesity in rats is associated with changes in the gut microbiota and gut inflammation. *American journal of physiology. Gastrointestinal and liver physiology* **299**. G440-448 (2010).
  111. T. Okada, S. Fukuda, K. Hase, S. Nishiumi, Y. Izumi, M. Yoshida, T. Hagiwara, R. Kawashima, M. Yamazaki, T. Oshio, T. Otsubo, K. Inagaki-Ohara, K. Kakimoto, K. Higuchi, Y. I. Kawamura, H. Ohno, T. Dohi. Microbiota-derived lactate accelerates colon epithelial cell turnover in starvation-refed mice. *Nat Commun* **4**. 1654 (2013).
  112. H. Suzuki. Differences in intraepithelial lymphocytes in the proximal, middle, distal parts of small intestine, cecum, and colon of mice. *Immunological investigations* **38**. 780-796 (2009).
  113. T. T. Kararli. Comparison of the gastrointestinal anatomy, physiology, and biochemistry of humans and commonly used laboratory animals. *Biopharm Drug Dispos* **16**. 351-380 (1995).
  114. C. T. Peterson, V. Sharma, L. Elmen, S. N. Peterson. Immune homeostasis, dysbiosis and therapeutic modulation of the gut microbiota. *Clin Exp Immunol* **179**. 363-377 (2015).
  115. K. Karlinger, T. Gyorke, E. Mako, A. Mester, Z. Tarjan. The epidemiology and the pathogenesis of inflammatory bowel disease. *European journal of radiology* **35**. 154-167 (2000).
  116. G. Latella, C. Papi. Crucial steps in the natural history of inflammatory bowel disease. *World J Gastroenterol* **18**. 3790-3799 (2012).
  117. M. A. Engel, M. Khalil, M. F. Neurath. Highlights in inflammatory bowel disease--from bench to bedside. *Clinical chemistry and laboratory medicine : CCLM / FESCC* **50**. 1229-1235 (2012).

118. G. Monteleone, R. Caruso, F. Pallone. Targets for new immunomodulation strategies in inflammatory bowel disease. *Autoimmun Rev* **13**. 11-14 (2014).
119. A. Geremia, P. Biancheri, P. Allan, G. R. Corazza, A. Di Sabatino. Innate and adaptive immunity in inflammatory bowel disease. *Autoimmun Rev* **13**. 3-10 (2014).
120. A. M. Globig, N. Hennecke, B. Martin, M. Seidl, G. Ruf, P. Hasselblatt, R. Thimme, B. Bengsch. Comprehensive intestinal T helper cell profiling reveals specific accumulation of IFN-gamma+IL-17+coproducing CD4+ T cells in active inflammatory bowel disease. *Inflamm Bowel Dis* **20**. 2321-2329 (2014).
121. C. Bezzio, F. Furfaro, R. de Franchis, G. Maconi, A. K. Asthana, S. Ardizzone. Ulcerative colitis: current pharmacotherapy and future directions. *Expert Opin Pharmacother* **15**. 1659-1670 (2014).
122. K. Bulut, J. J. Meier, N. Ansorge, P. Felderbauer, F. Schmitz, P. Hoffmann, W. E. Schmidt, B. Gallwitz. Glucagon-like peptide 2 improves intestinal wound healing through induction of epithelial cell migration in vitro-evidence for a TGF-beta-mediated effect. *Regul Pept* **121**. 137-143 (2004).
123. S. Wirtz, C. Neufert, B. Weigmann, M. F. Neurath. Chemically induced mouse models of intestinal inflammation. *Nature protocols* **2**. 541-546 (2007).
124. L. A. Dieleman, M. J. Palmen, H. Akol, E. Bloemena, A. S. Pena, S. G. Meuwissen, E. P. Van Rees. Chronic experimental colitis induced by dextran sulphate sodium (DSS) is characterized by Th1 and Th2 cytokines. *Clin Exp Immunol* **114**. 385-391 (1998).
125. M. Yue, Z. Shen, C. H. Yu, H. Ye, Y. M. Li. The therapeutic role of oral tolerance in dextran sulfate sodium-induced colitis via Th1-Th2 balance and gammadelta T cells. *Journal of digestive diseases* **14**. 543-551 (2013).
126. H. S. Cooper, S. N. Murthy, R. S. Shah, D. J. Sedergran. Clinicopathologic study of dextran sulfate sodium experimental murine colitis. *Laboratory investigation; a journal of technical methods and pathology* **69**. 238-249 (1993).
127. Y. L. Jones-Hall, M. B. Grisham. Immunopathological characterization of selected mouse models of inflammatory bowel disease: Comparison to human disease. *Pathophysiology* **21**. 267-288 (2014).
128. P. Desreumaux, S. Ghosh. Review article: mode of action and delivery of 5-aminosalicylic acid - new evidence. *Aliment Pharmacol Ther* **24 Suppl 1**. 2-9 (2006).
129. G. Bamias, G. Kaltsa, S. D. Ladas. Cytokines in the pathogenesis of ulcerative colitis. *Discov Med* **11**. 459-467 (2011).
130. M. H. Zaki, M. Lamkanfi, T. D. Kanneganti. The Nlrp3 inflammasome: contributions to intestinal homeostasis. *Trends Immunol* **32**. 171-179 (2011).
131. J. Dabritz, T. Weinhage, G. Varga, T. Wirth, K. Walscheid, A. Brockhausen, D. Schwarzmaier, M. Bruckner, M. Ross, D. Bettenworth, J. Roth, J. M. Ehrchen, D. Foell. Reprogramming of monocytes by GM-CSF contributes to regulatory immune functions during intestinal inflammation. *J Immunol* **194**. 2424-2438 (2015).
132. D. C. Lacey, A. Achuthan, A. J. Fleetwood, H. Dinh, J. Roiniotis, G. M. Scholz, M. W. Chang, S. K. Beckman, A. D. Cook, J. A. Hamilton. Defining GM-CSF- and macrophage-CSF-dependent macrophage responses by in vitro models. *J Immunol* **188**. 5752-5765 (2012).
133. J. B. Sun, C. Czerkinsky, J. Holmgren. B Lymphocytes Treated In Vitro with Antigen Coupled to Cholera Toxin B Subunit Induce Antigen-Specific Foxp3(+) Regulatory T Cells and Protect against Experimental Autoimmune Encephalomyelitis. *Journal of Immunology* **188**. 1686-1697 (2012).

134. M. Doulberis, K. Angelopoulou, E. Kaldrymidou, A. Tsingotjidou, Z. Abas, S. E. Erdman, T. Poutahidis. Cholera-toxin suppresses carcinogenesis in a mouse model of inflammation-driven sporadic colon cancer. *Carcinogenesis* **36**. 280-290 (2015).
135. D. Ma, D. Wolvers, A. M. Stanis, J. Bienenstock. Interleukin-10 and nerve growth factor have reciprocal upregulatory effects on intestinal epithelial cells. *Am J Physiol Regul Integr Comp Physiol* **284**. R1323-1329 (2003).
136. Y. Jung, M. E. Rothenberg. Roles and regulation of gastrointestinal eosinophils in immunity and disease. *J Immunol* **193**. 999-1005 (2014).
137. A. Walsh, R. Palmer, S. Travis. Mucosal healing as a target of therapy for colonic inflammatory bowel disease and methods to score disease activity. *Gastrointest Endosc Clin N Am* **24**. 367-378 (2014).
138. B. P. Vaughn, S. Shah, A. S. Cheifetz. The role of mucosal healing in the treatment of patients with inflammatory bowel disease. *Curr Treat Options Gastroenterol* **12**. 103-117 (2014).
139. A. U. Dignass, D. K. Podolsky. Cytokine modulation of intestinal epithelial cell restitution: central role of transforming growth factor beta. *Gastroenterology* **105**. 1323-1332 (1993).
140. M. F. Neurath. New targets for mucosal healing and therapy in inflammatory bowel diseases. *Mucosal Immunol* **7**. 6-19 (2014).
141. F. Verrecchia, A. Mauviel. Transforming growth factor-beta signaling through the Smad pathway: role in extracellular matrix gene expression and regulation. *J Invest Dermatol* **118**. 211-215 (2002).
142. K. R. Cutroneo. TGF-beta-induced fibrosis and SMAD signaling: oligo decoys as natural therapeutics for inhibition of tissue fibrosis and scarring. *Wound Repair Regen* **15 Suppl 1**. S54-60 (2007).
143. M. Principi, F. Giorgio, G. Losurdo, V. Neve, A. Contaldo, A. Di Leo, E. Ierardi. Fibrogenesis and fibrosis in inflammatory bowel diseases: Good and bad side of same coin? *World J Gastrointest Pathophysiol* **4**. 100-107 (2013).
144. J. W. Penn, A. O. Grobbelaar, K. J. Rolfe. The role of the TGF-beta family in wound healing, burns and scarring: a review. *Int J Burns Trauma* **2**. 18-28 (2012).
145. M. K. Kim, Y. I. Maeng, W. J. Sung, H. K. Oh, J. B. Park, G. S. Yoon, C. H. Cho, K. K. Park. The differential expression of TGF-beta1, ILK and wnt signaling inducing epithelial to mesenchymal transition in human renal fibrogenesis: an immunohistochemical study. *Int J Clin Exp Pathol* **6**. 1747-1758 (2013).
146. Y. Q. Zhang, Y. J. Liu, Y. F. Mao, W. W. Dong, X. Y. Zhu, L. Jiang. Resveratrol ameliorates lipopolysaccharide-induced epithelial mesenchymal transition and pulmonary fibrosis through suppression of oxidative stress and transforming growth factor-beta1 signaling. *Clin Nutr* **34**. 752-760 (2015).
147. M. R. Hufeldt, D. S. Nielsen, F. K. Vogensen, T. Midtvedt, A. K. Hansen. Variation in the gut microbiota of laboratory mice is related to both genetic and environmental factors. *Comp Med* **60**. 336-347 (2010).
148. F. Hildebrand, T. L. Nguyen, B. Brinkman, R. G. Yunta, B. Cauwe, P. Vandenabeele, A. Liston, J. Raes. Inflammation-associated enterotypes, host genotype, cage and inter-individual effects drive gut microbiota variation in common laboratory mice. *Genome Biol* **14**. R4 (2013).
149. W. Pang, F. K. Vogensen, D. S. Nielsen, A. K. Hansen. Faecal and caecal microbiota profiles of mice do not cluster in the same way. *Lab Anim* **46**. 231-236 (2012).

150. J. Tabarkiewicz, K. Pogoda, A. Karczmarczyk, P. Pozarowski, K. Giannopoulos. The Role of IL-17 and Th17 Lymphocytes in Autoimmune Diseases. *Arch Immunol Ther Exp (Warsz)*. (2015).
151. B. Tong, Y. Dou, T. Wang, J. Yu, X. Wu, Q. Lu, G. Chou, Z. Wang, L. Kong, Y. Dai, Y. Xia. Norisoboldine ameliorates collagen-induced arthritis through regulating the balance between Th17 and regulatory T cells in gut-associated lymphoid tissues. *Toxicol Appl Pharmacol* **282**. 90-99 (2015).
152. P. Pandiyan, L. Zheng, M. J. Lenardo. The molecular mechanisms of regulatory T cell immunosuppression. *Frontiers in immunology* **2**. 60 (2011).
153. B. D. Singer, L. S. King, F. R. D'Alessio. Regulatory T cells as immunotherapy. *Frontiers in immunology* **5**. 46 (2014).
154. P. Pandiyan, J. Zhu. Origin and functions of pro-inflammatory cytokine producing Foxp3 regulatory T cells. *Cytokine*. (2015).
155. G. Beriou, C. M. Costantino, C. W. Ashley, L. Yang, V. K. Kuchroo, C. Baecher-Allan, D. A. Hafler. IL-17-producing human peripheral regulatory T cells retain suppressive function. *Blood* **113**. 4240-4249 (2009).
156. K. S. Voo, Y. H. Wang, F. R. Santori, C. Boggiano, Y. H. Wang, K. Arima, L. Bover, S. Hanabuchi, J. Khalili, E. Marinova, B. Zheng, D. R. Littman, Y. J. Liu. Identification of IL-17-producing FOXP3+ regulatory T cells in humans. *Proceedings of the National Academy of Sciences of the United States of America* **106**. 4793-4798 (2009).
157. D. S. Chabot-Richards, T. I. George. Leukocytosis. *Int J Lab Hematol* **36**. 279-288 (2014).
158. Y. Dai, J. B. Jiang, Y. L. Wang, Z. T. Jin, S. Y. Hu. Functional and protein-protein interaction network analysis of colorectal cancer induced by ulcerative colitis. *Mol Med Rep*. (2015).
159. G. Rogler. Chronic ulcerative colitis and colorectal cancer. *Cancer Lett* **345**. 235-241 (2014).
160. R. Siegel, D. Naishadham, A. Jemal. Cancer statistics, 2012. *CA Cancer J Clin* **62**. 10-29 (2012).
161. Y. Wang, G. Han, K. Wang, G. Liu, R. Wang, H. Xiao, X. Li, C. Hou, B. Shen, R. Guo, Y. Li, G. Chen. Tumor-derived GM-CSF promotes inflammatory colon carcinogenesis via stimulating epithelial release of VEGF. *Cancer Res* **74**. 716-726 (2014).
162. J. P. Thiery. Epithelial-mesenchymal transitions in tumour progression. *Nat Rev Cancer* **2**. 442-454 (2002).
163. M. Guarino. Epithelial-mesenchymal transition and tumour invasion. *Int J Biochem Cell Biol* **39**. 2153-2160 (2007).
164. I. Matos, A. F. Bento, R. Marcon, R. F. Claudino, J. B. Calixto. Preventive and therapeutic oral administration of the pentacyclic triterpene alpha,beta-amyrin ameliorates dextran sulfate sodium-induced colitis in mice: the relevance of cannabinoid system. *Mol Immunol* **54**. 482-492 (2013).
165. L. Wang, Y. Wang, Z. Song, J. Chu, X. Qu. Deficiency of interferon-gamma or its receptor promotes colorectal cancer development. *J Interferon Cytokine Res* **35**. 273-280 (2015).
166. R. G. Urdinguio, A. F. Fernandez, A. Moncada-Pazos, C. Huidobro, R. M. Rodriguez, C. Ferrero, P. Martinez-Camblor, A. J. Obaya, T. Bernal, A. Parra-Blanco, L. Rodrigo, M. Santacana, X. Matias-Guiu, B. Soldevilla, G. Dominguez, F. Bonilla, S. Cal, C. Lopez-Otin, M. F. Fraga. Immune-dependent and independent antitumor activity of GM-CSF aberrantly expressed by mouse and human colorectal tumors. *Cancer Res* **73**. 395-405 (2013).

167. J. Massague, S. W. Blain, R. S. Lo. TGFbeta signaling in growth control, cancer, and heritable disorders. *Cell* **103**. 295-309 (2000).
168. M. Fakhoury, R. Negrulj, A. Mooranian, H. Al-Salami. Inflammatory bowel disease: clinical aspects and treatments. *Journal of inflammation research* **7**. 113-120 (2014).
169. S. Jones, W. D. Chen, G. Parmigiani, F. Diehl, N. Beerenwinkel, T. Antal, A. Traulsen, M. A. Nowak, C. Siegel, V. E. Velculescu, K. W. Kinzler, B. Vogelstein, J. Willis, S. D. Markowitz. Comparative lesion sequencing provides insights into tumor evolution. *Proceedings of the National Academy of Sciences of the United States of America* **105**. 4283-4288 (2008).
170. J. Massague. TGFbeta in Cancer. *Cell* **134**. 215-230 (2008).
171. T. Triulzi, E. Tagliabue, A. Balsari, P. Casalini. FOXP3 expression in tumor cells and implications for cancer progression. *J Cell Physiol* **228**. 30-35 (2013).
172. E. Pastille, K. Bardini, D. Fleissner, A. Adamczyk, A. Frede, M. Wadwa, D. von Smolinski, S. Kasper, T. Sparwasser, A. D. Gruber, M. Schuler, S. Sakaguchi, A. Roers, W. Muller, W. Hansen, J. Buer, A. M. Westendorf. Transient ablation of regulatory T cells improves antitumor immunity in colitis-associated colon cancer. *Cancer Res* **74**. 4258-4269 (2014).
173. M. Kim, T. Grimmig, M. Grimm, M. Lazariotou, E. Meier, A. Rosenwald, I. Tsaour, R. Blaheta, U. Heemann, C. T. Germer, A. M. Waaga-Gasser, M. Gasser. Expression of Foxp3 in colorectal cancer but not in Treg cells correlates with disease progression in patients with colorectal cancer. *PLoS One* **8**. e53630 (2013).
174. M. S. Mitchell. Immunotherapy as part of combinations for the treatment of cancer. *International immunopharmacology* **3**. 1051-1059 (2003).
175. C. Grande, J. L. Firvida, V. Navas, J. Casal. Interleukin-2 for the treatment of solid tumors other than melanoma and renal cell carcinoma. *Anticancer Drugs* **17**. 1-12 (2006).
176. M. F. Neurath. Cytokines in inflammatory bowel disease. *Nat Rev Immunol* **14**. 329-342 (2014).
177. M. Bersudsky, L. Luski, D. Fishman, R. M. White, N. Ziv-Sokolovskaya, S. Dotan, P. Rider, I. Kaplanov, T. Aychek, C. A. Dinarello, R. N. Apte, E. Voronov. Non-redundant properties of IL-1alpha and IL-1beta during acute colon inflammation in mice. *Gut* **63**. 598-609 (2014).
178. T. A. Hamilton, C. Zhao, P. G. Pavicic, Jr., S. Datta. Myeloid colony-stimulating factors as regulators of macrophage polarization. *Frontiers in immunology* **5**. 554 (2014).
179. H. Liu, N. R. Patel, L. Walter, S. Ingersoll, S. V. Sitaraman, P. Garg. Constitutive expression of MMP9 in intestinal epithelium worsens murine acute colitis and is associated with increased levels of proinflammatory cytokine Kc. *American journal of physiology. Gastrointestinal and liver physiology* **304**. G793-803 (2013).
180. A. Egesten, M. Eliasson, A. I. Olin, J. S. Erjefalt, A. Bjartell, P. Sangfelt, M. Carlson. The proinflammatory CXC-chemokines GRO-alpha/CXCL1 and MIG/CXCL9 are concomitantly expressed in ulcerative colitis and decrease during treatment with topical corticosteroids. *Int J Colorectal Dis* **22**. 1421-1427 (2007).
181. P. A. Phipps, M. R. Stanford, J. B. Sun, B. G. Xiao, J. Holmgren, T. Shinnick, A. Hasan, Y. Mizushima, T. Lehner. Prevention of mucosally induced uveitis with a HSP60-derived peptide linked to cholera toxin B subunit. *Eur J Immunol* **33**. 224-232 (2003).
182. K. J. Baldauf, J. M. Royal, K. T. Hamorsky, N. Matoba. Cholera toxin B: one subunit with many pharmaceutical applications. *Toxins (Basel)* **7**. 974-996 (2015).
183. H. Oshima, M. Nakayama, T. S. Han, K. Naoi, X. Ju, Y. Maeda, S. Robine, K. Tsuchiya, T. Sato, H. Sato, M. M. Taketo, M. Oshima. Suppressing TGFbeta signaling in regenerating

- epithelia in an inflammatory microenvironment is sufficient to cause invasive intestinal cancer. *Cancer Res* **75**. 766-776 (2015).
184. M. Stahle-Backdahl, J. Maim, B. Veress, C. Benoni, K. Bruce, A. Egesten. Increased presence of eosinophilic granulocytes expressing transforming growth factor-beta1 in collagenous colitis. *Scand J Gastroenterol* **35**. 742-746 (2000).
  185. K. Suzuki, X. Sun, M. Nagata, T. Kawase, H. Yamaguchi, V. Sukumaran, Y. Kawauchi, H. Kawachi, T. Nishino, K. Watanabe, H. Yoneyama, H. Asakura. Analysis of intestinal fibrosis in chronic colitis in mice induced by dextran sulfate sodium. *Pathol Int* **61**. 228-238 (2011).
  186. D. A. Hill, D. Artis. Intestinal bacteria and the regulation of immune cell homeostasis. *Annu Rev Immunol* **28**. 623-667 (2010).
  187. S. Gu, D. Chen, J. N. Zhang, X. Lv, K. Wang, L. P. Duan, Y. Nie, X. L. Wu. Bacterial community mapping of the mouse gastrointestinal tract. *PLoS One* **8**. e74957 (2013).
  188. V. R. Velagapudi, R. Hezaveh, C. S. Reigstad, P. Gopalacharyulu, L. Yetukur, S. Islam, J. Felin, R. Perkins, J. Boren, M. Oresic, F. Backhed. The gut microbiota modulates host energy and lipid metabolism in mice. *J Lipid Res* **51**. 1101-1112 (2010).
  189. K. K. Gkouskou, C. Deligianni, C. Tsatsanis, A. G. Eliopoulos. The gut microbiota in mouse models of inflammatory bowel disease. *Front Cell Infect Microbiol* **4**. 28 (2014).
  190. M. Gross, T. M. Salame, S. Jung. Guardians of the Gut - Murine Intestinal Macrophages and Dendritic Cells. *Frontiers in immunology* **6**. 254 (2015).
  191. G. Leoni, P. A. Neumann, R. Sumagin, T. L. Denning, A. Nusrat. Wound repair: role of immune-epithelial interactions. *Mucosal Immunol* **8**. 959-968 (2015).
  192. J. E. Qualls, H. Tuna, A. M. Kaplan, D. A. Cohen. Suppression of experimental colitis in mice by CD11c+ dendritic cells. *Inflamm Bowel Dis* **15**. 236-247 (2009).
  193. T. Lysakova-Devine, C. O'Farrelly. Tissue-specific NK cell populations and their origin. *J Leukoc Biol* **96**. 981-990 (2014).
  194. P. Kiesler, I. J. Fuss, W. Strober. Experimental Models of Inflammatory Bowel Diseases. *Cell Mol Gastroenterol Hepatol* **1**. 154-170 (2015).
  195. F. Furfarò, C. Bezzio, S. Ardizzone, A. Massari, R. de Franchis, G. Maconi. Overview of biological therapy in ulcerative colitis: current and future directions. *J Gastrointest Liver Dis* **24**. 203-213 (2015).
  196. D. R. Principe, J. A. Doll, J. Bauer, B. Jung, H. G. Munshi, L. Bartholin, B. Pasche, C. Lee, P. J. Grippo. TGF-beta: duality of function between tumor prevention and carcinogenesis. *J Natl Cancer Inst* **106**. djt369 (2014).
  197. M. Schiller, D. Javelaud, A. Mauviel. TGF-beta-induced SMAD signaling and gene regulation: consequences for extracellular matrix remodeling and wound healing. *J Dermatol Sci* **35**. 83-92 (2004).
  198. I. Marafini, F. Zorzi, S. Codazza, F. Pallone, G. Monteleone. TGF-Beta signaling manipulation as potential therapy for IBD. *Curr Drug Targets* **14**. 1400-1404 (2013).
  199. S. Sedda, I. Marafini, V. Dinallo, D. Di Fusco, G. Monteleone. The TGF-beta/Smad System in IBD Pathogenesis. *Inflamm Bowel Dis*. (2015).
  200. S. Dionne, S. Laberge, C. Deslandres, E. G. Seidman. Modulation of cytokine release from colonic explants by bacterial antigens in inflammatory bowel disease. *Clin Exp Immunol* **133**. 108-114 (2003).
  201. J. Babickova, L. Tothova, E. Lengyelova, A. Bartonova, J. Hodosy, R. Gardlik, P. Celec. Sex Differences in Experimentally Induced Colitis in Mice: a Role for Estrogens. *Inflammation*. (2015).

202. S. Matsuzaki, T. Hiratsuka, M. Taniguchi, K. Shingaki, T. Kubo, K. Kiya, T. Fujiwara, S. Kanazawa, R. Kanematsu, T. Maeda, H. Takamura, K. Yamada, K. Miyoshi, K. Hosokawa, M. Tohyama, T. Katayama. Physiological ER Stress Mediates the Differentiation of Fibroblasts. *PLoS One* **10**. e0123578 (2015).
203. L. Costantini, E. Snapp. Probing endoplasmic reticulum dynamics using fluorescence imaging and photobleaching techniques. *Curr Protoc Cell Biol* **60**. Unit 21 27 (2013).
204. B. He, P. Lin, Z. Jia, W. Du, W. Qu, L. Yuan, W. Dai, H. Zhang, X. Wang, J. Wang, X. Zhang, Q. Zhang. The transport mechanisms of polymer nanoparticles in Caco-2 epithelial cells. *Biomaterials* **34**. 6082-6098 (2013).
205. M. Lepretti, G. Paoella, D. Giordano, A. Marabotti, F. Gay, A. Capaldo, C. Esposito, I. Caputo. 4-Nonylphenol reduces cell viability and induces apoptosis and ER-stress in a human epithelial intestinal cell line. *Toxicol In Vitro* **29**. 1436-1444 (2015).
206. W. L. Conte, H. Kamishina, R. L. Reep. The efficacy of the fluorescent conjugates of cholera toxin subunit B for multiple retrograde tract tracing in the central nervous system. *Brain Struct Funct* **213**. 367-373 (2009).
207. P. H. Luppi, P. Fort, M. Jouvet. Iontophoretic application of unconjugated cholera toxin B subunit (CTb) combined with immunohistochemistry of neurochemical substances: a method for transmitter identification of retrogradely labeled neurons. *Brain Res* **534**. 209-224 (1990).
208. T. Terai, T. Nagano. Small-molecule fluorophores and fluorescent probes for bioimaging. *Pflugers Arch* **465**. 347-359 (2013).
209. H. Seno, H. Miyoshi, S. L. Brown, M. J. Geske, M. Colonna, T. S. Stappenbeck. Efficient colonic mucosal wound repair requires Trem2 signaling. *Proceedings of the National Academy of Sciences of the United States of America* **106**. 256-261 (2009).
210. J. Terc, A. Hansen, L. Alston, S. A. Hirota. Pregnane X receptor agonists enhance intestinal epithelial wound healing and repair of the intestinal barrier following the induction of experimental colitis. *Eur J Pharm Sci* **55**. 12-19 (2014).
211. V. J. Findlay, C. Wang, D. K. Watson, E. R. Camp. Epithelial-to-mesenchymal transition and the cancer stem cell phenotype: insights from cancer biology with therapeutic implications for colorectal cancer. *Cancer Gene Ther* **21**. 181-187 (2014).
212. A. Henriques, A. Rodriguez-Caballero, W. G. Nieto, A. W. Langerak, I. Criado, Q. Lecrevisse, M. Gonzalez, M. L. Pais, A. Paiva, J. Almeida, A. Orfao. Combined patterns of IGHV repertoire and cytogenetic/molecular alterations in monoclonal B lymphocytosis versus chronic lymphocytic leukemia. *PLoS One* **8**. e67751 (2013).
213. L. Beaugerie, S. H. Itzkowitz. Cancers complicating inflammatory bowel disease. *The New England journal of medicine* **372**. 1441-1452 (2015).
214. T. Kodani, A. Rodriguez-Palacios, D. Corridoni, L. Lopetuso, L. Di Martino, B. Marks, J. Pizarro, T. Pizarro, A. Chak, F. Cominelli. Flexible colonoscopy in mice to evaluate the severity of colitis and colorectal tumors using a validated endoscopic scoring system. *J Vis Exp*. e50843 (2013).
215. E. H. Huang, J. J. Carter, R. L. Whelan, Y. H. Liu, J. O. Rosenberg, H. Rotterdam, A. M. Schmidt, D. M. Stern, K. A. Forde. Colonoscopy in mice. *Surg Endosc* **16**. 22-24 (2002).
216. I. Lonngren, J. Holmgren. Subunit structure of cholera toxin. *J Gen Microbiol* **76**. 417-427 (1973).



## CURRICULUM VITAE

### Keegan James Baldauf, M.S.

Louisville, Kentucky

(419) 651-4880

keegan.baldauf@outlook.com

---

PhD in Pharmacology and Toxicology interested in the development of new drug therapies. Expertise in designing and conducting numerous studies *in vitro* and *in vivo* which involved new methodologies and lab techniques. Participating in small Phase 1 clinical trial protocol design and recruiting of clinicians to administer the study. Recognized for ability to write a high volume of reports with consistent quality and experience in presenting at regional, national and international meetings. Active mentor to undergraduate students and research staff.

#### **EDUCATION**

Ph.D., Pharmacology and Toxicology, University of Louisville, Louisville, KY

October 2015

M.S., Pharmacology and Toxicology, University of Louisville, Louisville, KY

2012

B.S., Molecular Biology and Biotechnology, Clarion University of Pennsylvania, Clarion, PA

2005

#### **PROFESSIONAL EXPERIENCE**

University of Louisville, Louisville, KY

Graduate Research Associate

June 2009 – Present

Technical experience in cell culture of human epithelial cell lines; *in vivo* experiments with mice; gene expression analysis; multi-color flow cytometry; immune cell isolation; Luminex serum and tissue protein analysis; ELISA; Immunohistochemistry; large data set analysis (Microarray).

- Led collaborations with faculty to develop new techniques in the lab leading to publication quality research including: immunohistochemistry, introduction of animal model for ulcerative colitis, flow cytometry and luminex.
- Proposed and performed both *in vitro* and *in vivo* (mouse) experiments.
- Training and supervising undergraduate students and research staff on techniques used in the lab.
- Proficient in organizing a strategy and developing techniques in the lab to achieve study goals.
- Presented at regional, national, and international meetings.

WIL Research Laboratories, LLC, Ashland, OH

Study Analyst

2006 - June 2009

Promoted to Study Analyst. Lead writer for complex study reports and monitored study progress from initiation to completion. Produced interim reports during studies and generated end of study reports in accordance with Good Laboratory Practice (GLP) Regulations and WIL Research Standard Operating Procedures. Reviewed study records, prepared methodology sections of the report, quality control and advanced scientific interpretation of the data, as well as writing results for submission to Regulatory Agencies. Led in the training of new personnel in the department and was the primary reviewer of reports generated by other analysts.

- Wrote and analyzed over 100 studies for Safety Pharmacology (cardiovascular and respiratory) and General Toxicology.
  - Coordinated Safety Pharmacology report writing which involved working with study directors, clients and other analysts to review protocol, timelines and writing of reports.
  - Worked directly with Quality Assurance on GLP studies to resolve data and report conflicts.
  - Reviewed incoming studies per month with Department Head to appropriately assign work to analysts, based on their availability, as well as tracked progress to ensure specific client deadlines were met.
- 
- Developed templates for Word text which improved consistency and efficiency of report writing and a study database for Safety Pharmacology studies which allowed analysts to access information on status of reports and pull past reports to ensure client language was consistent.

### **CONTINUING EDUCATION**

General Toxicology Course, Ashland University

Continuing Education Program for Data Analysis, WIL Research Laboratories, LLC

### **HONORS**

T32 Training Grant, Predoctoral Fellowship

Masters Basic-Science Graduate Student Award, Research! Louisville

Integrated Programs in Biomedical Sciences Scholarship, University of Louisville

### **SELECTED PUBLICATIONS**

Baldauf KJ, Royal JM, Hamorsky KT, Matoba N. Cholera Toxin B: one subunit with many pharmaceutical applications. *Toxins*. 2015 Mar 20. 7(3):974-96.

Ding X, Beier JI, Baldauf KJ, Jokinen JD, Zhong H, Arteel GE. Acute ethanol preexposure promotes liver regeneration after partial hepatectomy in mice by activating ALDH2. *Am J Physiol Gastrointest Liver Physiol*. 2014 Jan 1. 306(1):G37-47.

Baldauf KJ, Kouokom J, Jala VR, Bodduluri H, Matoba N. (2013) A Plant-Produced Cholera Toxin B Subunit Prevents Acute Colitis in a Mouse Model. *ICMI Abstract Supplement* (83).

Hamorsky KT, Kouokam JC, Bennett LJ, Baldauf KJ, Kajjura H, Fujiyama K, Matoba N. Rapid and scalable plant-based production of a cholera toxin B subunit variant to aid in mass vaccination against cholera outbreaks. *PLoS Negl Trop Dis*. 2013. 7(3):e2046.

Baldauf KJ, Jokinen JD, Falkner, K. Beier JI, Arteel GE. (2012) Acetaldehyde Dehydrogenase 2 (ALDH2) activation protects hepatocytes from mitochondrial damage and death cause by 4-hydroxynonenal. Society of Toxicology 2012 Annual Meeting (108).

Baldauf KJ, Schmidt, RH, Ding X, Beier JI, Tan M, and Arteel GE (2010) Sulforaphane Enhances Liver Regeneration after Partial Hepatectomy in Mice. Hepatology 52:617A

#### SELECTED PRESENTATIONS

2015 Poster Presenter, Ohio Valley Society of Toxicology, Cincinnati, OH. Cholera Toxin B Subunit Protects against Colitis-Associated Colon Cancer in a Mouse Model.

2013 Poster Presenter, International Conference on Mucosal Immunology, Vancouver, BC. A Plant-Produced Cholera Toxin B Subunit Prevents Acute Colitis in a Mouse Model.

2012 Poster Presenter, Society of Toxicology, San Francisco, CA. Acetaldehyde Dehydrogenase 2 (ALDH2) activation protects hepatocytes from mitochondrial damage and death caused by 4-hydroxynonenal.

2010 Poster Presenter, American Association for the Study of Liver Diseases Liver Meeting, Boston, MA. Sulforaphane Enhances Liver Regeneration after Partial Hepatectomy in Mice.